Final Report:

4-D High-Resolution Seismic Reflection Monitoring of Miscible CO_2 Injected into a Carbonate Reservoir

Type of Report
Final Report

Reporting Period Start Date
September 1, 2003

Reporting Period End Date
August 31, 2007

Principal Authors
Richard D. Miller
Abdelmoneam E. Raef
Alan P. Byrnes
William E. Harrison

Kansas Geological Survey
Open-File Report 2023-58

Date of Report
September 2007

DOE Award Number
DE-FC26-03NT15414

Name and Address of Submitting Organization

Univ. of Kansas Center for Research, Inc.
242 Youngberg Hall
2385 Irving Hill Road
Lawrence, KS 66045-7563

Kansas Geological Survey
University of Kansas
1930 Constant Avenue
Lawrence, KS 66047-3726

Disclaimer

Abstract

The objective of this research project was to acquire, process, and interpret multiple high-resolution 3-D compressional wave and 2-D, 2-C shear wave seismic data in the hopes of observing changes in fluid characteristics in an oil field before, during, and after the miscible carbon dioxide (CO_2) flood that began around December 1, 2003, as part of the DOE-sponsored Class Revisit Project (DOE #DE-AC26-00BC15124). Unique and key to this imaging activity is the high-resolution nature of the seismic data, minimal deployment design, and the temporal sampling throughout the flood. The 900-m-deep test reservoir is located in central Kansas oomoldic limestones of the Lansing-Kansas City Group, deposited on a shallow marine shelf in Pennsylvanian time. After 30 months of seismic monitoring, one baseline and eight monitor surveys clearly detected changes that appear consistent with movement of CO_2 as modeled with fluid simulators and observed in production data. Attribute analysis was a very useful tool in enhancing changes in seismic character present, but difficult to interpret on time amplitude slices. Lessons learned from and tools/techniques developed during this project will allow high-resolution seismic imaging to be routinely applied to many CO_2 injection programs in a large percentage of shallow carbonate oil fields in the midcontinent.

4-D High-Resolution Seismic Reflection Monitoring of Miscible CO_2 Injected into a Carbonate Reservoir

Final Report

TABLE OF CONTENTS

4-D High-Resolution Seismic Reflection Monitoring of Miscible CO_2 Injected into a Carbonate Reservoir

Final Report

EXECUTIVE SUMMARY

Efficiency of enhanced oil recovery (EOR) programs relies heavily on accurate reservoir models. Movement of miscible carbon dioxide (CO_2) injected into a thin (~5 m), shallow-shelf, oomoldic carbonate reservoir around 900 m deep in Russell County, Kansas, was successfully monitored using high-resolution 4-D/time-lapse seismic techniques. High-resolution seismic methods show great potential for incorporation into CO_2-flood management, highlighting the necessity of frequently updated reservoir-simulation models, especially for carbonates. Use of an unconventional approach to acquisition and interpretation of the high-resolution time-lapse/4-D seismic data was key to the success of this monitoring project.

Interpretations of geologic features from seismic data have provided location-specific reservoir properties that appear to strongly influence fluid movement in this production interval. Lineaments identified on seismic sections likely (based on time-lapse monitoring and production data) play a role in sealing and/or diverting flow through the reservoir. Distribution and geometries associated with similarity seismic facies and seismic lineament patterns are suggestive of a complex ooid shoal depositional environment. By incorporating these features, using properties consistent with core data, a more realistic reservoir simulator results, honoring the production and core properties. Flow models after simulator updating (sealing lineaments and preferential permeability manifested by faster progression of the CO_2 bank) show improvement in detail and provide correlation with the material balance.

Amplitude envelope attribute data possess changes in texture generally consistent with expectations and CO_2 volumetrics. Arguably, a multitude of different boundaries could be drawn to define the shape of the CO_2 plume, but the shapes suggested match the physical restraints, based on engineering data and the estimated amplitude response. Focusing on the injection well area and continuity of the characteristics defining the anomalous area, it is not difficult to identify a notable change in data character and texture likely associated with the displacement of reservoir fluids with CO_2.

Advancement of the CO_2 from the injector seems to honor both the lineaments identified on baseline data and changes in containment pressures. Overlaying the amplitude envelope attribute map with the lineament attribute map provides an enhanced view, and therefore perspective, of the overwhelming variability in the reservoir rocks and the associated consistency and control these features or irregularities have on fluid movement.

Increased northerly movement of the CO_2, as interpreted on seismic data and inferred from production data, after several months of CO_2 injection and oil production, stimulated an increase in injection rates at the water flood wells. After several months of increased water injection, the CO_2 advancement to the northwest was halted and some regression was observed on seismic data.

Production of CO_2 at a well significantly outside the designed flood to the northwest was consistent with the 4-D seismic, but a complete surprise to the petroleum engineers operating the flood. Seismic data early on suggested preferential northerly movement and once the CO_2 plume moved outside the high-fold footprint of the seismic volume it could no longer be tracked. Clearly the seismic monitoring could have dramatically improved the flood efficiency if the operators would have put more confidence in and heeded the images produced during the early stages of this flood.

Shortness of turnaround time of time-lapse seismic monitoring in the Hall-Gurney field provided timely support for reservoir-simulation adjustments and flood-management of the pilot study. Initial reservoir flow simulations utilized models based on pre-CO_2 oil production history, measured rock properties from core, water injectivity testing, and interwell testing. These data did not completely constrain the possible permeability architecture in the reservoir and CO_2-flood performance did not match pre-CO_2 injection predicted performance. 4-D seismic data, obtained and interpreted while the CO_2 flood was ongoing, was interpreted independent of simulations updated with the most current production data; therefore, to a limited extent, the interpretations of CO_2 movement based on seismic data were performed without field production input. Seismic predictions of CO_2 breakthrough at well 12 and the delay at well 13 were based on seismic data alone after the second monitor survey. Following initial seismic prediction, seismic and flood performance data were integrated to both validate the 4-D interpretation and confirm it was not inconsistent with flood performance, and to provide seismic input of flood progress to the flood management process. In general, seismically predicted changes in the CO_2 plume and measurements at production wells have been consistent throughout the flood.

Interpretations of time-lapse seismic data are consistent with and have assisted understanding of field response for the pilot. In a similar fashion, 4-D seismic have provided input to reservoir simulations investigating full-field EOR-CO_2 floods. Key observations from seismic data include

- accurate indication of solvent "CO_2" breakthrough in well 12,
- predicted delayed response in well 13,
- interpretation of a permeability barrier between wells 13 and CO2I#1, and
- consistency with reservoir simulation prediction of CO_2 movement and volume estimated to have moved north, outside the pattern.

Time-lapse seismic monitoring of EOR-CO_2 can reveal weak anomalies in thin carbonates below temporal resolution and can be successful with moderate cross-equalization and attention to consistency in acquisition and processing details. Most of

all, methods applied here avoid the complications associated with inversion-based attributes and extensive cross-equalization techniques. Spatial textural, rather than spatially sustainable magnitude, time-lapse anomalies were observed and should be expected for thin, shallow carbonate reservoirs. Non-inversion, direct seismic attributes proved both accurate and robust for monitoring the development of this EOR-CO_2 flood.

Weak-anomaly enhancement of selected non-inversion, 4-D seismic attribute data represented a significant interpretation development and proved key to seismic monitoring of CO_2 movement. Also noteworthy was the improved definition of heterogeneities affecting the expanding flood bank. Among other findings, this time-lapse seismic feasibility study demonstrated that miscible CO_2 injected into a shallow, thin carbonate reservoir could be monitored, even below the classic temporal seismic resolution limits.

Project Goal

A primary goal of this project has been to seismically delineate the movement of a miscible CO_2 floodbank through this thin oomoldic limestone petroleum reservoir with sufficient resolution to identify reservoir heterogeneities and their influence on sweep uniformity and efficiency. A secondary goal was to evaluate the feasibility of the high-resolution seismic method as a highly repeatable tool for monitoring the long-term stability of the CO_2 volume and in so doing develop a cost-effective, reliable approach for routinely appraising the nature and distribution of sequestered CO_2 and thus providing the assurance of CO_2 sequestration that may be required in future sequestration efforts.

This project has addressed questions that independently and together are relevant to the CO_2 flood management and CO_2 sequestration. These questions include:

Flood Management

Where is CO_2 moving?
Is CO_2 leaving the flood pattern area?
What is the sweep efficiency?
Are there areas of bypassed oil?
If CO_2 is moving, what is the mechanism?
How can the injection and production program be improved in near real-time to optimize the sweep or recovery?

CO_2 Sequestration

Where is CO_2 moving?
What is the nature (phase properties, saturation, dissolved concentration) and distribution of CO2?
Is CO_2 leaving the flood pattern area?
If CO_2 is moving, what is the mechanism?
How does CO_2 in the reservoir change with time?
Can high-resolution seismic reflection provide the assurances necessary to accurately monitor CO2 distribution?

Background

Over the last decade, time-lapse 3-D (or 4-D) seismic reflection profiling has proven to be an effective tool for evaluating conventional EOR programs. Consistency and repeatability of 3-D surveys has been the most persistently identified problem associated with time-lapse monitoring of reservoir production. Seismic monitoring has been considered viable only for the most prolific fields, which possess the greatest potential for significant returns from identification of stranded reserves. Using historical criteria, the vast majority of midcontinent reservoirs would not be considered candidates for 4-D monitoring.

The potential of seismically monitoring the injection of miscible CO_2 into thin carbonate reservoirs has only recently been studied. Field tests to date of this technique have used conventional approaches with limited evaluation of the economics of routine application or spatial and temporal sampling necessary for application to most midcontinent-size reservoirs. Changes in reservoir characteristics between baseline and one, or at most two, monitoring surveys have previously assumed linearity and not been designed to be incorporated into the production scheme.

Technical Progress

Seismic data acquisition and preliminary processing on the nine 3-D reflection surveys (one baseline and eight monitor) proposed for budget periods 1, 2, and 3 were completed as planned. Consistent with the proposed time line, evaluation of various interpretation approaches has produced images with strong agreement to production models, volumetrics, and observations that provide the essential ground truth for this study. Data acquisition was completed on schedule with the utmost care taken to insure the highest possible data quality, repeatability, and field efficiency. Preliminary data processing on the nine seismic volumes is complete with secondary processing started to enhance data resolution and interpretation potential beyond any documented studies at these depths and for beds this thin. However, due to premature termination of this project, this highly encouraging secondary processing will not be continued. Interpretations are still very crude and working with processed data that are still being optimized for consistency, resolution, and signal-to-noise. Enhancing these crude interpretations will also not be completed due to premature termination of funding.

Several unique approaches to data equalization have allowed differencing and interpretation consistent with our previous work, enhancing confidence in the image and growth pattern suggested from preliminary processing. A variety of unexpected data and reservoir characteristics have been identified and explained, providing engineers with detailed scenarios of fluid movement unlike any reservoir study in the literature. As part of the ongoing evaluation task, unique and consistent anomalies in both amplitude and frequency data suggest the presence of CO_2 in the rock can be imaged at these depths and reservoir characteristics. In addition, as key aspects of the data are identified and enhanced with specialized processing flows, images of the CO_2 plume would have become vivid, but these enhancements will not be formulated, again due to termination of this project.

After extensive equalization of reflection data to minimize and eliminate noise and balance data signal characteristics with properties inconsistent from survey to survey and not related to fluid changes in the reservoir, time slices from the reservoir interval were differenced, resulting in interpretable patterns consistent with previous analysis. Tasks one through twelve were completed as proposed and in accordance with our timeline.

Project Results

The efficiency of enhanced oil recovery (EOR) programs relies heavily on accurate reservoir models. Movement of miscible carbon dioxide (CO_2) injected into a thin (~5 m), shallow-shelf, oomoldic carbonate reservoir around 900 m deep in Russell County, Kansas, was successfully monitored using high-resolution 4D/time-lapse seismic techniques. High-resolution seismic methods showed great potential for incorporation into CO_2-flood management, highlighting the necessity of frequently updated reservoir-simulation models, especially for carbonates. Use of an unconventional approach to acquisition and interpretation of the high-resolution time-lapse/4D seismic data was key to the success of this monitoring project.

Weak-anomaly enhancement of selected non-inversion, 4D-seismic attribute data represented a significant interpretation development and proved key to seismic monitoring of CO_2 movement. Also noteworthy was the improved definition of heterogeneities affecting the expanding floodbank. Among other findings, this time-lapse seismic feasibility study demonstrated that miscible CO_2 injected into a shallow, thin carbonate reservoir could be monitored, even below the classic temporal seismic resolution limits.

Differences interpreted on consecutive time-lapse seismic horizon slices are consistent with CO_2 injection volumetrics, match physical restraints based on engineering data and model amplitude response, and honor production data. Textural characteristics in amplitude envelope images appear to correspond to non-uniform expansion of the CO_2 through the reservoir, honoring both the lineaments identified on baseline data and changes in containment pressures. Interpretations of a set of time-lapse seismic images can be correlated to a mid-flood alteration of the injection/ production scheme intended to improve containment and retard excessive northward movement of the CO_2.

EXPERIMENTAL

Program Development

Permits and access agreements were secured for the 810 shot points and 240 receiver stations that make up the 3.6 km^2 3-D deployment (Figure 1). The design provides uniform 20- to 24-fold coverage across an approximately 600 m x 450 m area centered on the flood pattern from start-up to breakthrough. Moving further away from the CO_2 injector, the two water injection wells planned for containment are all within the minimum 12-fold boundary. The 2-D, 2-C shear wave lines intersected near the injection well and extend about 400 m away from the injector. Even if the flood strays significantly from the current expected sweep pattern this 3-D design should provide the necessary offsets, offset distribution, azimuthal control, and fold to monitor the CO_2 movement and eventual fate.

Patch design has limited the bin (cell) size to a maximum 10 m × 10 m area while maintaining relatively uniform fold, offset, and azimuthal distributions. Shot lines are perpendicular to receiver lines and staggered to form a modified brick pattern. This pattern made access and movement along shot lines precarious in some areas. This style patch complicates the acquisition (source and receiver deployments), but it provides the optimum traces and trace distribution for each bin.

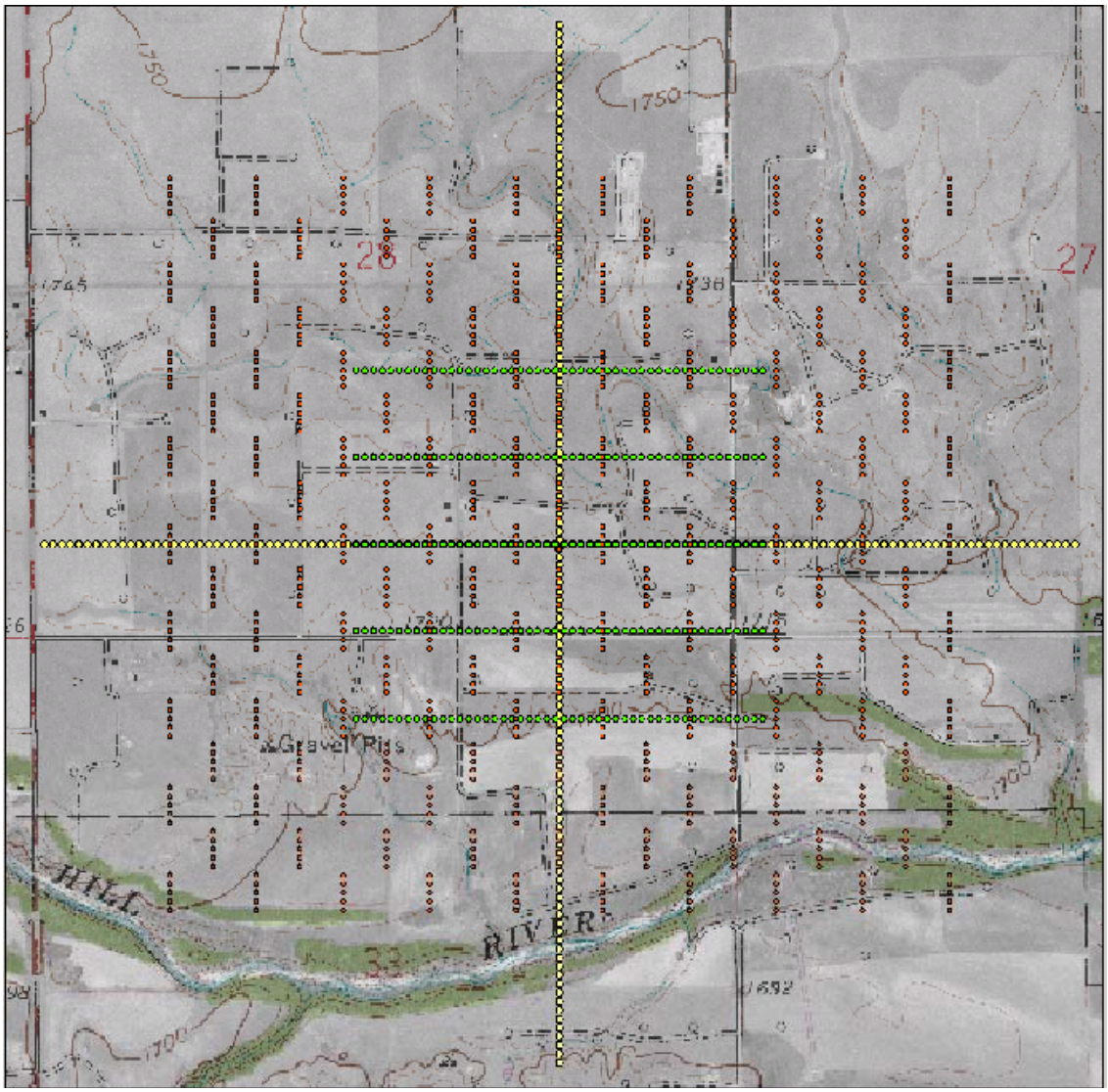

Figure 1. This orthophoto is from the Colliver lease southeast of Russell, Kansas. It is overlain by the current working 3-D compressional and shear wave, high-resolution seismic reflection survey to be acquired 12 times over the next six years. The center of this grid is approximately 20 ft north of the injection well. During a site visit on June 18, 2003, the grid was located with the KGS's Trimble DGPS system. With the grid centered on the CO_2 injector, receiver line 4 (forth from the north) was in the center of the east/west county road and receiver line 2 crossed directly through the oil storage tanks and metal building located northwest of the injection well. Site reconnaissance left us with the opinion that with the exception of the shot location in the river and in few of the deeper ditches (approximately 10 to 15), all shot stations should be accessible.

A 240-channel Geometrics Geode distributed system networked to a StrataVisor NZ acquisition controller recorded the seismic data. A single IVI minivib2 with a prototype high-output Atlas rotary control valve swept five times at each source location. Sweep frequencies for the P-wave survey span from 25 to 250 Hz over a 10 second duration. Receivers were three digital grade 10 Hz Mark Products Ultra2w geophones wired in series with 14 cm oversized spikes. Geophones were planted in a fresh spot but within a half-km of the station location as defined during the baseline and previous three monitor surveys. The three-geophone spread formed a 0.5 m equilateral triangle.

Shear wave data were acquired using an IVI minivib1 with a sweep frequency that ranges from around 15 to 150 Hz and the same seismograph but with 14 Hz horizontal geophones. The spread design and recording parameters were identical to the baseline survey. The resulting data were initially processed in 2-D with follow-up work in 3-D.

Absolute source and receiver location over the 3.6 km^2 survey grid were maintained using a Trimble survey-grade DGPS system. The original digital map developed during the baseline survey was used to exactly relocate each station for each of the repeat 3-D surveys.

3-D stacked cubes ready for interpreting were generated using the 2-D/3-D ProMax (a product of Landmark) processing package currently running at the KGS on a dual processor SGI Octane workstation. Refinements to processing flows and reprocessing of previous data sets were continuous throughout the project. Optimal processing of these 3-D data have involved techniques and algorithms developed for petroleum applications but carefully analyzed and applied in a fashion consistent with the needs of shorter wavelength and lower signal-to-noise ratio high-resolution data. Cross-equalization techniques have not been necessary with the consistency in data acquisition but will be appraised with each new data set.

Interpretation of these seismic data began during year 1. Volumes including instantaneous frequency, amplitude, and phase, along with impedance and coherency, were generated, compared, and differenced in search of the seismic attribute or attributes most sensitive to CO_2 (fluid) movement in the reservoir. Successes with instantaneous frequency were observed on initial surveys. Landmark's interpretation software Kingdom Suites has proven extremely adaptable to the high-resolution nature of these data and continued to be the primary interpretation software throughout the project.

Time Line and Progress

This six-year project was designed to be acquisition and processing intensive during the first three years and interpretation and analysis intensive during the last three years. With funding terminated after year 3, only preliminary interpretation and analysis was possible. All data acquisition and processing tasks were completed on schedule. With the unpredictability of any field-scale demonstration project, much of the field simulation and engineering was altered due to unexpected performance.

Program termination

	Budget Period I	Budget Period II	Budget Period III	Budget Period IV	Budget Period V	Budget Period VI
Task	Year 1 2003 - 2004	Year 2 2004-2005	Year 3 2005-2006	Year 4 2006-2007	Year 5 2007-2008	Year 6 2008-2009
1. Seismic survey design						
2. Pre-injection 3-D survey						
3. Compare simulation to survey (CO_2 flood begins)						
4. First time-lapse 3-D survey						
5. Second time-lapse 3-D survey						
6. Third time-lapse 3-D survey						
7. Fourth time-lapse 3-D survey						
8. Fifth time-lapse 3-D survey						
9. Sixth time-lapse 3-D survey						
10. Seventh time-lapse 3-D survey						
11. Eighth time-lapse 3-D survey						
12. Evaluation of flood efficiency						
13. Ninth time-lapse 3-D survey						
14. Tenth time-lapse 3-D survey (CO_2 flood ends)						
15. Eleventh time-lapse 3-D survey						
16. Final project evaluation and report writing						

PROGRAM CHRONOLOGY

Pre-Survey Preparations

During the June 18, 2003, visit, several key farmers who had land within the grid were contacted. Each expressed a strong interest in the project and willingness to work with us to insure year-around access.

After on-site discussions with a representative from Murfin Drilling (operators of this lease), a location for a semi-permanent monument was established immediately south of the injection well. Once the marker was placed it was located absolutely and was used to definitively locate and deploy the grid each time survey data were acquired.

A digital terrain map was generated using a Trimble DGPS system. Development of a high-resolution digital map of actual shot and receiver locations based on surface access was critical for pre-survey modeling and design. Stations that could not be occupied due to access problems were identified, with new locations (generally offset from the ideal) incorporated into final designs and survey parameters. To minimize the adverse affect of inaccessible stations on fold and azimuthal and offset distribution, it was sometimes necessary to locate replacement stations in particular directions and at specific distances from the receiver grid. For 4-D seismic surveys to be effective it is imperative that each shot and receiver station be accurately reoccupied during each time-lapse 3-D survey, effectively minimizing any changes in the recorded data not related to the injection of CO_2. To that end, the digital terrain map provides absolute reoccupation of sources and receivers.

Much of the acquisition on this project was carried out at night to minimize surface noise associated with wind and cultural activities (vehicle traffic). It was imperative that our seismic activities minimally impact current and future agricultural activities within the affected one square mile. With that, a digital tracking log was built to help guide the vibratory source (13,000 lb center articulated, four-wheel-drive vehicle with >3 psi ground pressure) around the site, avoiding fences, ditches, pipelines, etc., and minimizing ground compaction and number of miles traveled through tilled farm fields. With the limited-sight conditions present during many of the 3-D surveys, a notebook computer and high-resolution GPS were outfitted for the vibrator, which directed the operator from point to point when weather or night operations permit little or no visibility.

The digital terrain map was constructed using a DGPS mapping system, including a six-wheel-drive ATV, Trimble DGPS, Garmin GPS, and notebook computer (Figure 2). Aided by orthophotos and topo maps, researchers drove and digitally mapped the "best" vibrator route (Figure 3). Key priorities were minimal ground disturbance and best path around obstacles in all weather conditions. The digital mapping system was developed and assembled at the Kansas Geological Survey's fabrication facility specifically for this project. This modular system uses custom software interfaced to two GPS receivers, allowing real time placement and guidance referenced to orthophotos (digital, high-resolution aerophotos) and digital topo maps.

Figure 2.

Figure 3.

A preliminary tracking log provided an overview of the route most easily traversed by the ATV and one that the researchers believed would accommodate the vibrator in all weather (Figure 4). The red lines track the path followed by the digital mapping unit. The blue dots are the ideal shot station locations. With the western two-thirds completed, all but about 10% of the shot stations were easily accessible. Some minor dozer work was necessary to reduce this missing 10% in the western two-thirds down to less than 5%. Once this preliminary mapping was completed, manual editing produced a uniform route with location accuracy around 5 cm.

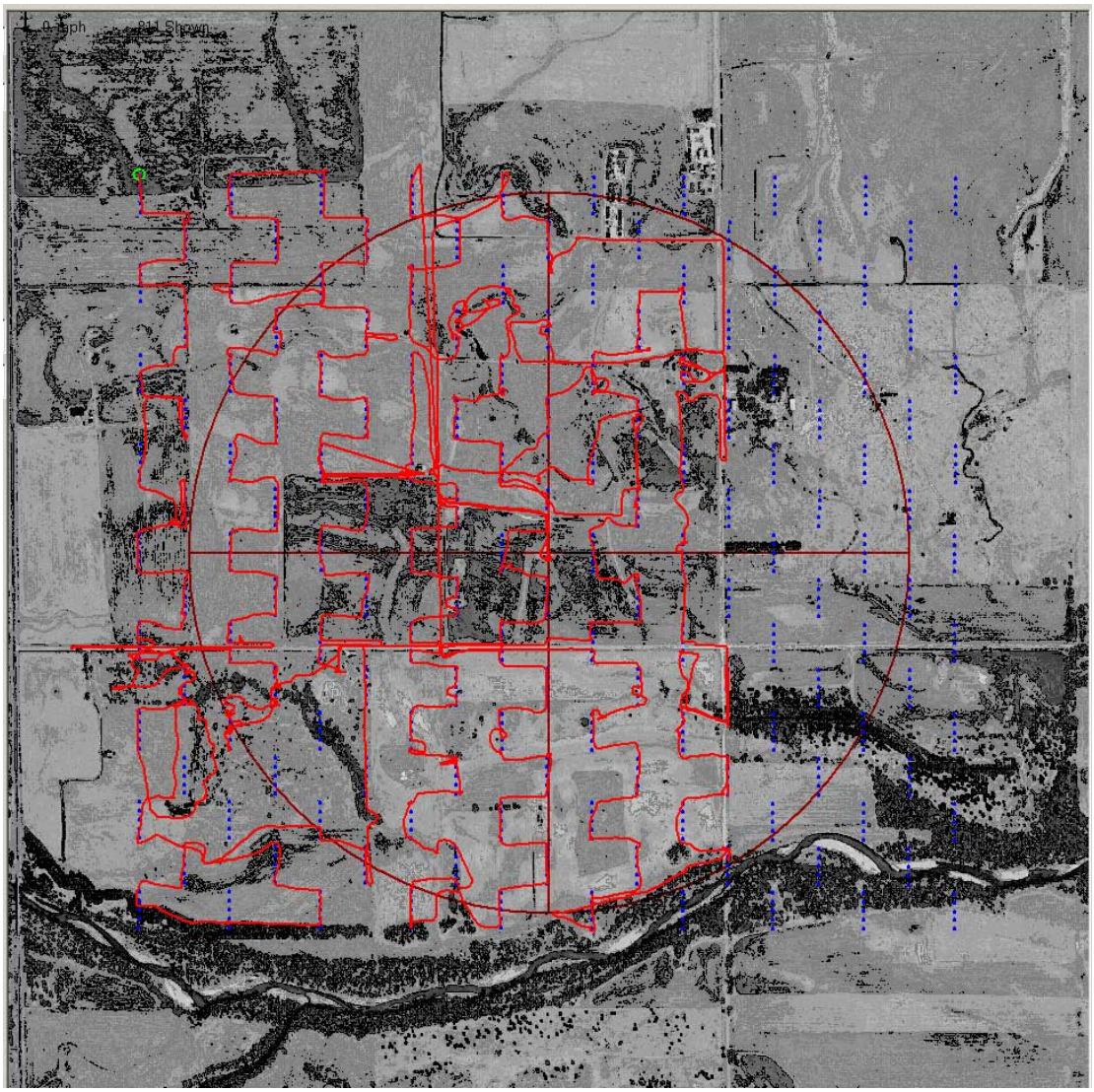
Figure 4. An orthophoto of the project area overlain by a preliminary tracking log.

After three site visits and extensive route mapping (necessary for computer-aided guidance system on vibrator), areas in need of line clearing were identified and permission to clear granted from the affected landowners/tenants. To insure the optimum trace configurations (azimuthal, offset, and fold symmetry) and year-to-year and season-to-season consistency in source locations over the six years of this monitoring program, source access paths were made as straight as possible and clear of overhanging trees that might interfere with satellite reception (Figure 5). To minimize the impact on the vegetation and to maximize the consistency in source and receiver coupling, paths were made narrow with as many of the large relief river terrace features cut and smoothed (in some cases as much as a meter) to reduce the potential static anomalies and to allow all-season travel along the paths.

A dozer, tracked hoe, and several trucks were used to clear the paths (Figure 5). Several of the source lines in the extreme southwestern end of the patch ended right at the

Smoky Hill River. Cuts up to 1 m were made through the steeper terraces, cutting away the loose sandy near-surface to expose a more compacted surface, a significant improvement in the coupling environment for the vibrator. To move the source through these areas, some manicuring was necessary and the more extreme slopes cut down. In most places the ground was just scraped, with the larger trees directly in the source line removed, leaving a path that was around 12 to 15 ft wide. The old gravel pit had several old mined-out ponds and channels that left a hummocky topography. With a few exceptions, the source paths are straight north/south.

Figure 5.

Seismic Data Acquisition: Baseline Survey

Acquisition of the baseline 3-D survey for the 4-D seismic monitoring project began on November 5, 2003. Digital data from preliminary GPS surveys were used to guide physical site preparations and were integral to the construction of an extremely accurate and precise station grid map. The station grid map incorporated the 3-D seismic survey designs with the site-specific information and allowances for surface obstacles. Ensuring the placement precision of this and all repeat source and receiver line deployments is critical to difference processing. Digital terrain maps with vibrator routes were built for all 800+ source locations across the site. Considering the proposed six-year duration of this surface seismic monitoring project, time spent at this stage to accurately map each detail of the data acquisition phase helped ensure maximum correlations between repeat surveys and minimized the need for radical equalization procedures during data processing.

Equipment was transported to the field site in two semi-trailers (Figure 6). One hauled cables, phones, and vibrator (Figure 6 left), while the other transported the ATVs used to haul cables and phones and house the recording equipment (Figure 6 right). The semi-tractor used to move the ATVs and seismograph to the site also houses the mobile processing facility (MPC), which contains three workstations, two printers/plotters, and enough desk space for three processors (Figure 6 right). All on-board computers are connected to each other and the seismograph via Ethernet cables.

Figure 6. Two semi-trailers transport equipment to the field: (left) cables, phones, and vibrator, and (right) ATVs and seismograph.

Each receiver line was located with a Trimble DGPS to ensure straight grid lines (Figure 7), with deviations in line-to-line spacing not exceeding a couple percent (1 m to 2 m). Three Mark Products U2 10 Hz geophones with 14 cm spikes were placed at the points of a half-meter equilateral triangle centered on the receiver station. With the receiver grid remaining on the ground for up to two weeks, the geophone connections were protected from moisture and ground leakage by suspending them in the air with plastic bowls (Figure 8). This practice reduced and generally eliminated all earth signal leakage. Each receiver was planted at the base of a hole dug down through the sod and into firm soil (Figure 9). This ensured good coupling and reduced the effects of wind noise.

Figure 7.

Figure 8.

Figure 9. (left and right)

A Geometrics NZ StrataVisor was used to record data from a 24-bit A/D, 241-channel Geode distributed seismograph system. Each Geode (11 individual units) contains 24 recording channels and is connected to the StrataVisor (controller) through reinforced Ethernet cables. The StrataVisor remotely controls the entire acquisition process and provides a variety of QC functions to ensure data quality. Interfaced to the StrataVisor was an IVI RTS (radio control unit for communicating with the vibrator and receiving the sweep from the vibrator) delivering the ground force pilot to the StrataVisor where it was recorded on an auxiliary channel. Two 24-channel Geodes were deployed in the center of each receiver line (Figure 10 left). These distributed seismographs transmitted digital data through four unique Ethernet lines daisy chained between units located at the center of each of the five receiver lines. An 85-amp-hour deep-cycle marine 12-volt battery powered two units for more than 40 hours of continuous use. The four Ethernet lines were all connected to the NZC controller located centrally within the

Figure 10. One of five Geode deployments (left) located in the center of each 48-station receiver line. The five Geode groupings were all connected to the Geometrics StrataVisor NZC seismic controller (right). Conducted from this John Deere Gator, seismic operations were all-weather and all-terrain. Here the Gator is configured for warm, dry conditions. Under wet or cold conditions an additional zip-on covering can be added to protect the operator and seismographs.

receiver patch (Figure 10 right). Warm and clear weather conditions allowed open-air operation of the seismic controller. Temperatures ranged from lows of 60ºF to highs near 90ºF.

Data were recorded uncorrelated, allowing maximum flexibility during processing to enhance the high fidelity of the data through precorrelation processing and unconventional approaches to correlation. Each sweep was recorded as a separate file, resulting in more than 4,000 files and a total of about 12 megabytes of data per survey. A single 3-D survey consumed about 40 gigabytes of storage space. The recording system was housed on the back of a specially modified John Deere Gator 6-wheel vehicle (Figures 11 and 12). Due to the need for quiet operation, six 12-volt lead acid batteries provided all power. Temperatures below freezing required housing the operator and system inside a specially designed insulated covering previously used during KGS research north of the Arctic Circle (Figure 13).

Figure 11. Two 24-channel Geodes next to an injection well.

Figure 12. Operating console inside Gator "dog house."

Figure 13. Cold weather cover.

Figure 14. Two 24-channel Geodes next to CO_2 injection well and DGPS (RTK) base station.

A differential GPS transmitter was set up directly over the CO_2 injection well and used for vibrator guidance, receiver placement, and well locations (Figure 14). The transmitter was up and operational during the entire baseline survey and was used on all monitor surveys to ensure source locations were within 0.5 m of the baseline survey and receivers were placed within centimeters of their original locations.

Figure 15. Installation of vibrator GPS receiver.

Capabilities for night operations were essential to avoid cultural and wind noise, which would severely contaminate this low-energy high-frequency data. To ensure safe and accurate movement and placement of the vibrator, a GPS guidance system specially designed at the KGS for this project was installed on the vibrator (Figure 15). The system allowed navigation around the site and to each shot location along predetermined optimum paths. From the cab of the vibrator the operator could move repeatedly along these predetermined routes within a few inches of the programmed safest route to a shot location, all in total darkness, if necessary. Once the vibrator was located and a sweep run, the onboard computer would log the exact pad location (within a few inches in x, y, and z).

Considering the study area for the 4-D seismic survey was just over one square mile, the diversity in terrain was significant and provided unique challenges (Figures 16-20). Source as well as receiver coupling was critical, and for that reason five individual sweeps were recorded at each location. Each of the 10-second linear up-sweeps spanned the 20 Hz to 250 Hz frequency range in a temporally uniform fashion. The first of the five sweeps was designed to seat the pad (compact the ground sufficiently that subsequent sweeps are as consistent as possible) while the remaining four sweeps were vertically stacked (once appropriate noise was edited from each) to enhance the signal-to-noise ratio. Areas such as freshly planted wheat fields were the softest and were the least conductive of high-frequency signal. Other areas such as pastures, roads, summer-

fallowed ground, waterways, alfalfa fields, and wooded areas all affected vibrator performance in slightly different ways. Of particular concern was maintaining source locations that would not only be accessible for the six-year duration of this study but also minimize dramatic swings in ground conditions due to seasonal changes. Dealing with this variability in source and receiver coupling was best accomplished during the recording phase rather than relying on processing to numerically compensate for these effects.

Figure 16. Site photo. Repeat location was used for all surveys.

Figure 17. Pasture area.

Figure 18. Wooded area near Smoky Hill River.

Figure 19. Wheat field stubble.

Figure 20. Native grasslands.

To insure acquisition of the highest quality data set, all shot records were re-viewed and preliminary processing completed on each vibrator sweep on-site (Figure 21 left). With the over 4000 uncorrelated, 12-second vibrator sweeps recorded as part of each 3-D survey, real time on-site QC was essential. Uncorrelated shot records were downloaded via Ethernet to on-site computers located in the mobile processing center (MPC) (Figure 21 right). Then the data were corrected for spectral attenuation, correlated, spectral balanced, edited, filtered, and vertically stacked. Data from shot stations with excessive noise or noise inconsistent with that observed on records from other shot stations in proximity were re-recorded to improve signal quality.


Figure 21. View from front of truck toward computer workstations (left); processing box (right) is climate controlled and mounted on truck frame with ride-controlled air suspension. A 12-kilowatt generator provides both 240-volt and 120-volt power. As data were acquired they were transmitted via Ethernet from the seismograph to the mobile processing center. Once data were transferred, preliminary processing was performed, which included long-term archive, format conversion, pre-correlation processing, correlation, noise editing, vertical stacking, application of geometry, and data inspection.

During data inspection and preliminary analysis, stations that needed reoccupation and reacquisition of data were defined. Ability to identify poor data areas and redeploy the source to these areas within hours of acquisition was only possible as a result of this in-field processing capability. About 15 percent of the shot locations were reoccupied in an attempt to improve data quality. This clearly enhanced the uniformity of the fold and resulted in a final data set with 3-D acquisition characteristics (fold, azimuthal and offset distribution, etc.) that more closely matched the ideal design criteria.

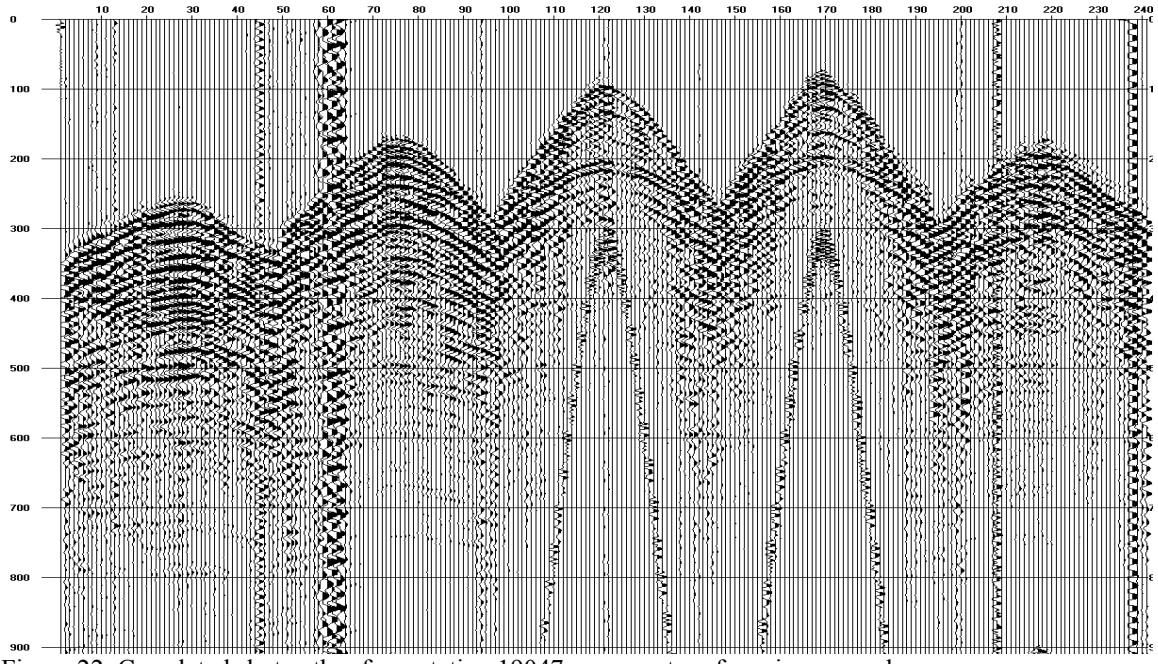

Figure 22. Correlated shot gather from station 19047, near center of receiver spread.

Data quality from the baseline survey was excellent (Figure 22). Data were cross-correlated with the synthetic pilot trace after whole trace gain was applied, boosting the amplitude of the high frequency signal (1 second AGC scale). After correlation, coherent

noise with an arrival pattern that changed from sweep-to-sweep (vehicles) was removed by zeroing affected portions of the data. Once the signal-to-noise ratio was maximized on each correlated sweep, the last four sweeps (five sweeps were recorded at each site, but the first sweep was only used to seat the base plate) were then vertically stacked.

A total of almost 800 240-channel shot gathers were recorded for each survey. Each shot gather is a four-shot vertical stack. With simple spectral balancing (band-limited spiking deconvolution) the dominant frequency of the reflection increased from around 70 Hz to over 100 Hz, which equates to an improvement in resolution potential from 35 ft to around 25 ft at depths in excess of 3000 ft (600 msec) (Figure 23). As the data processing continues, the dominant frequency from 3000 ft could exceed 150 Hz, thereby providing vertical resolution potential of around 15 ft with an upper usable corner frequency of over 200 Hz, making the thinnest possible bed resolution at around 12 ft within the Lansing-Kansas City (L-KC) formation. Approximate two-way travel time of the interval of interest (L-KC) using NMO calculated average velocities is 600 ms. Several high quality reflections are evident between 500 and 800 msec. The top of the Arbuckle is likely the reflection at around 750 msec at longer offset traces with basement around 800 msec (Figure 23). Processing of the 3-D baseline data set into a stacked volume was completed by mid-February 2004.

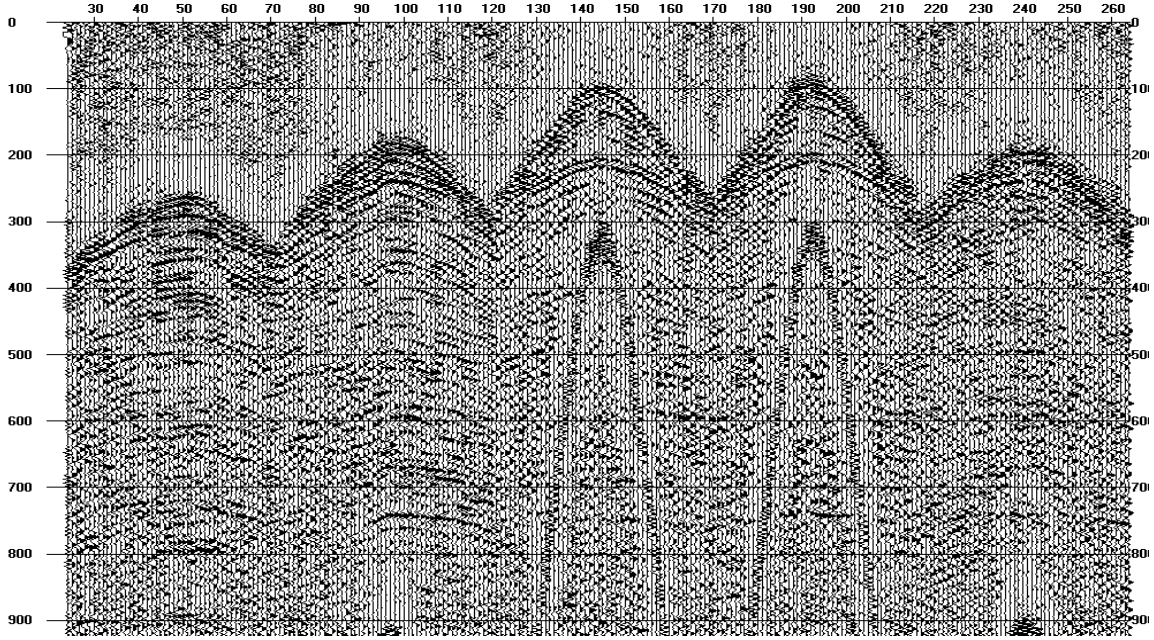

Figure 23. Four-shot vertical stack with spectral balancing.

Without doubt equipment upgrades and prototype components used to acquire these 3-D data more than doubled the overall signal-to-noise ratio and noticeably boosted the dominant frequency (Figure 24). Walkaway tests acquired during August 2002, using a 240-channel Geometrics Strataview seismograph (21-bit A/D) and IVI minivib1 (1500 ft-lbs @ 200 Hz) with the standard factory valve, produced data with excellent potential and quite adequate for the proposed 4-D monitoring project (Figure 24). However, upgrading the seismograph from 21 to 24 bits of dynamic range (going from a

Geometrics StrataView to a distributed Geometrics Geode system) and quadrupling the power output of the vibrator by going to a minivib2 with a high output Atlas rotary valve dramatically elevated the potential effectiveness of this technique to monitor, track, and allow prediction of CO_2 movement with little increase in overall cost.

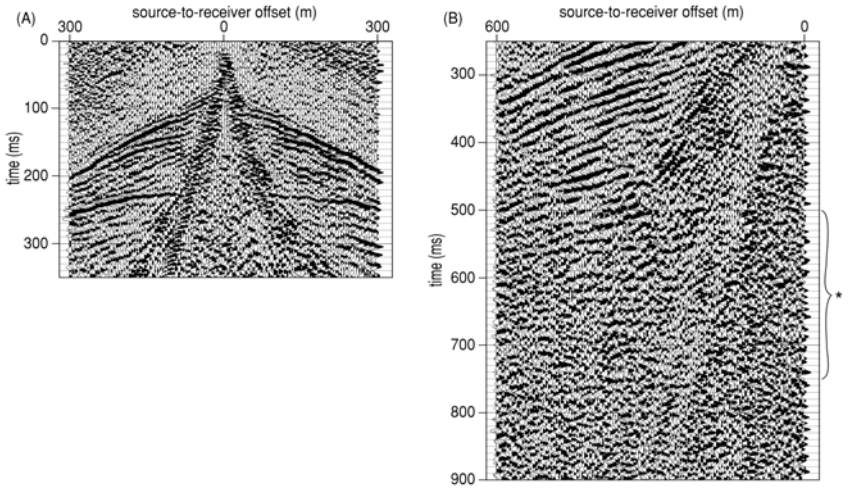

Figure 24. 2-D shot gather acquired during August 2002 testing with the minivib1 and Strataviews.

Seismic Data Acquisition: Monitor Survey One

Deployment of recording equipment for the first 3-D monitoring survey began on January 17, 2004, approximately six weeks after the baseline 3-D survey and start of CO_2 injection at the 10-acre enhanced oil recovery (EOR) demonstration site in southeastern Russell County, Kansas (Figure 25). Based on rough reservoir model estimations and the assumption CO_2 is moving uniformly away (horizontally) from the injection well, the CO_2 front should be at least 75 m, roughly seven bins or subsurface seismic sample points, out from the injection well.

As on all surveys, high-resolution GPS was used to navigate the site, insuring each source location was reoccupied within 0.5 m on all subsequent acquisition trips (Figure 26). Besides navigation, the DGPS system was programmed to provide a digital terrain map with an overall accuracy of better than 0.5 cm for each occupation point (Figure 27). Reflection data were acquired intermittently over five days with stoppages for excessive wind, construction around the tank battery, and activity associated with well rework rigs. Night recording proved beneficial in minimizing wind and cultural noise.

Time-lapse analysis of these two data sets (baseline and the first of eleven 3-D monitoring surveys) required minimal, if any, special equalization procedures to compensate for changes in ground or recording conditions. Data acquisition on the first monitoring survey mimicked the baseline survey as closely as possible. Ground conditions across the site were nearly identical to what they were in November just two months prior (Figure 28). With no appreciable new moisture and with ground conditions that were already extremely dry, from a seismic data perspective surface or near-surface conditions were unchanged between this survey and the baseline 3-D survey collected six weeks prior.

Figure 25. Kevin Axelson, Foreman for Murfin Drilling Company, monitors CO_2 pressure.

Figure 26. Vibrator tracking log showing all source stations occupied and routes driven.

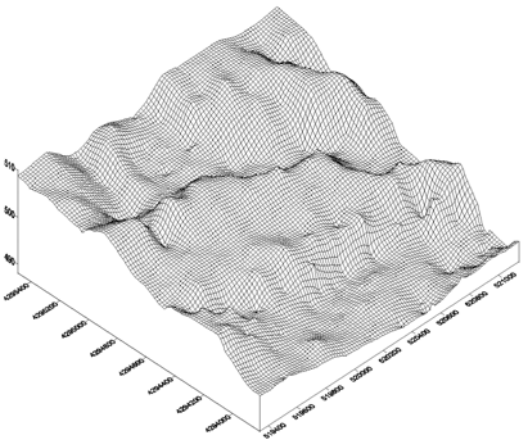

Figure 27. Digital terrain map from vibrator.

Figure 28. Ground condition on January 17. Air temperature was 40° F & wind at 25 mph.

Cables were laid along receiver stakes placed during baseline survey (Figure 29 left). Geophones were planted in the same locations (+/-10 cm) and with nearly identical coupling (Figure 29 right). To insure as near identical recording conditions as possible, no data were recorded when wind speeds are in excess of 15 mph, with reluctance to record when the wind exceeds 10 mph. These general ground rules for recording in this notoriously windy area were used during the baseline survey and all subsequent 3-D monitoring surveys.

Figure 29. (left) cable laid with ATV along stakes and (right) geophones planted at surveyed stake.

With time lapse (4-D) seismic imaging comes an exorbitant amount of attention paid to all sources of noise, especially noise that changes from record-to-record and day-to-day (Figure 30). This concern stems from the need for complete repeatability in every recorded data point. Sources of noise at the CO_2 pilot study site in southeastern Russell County include wind, rain/sleet, injector pumps, injection wells, pipelines, oil-production pumps, vehicle traffic, livestock/wildlife, and power lines. Each of these noise sources produces seismic energy impacting the recorded signal in a range of ways.

Figure 30. During normal operations CO_2 will occasionally vent from storage tanks.

Changes in near-surface conditions that occurred during the acquisition of the 3-D monitoring surveys ad little to no effect on the recorded data (Figure 31). Receivers were well seated (14 cm) into solid material and all electronic connecting points were insulated from the ground by elevating the takeouts with plastic tubs and therefore protecting the takeout from leakage (Figure 32). The 240-channel Geometrics Geode recording system is designed to operate in all weather conditions (Figure 33).

Figure 31. Data collection: January 23, 2004 (50º, calm, & clear) vs. January 25, 2004 (25º, freezing rain, and cloudy).

Figure 32. Ten-hertz geophones with tubs to insulate connector.

Figure 33. Ice covered Geode.

Coherent noise that moves either during the 10-second seismic sweep or from sweep to sweep at a single source station has the least impact on the eventual consistency in data characteristics between any two surveys acquired at different times of the year. Moving coherent noise is generally a vehicle, an animal, or humans. Since the source point for this type of noise changes from shot to shot throughout the recording time, it can be muted or zeroed from one record in a surgical fashion (Figure 34). In this example, when the four sweeps from each station are vertically stacked, contributions from records with good signal are added to the zeroed or muted portions of records where noise had previously dominated to produce a continuous high signal-to-noise ratio section.

Removing coherent noise that is stationary is more difficult and has a marked negative effect on stacked sections in comparison to moving coherent noise. Examples of sources of coherent stationary noise include injection wells, injection pumps, pipelines,

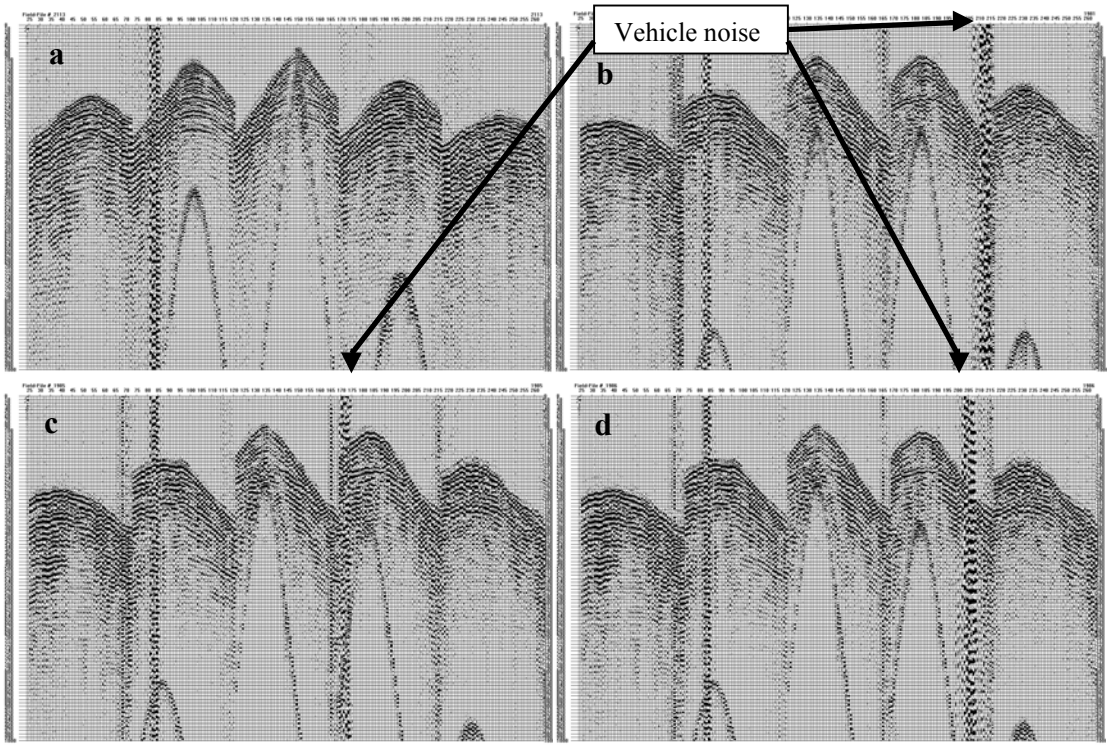

Figure 34. (a) Quiet record with water injector pump at trace #84, compared to records (b), (c), and (d) with vehicle noise moving across the records.

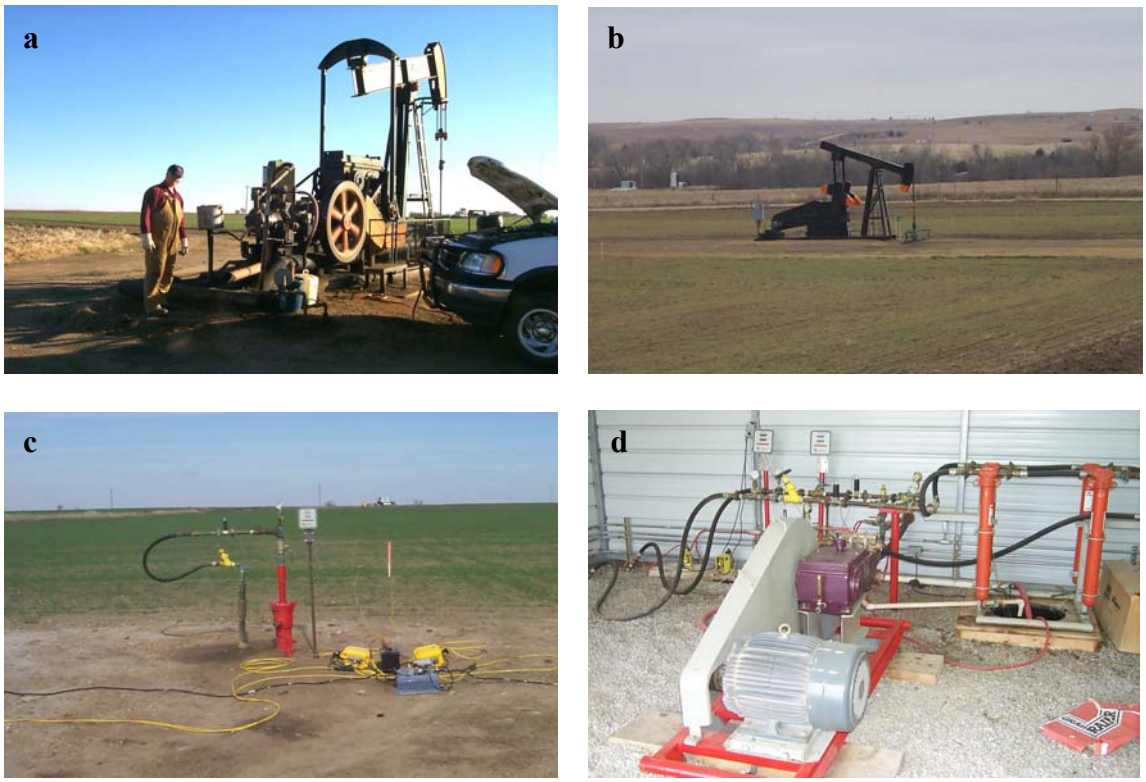

Figure 35. (a) Single cylinder gas engine powered pump jack, (b) electric-powered pump jack—Colliver #12, (c) water injection well with fluid flow meter, (d) piston pump for water injection.

oil-production pumps, and power lines (Figure 35). With the stationary nature of these noise sources, all records recorded for all source locations had this noise at the same place (Figure 36). Therefore the method used for moving noise sources—muting bad segments and then adding the muted (zeroed) portion to good signal from other records taken at this site—will not work here. Two different techniques were used to reduce or eliminate this type of noise, depending on the specific characteristics of the noise. One technique involved filtering in the frequency domain for the noise source, which has dominant frequency signatures within a narrow range or a range outside the seismic source bandwidth. Another technique is cancellation when the phase characteristics of the noise source vary through time and from record to record.

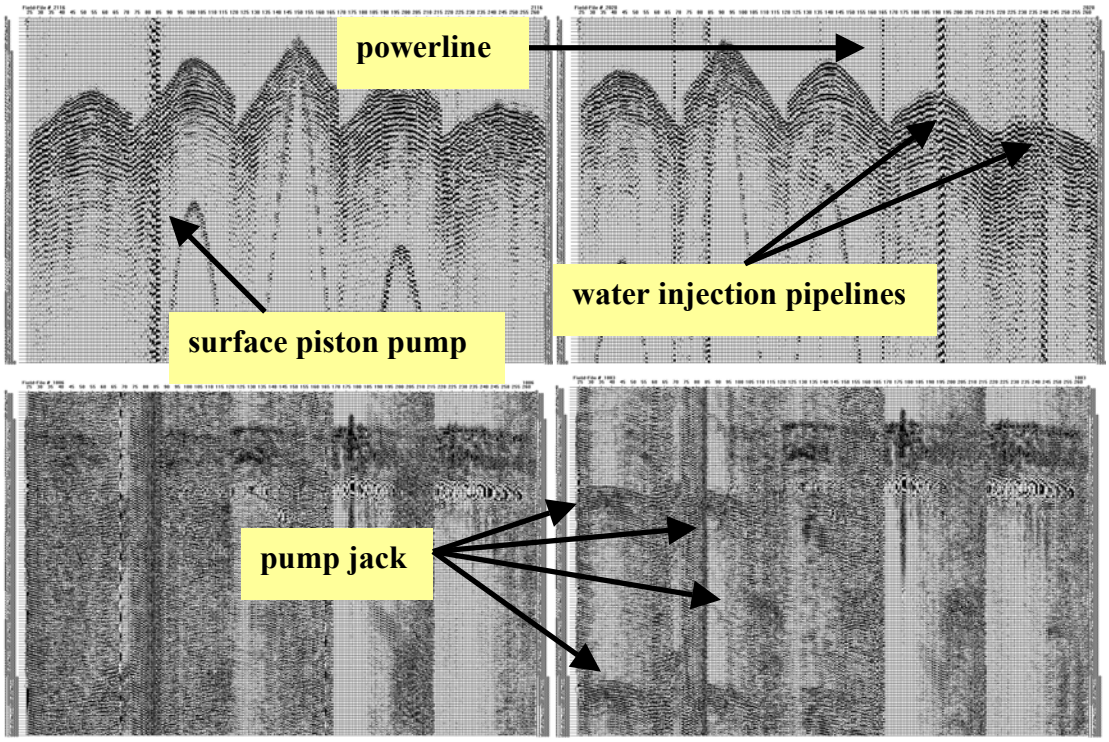

Figure 36. (top) Correlated shot gather with stationary noise. (bottom) 12-second uncorrelated shot gather with pump-jack noise (right) and without (left).

At this site there are two predominant sources of fixed, continuous, coherent noise: pumps and pipelines. Oil-production well pumps produce a periodic low-frequency long-duration pulse consistent with the stroke of the pump jack (Figure 35). Correlation of the pilot with the recorded sweep tends to reduce this kind of noise, generally to levels that can be tolerated, but not preferred, on 4-D data sets. This kind of pump jack noise is bothersome but not nearly as detrimental to the overall data quality as ground vibrations emitted by high-pressure piston pumps. High-pressure piston pumps put continuous high amplitude relatively broadband noise into the ground.

In the case of the fresh-water injection pump located inside the utility shed on-site, all receivers within 150 ft are inundated with this high amplitude broadband noise (Figure 36, top). The only signal enhancement weapons that seem to work to a very limited degree against this kind of noise are spectral balancing and vertical stacking.

Fortunately, these pumps do not saturate the available dynamic range of the seismograph, permitting recording of some signal (be it extremely low amplitude). This extremely small percentage of signal increases relative to the noise by vertically stacking each sweep recorded at a shot station. Building the signal strength in this fashion is possible as a consequence of the uniformity in arrival times and character of signal on all shot gathers compared to the more random phase-time relationship that coherent and continuous single-point noise will have from shot to shot.

Pipelines used to move the fluid from pump to well bore emit noise generated by surface piston pumps, which are used to move fluid around an oil field (Figure 36, top). A tremendous amplitude of pump noise can be seen every place a pipeline passes beneath a receiver line. With water injection at this site used to contain the CO_2, pumping of water through these pipes and into the injection wells occurs based on need as determined by borehole pressures. Therefore, high-amplitude pipeline noise dominates several traces on any line that passes over the pipeline for periods of 1 to 2 hours every 2 to 4 hours all day. This noise always affects the same receivers but is recorded at some shot stations and not at others, depending on when the well is pressured up. As a result, no two complete 3-D data sets have this pipeline noise on all the same shot gathers. Differences in this noise appear as changes from baseline on later monitoring surveys.

Wind is a source of noise that is the least controllable and can be the most detrimental to time-lapse seismic recording (Figure 37). No two days have the same wind conditions, so it is impossible to record two data sets that will difference to equal zero,

Figure 37. Data acquisition was not possible on January 26, 2004 (10º F, snowing, and 30 mph wind). Many days with excessively noisy conditions related to weather were unfit for recording data.

even when using the same source, identical source locations, and exactly the same receiver grid. This project requires four to six 18-hour days to record data from all the source locations. Across that six-day span, noise from wind is stronger some days than others, making shots recorded on one side of the grid noisier than shots from the other side, independent of near-surface conditions or source-to-receiver offsets. On this project, no data are recorded when wind velocity exceeds 15 mph. This is an experience-based value that resulted in an acceptable signal-to-noise ratio on recorded seismic data.

Adjustments made to the data-acquisition procedures insured changes from the dry, warm conditions present at the start of this survey to the snow/ice covered ground and frigid temperatures endured during the latter days of this first 3-D monitoring survey (Figure 38) had little or no distinguishable effects on the recorded data. For example, the vibrator pad was continuously cleared of snow to maintain optimum coupling. KGS experience acquiring data in Arctic regions was extremely beneficial in and critical to maintaining the highest possible data quality even when temperatures dropped below -6ºF with a stout breeze and light snow cover on the ground.

Figure 38. (a & b) Conditions during week of January 19, 2004; (c & d) conditions during week of January 26, 2004.

Qualitative analysis was used to determine if shot records possessed unacceptable noise levels. Determining stations that needed to be reoccupied was generally a straight-forward process. High frequency random noise, elevated by as much as 6 dB over adjacent stations, could be easily identified. In general, noise level increases of as little as 3 dB were sufficient to justify reacquiring all five sweeps at that location (Figure 39).

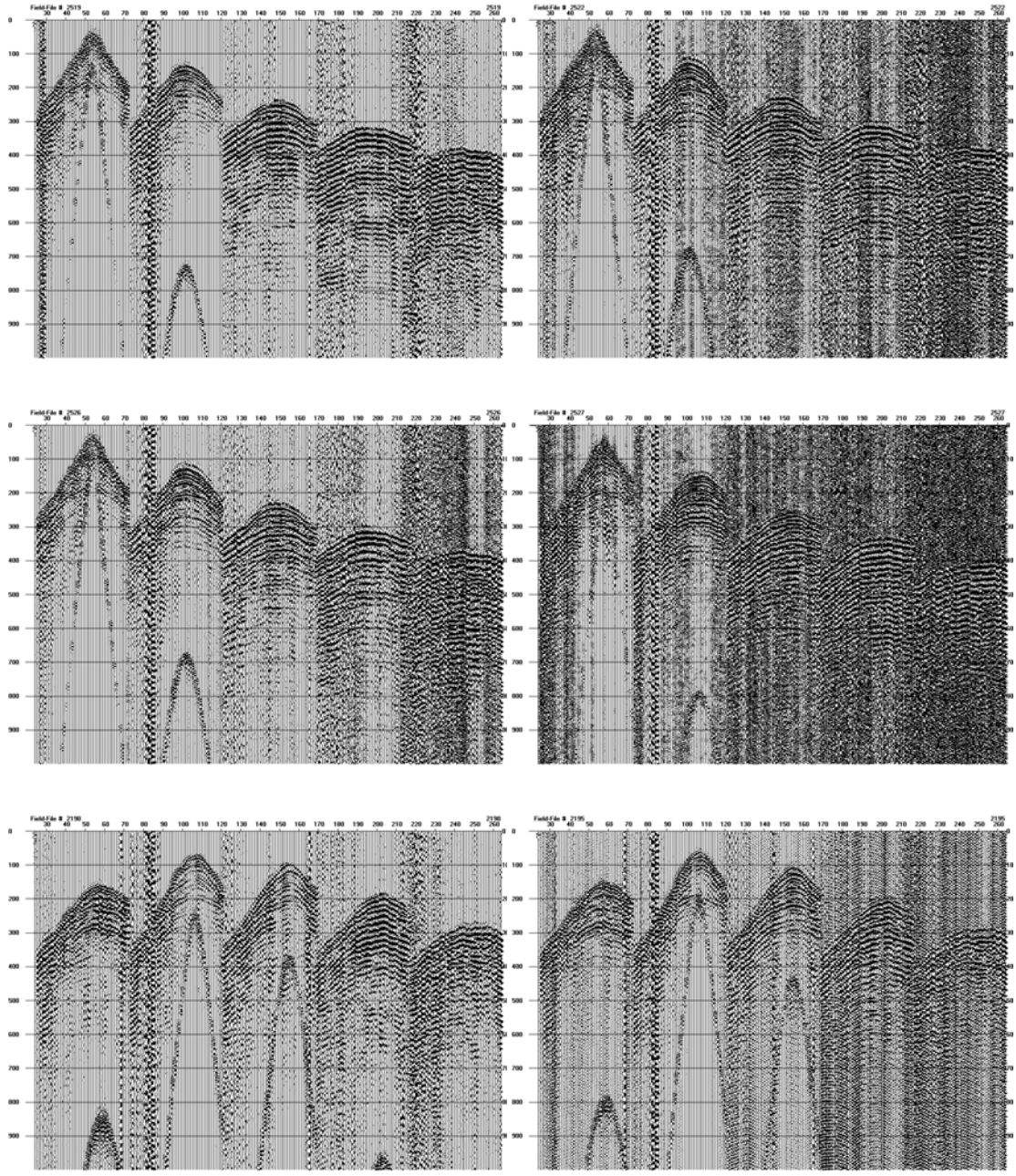

Figure 39. Average, relatively low noise, correlated shot gather (left) with adjacent shot station (right) possessing elevated noise levels.

Visually dramatic increases in noise between two source stations located within 20 m of each other are usually related to earth coupling of the vibrator or gusty winds. Either way, reacquiring the data can only be accomplished real-time while all the equipment and crew are on-site and the CO_2 position is relatively constant (at least with respect to the size of the seismic wavelet). Considering the need that time-lapse analysis has for high S/N data, this step is imperative for obtaining the highest resolution, most representative series of snap shots of the CO_2 movement through this shallow (950 m), thin (5 m) reservoir.

Changes in reflections from within the interval of interest can be observed on raw shot records (Figures 41 and 42). It is not clear that these changes are related to the presence of CO_2. It will require significantly more processing to determine this. However, it is encouraging to see reflection characteristics changing within thin zones near the depth interval receiving CO_2, while reflection characteristics from rock layers shallower and deeper remain consistent between these two data sets separated in time by over six weeks. It would be premature to suggest these changes in reflection character are direct indicators of changes to reservoir characteristics due uniquely to the presence of CO_2 during this late January survey where it was not during the mid-November baseline survey.

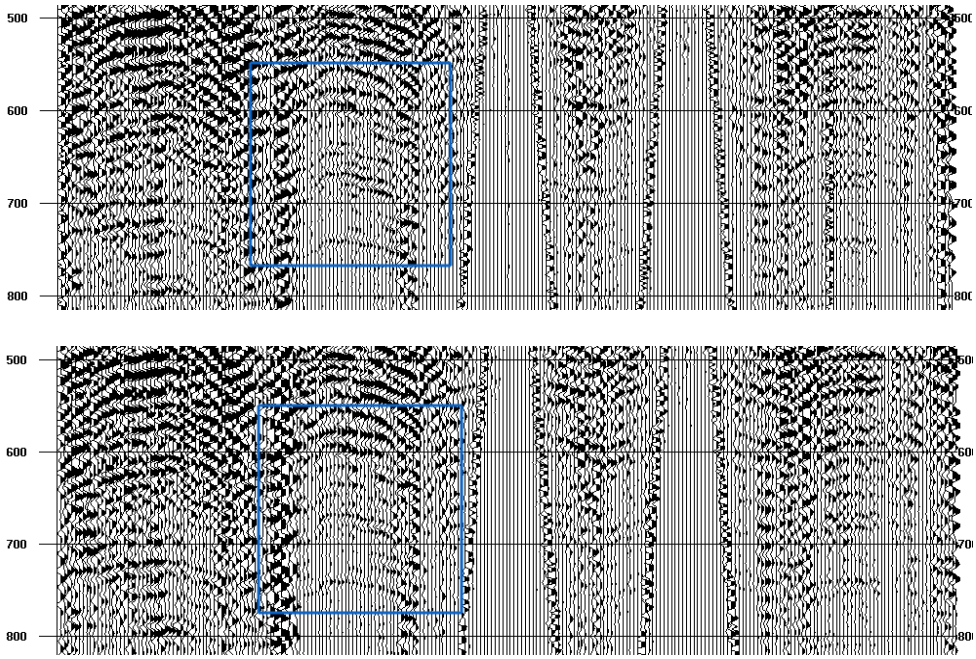

Figure 40. Before CO_2 injection (top) compared to after CO_2 injection (bottom). Reflections from the L-KC should be arriving around 600 msec (+/- 100 msec). Exact time depths are being determined from VSP and synthetic seismograms produced from nearby sonic logs. The boxed areas are enlarged in Figure 41.

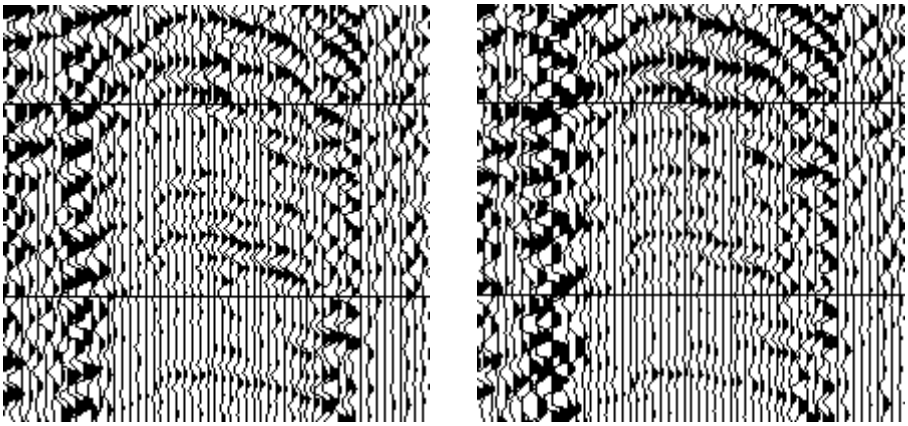

Figure 41. Before CO_2 (left) and after CO_2 (right). This enlarged section of the shot gather from station 19047 is from line 2. Reflections from the middle portion of these records have midpoints within a few hundred meters of the injection well and therefore are sampling the zone proposed to be already affected by the CO_2 flood.

Seismic Data Acquisition: Monitor Survey Two

Incorporating all well data available at this point in the flood, engineers projected CO_2 breakthrough in Colliver 12 as early as April 1, significantly ahead of preliminary schedules. Predictions of premature breakthrough at this oil-producing well were revised based on models that incorporated wellhead data acquired during water-injection tests run just months before commencing the CO_2 flood. These newer models suggested movement along the CO_2 front was being influenced by high-permeability "fingers." These high-perm zones influence connectivity between Colliver 12, 14, and CO2I#1 and are likely quite thin (on the order of a seismic wavelength). It was anticipated from seismic-waveform models produced from pressure and phase relationships that as the CO_2 front passed the amplitude of the reflectivity of L-KC, the C-zone reflector would change sufficiently to allow easy tracking of the CO_2 plume from comparison of images from the first two 3-D seismic surveys.

After deliberation among geologists, engineers, and geophysicists, the optimum second snapshot of the CO_2 flood-monitoring survey (third 3-D survey; one baseline and two monitoring) needed to begin around March 15 (Figure 42). Based on previous experience, this third 3-D survey was expected to take about 10 days. Geophones were left frozen in place after the January 2004 survey and were used for this survey without disturbing them (Figure 43). Considering the effort taken between surveys to reoccupy identical stations and plant geophones well into competent soil, leaving the receivers in place did not result in distinguishable changes in survey-to-survey consistency. However, this difference was studied and if significant improvement in waveform consistency would have been observed receivers would have been left in the ground where possible, although tillage of farm fields would not have permitted phones to remain planted in some areas of the site.

Figure 42. Installing cable protector across road.

Figure 43. Connecting geophones still in place after January 2004 survey to cable laid down for March 2004 survey.

Critical to data quality during the second monitoring survey at the CO_2 injection site was the avoidance of excessive wind noise. March is known as particularly windy in central and western Kansas. Noise from wind is difficult to attenuate using post-acquisition processing techniques on seismic data due to its somewhat random arrival pattern and broadband spectral characteristics. Major efforts were taken to minimize the recording of excessive wind noise. Most significant of these efforts were recording at

night and only recording when winds were less than 15 mph (an empirically based wind speed based on noise levels observed at the seismograph during recording). As a result of these strict acquisition guidelines, several days might pass without data being recorded while other days more than 240 shotpoints were recorded in a twenty-hour work period.

With temperatures in the 60s, ground surface dry, and winds less than 15 mph, background noise levels and site access conditions were as close to ideal for this part of the world as possible for seismic-data acquisition during March. When the wind exceeded 15 mph, the data quality dropped sufficiently that acquisition was halted (Figure 44). Generally, during the afternoons wind velocities exceeded acceptable levels for recording. To counter these unacceptable noise levels, data acquisition began around 3:00 am and continued until wind levels exceeded preset thresholds, usually occurring around 12:30 pm to 1:00 pm (Figures 44 and 45). The requirement for low wind noise is significantly more important for 4-D (time-lapse) than for standard 3-D. For 4-D to be effective, detectable changes in reflection signatures must primarily be related to changes in reservoir flood properties and not due to changes in noise levels or ground conditions.

Figure 44. Wind gusting at 30 mph in afternoons.

Figure 45. No wind, night and mornings.

Wind noise became a noticeable problem when gusts exceeded 15 mph. Shot records from the end of the first day showed the adverse affects of winds gusting to around 20 mph around 1:00 pm (Figure 46). Reacquiring noisy data from day 1 just 14 hours later on day 2 when winds were calm resulted in a noticeable improvement in the signal-to-noise ratio (Figure 47). A great deal of on-site effort went into identifying shot records possessing unacceptable noise levels and reacquiring those stations when conditions were more conducive to the highest quality data possible.

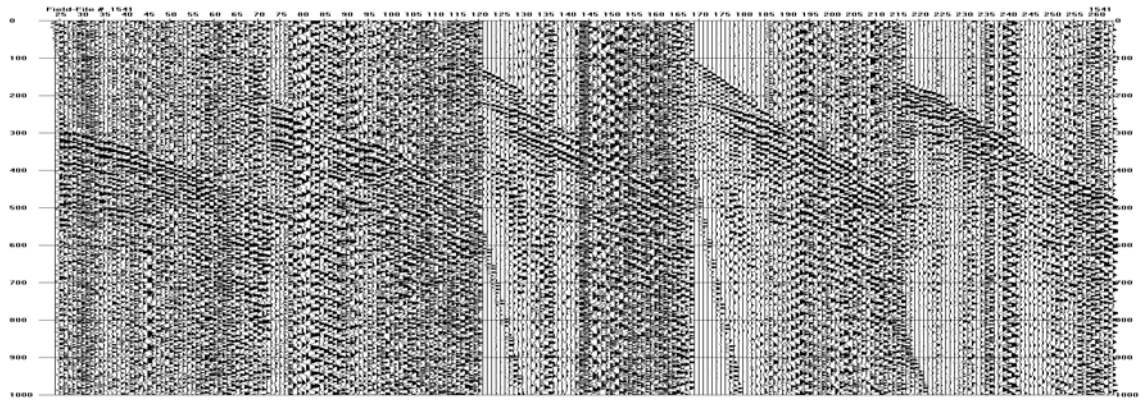

Figure 46. Correlated single sweep from station 13049 with 20 mph gusty winds.

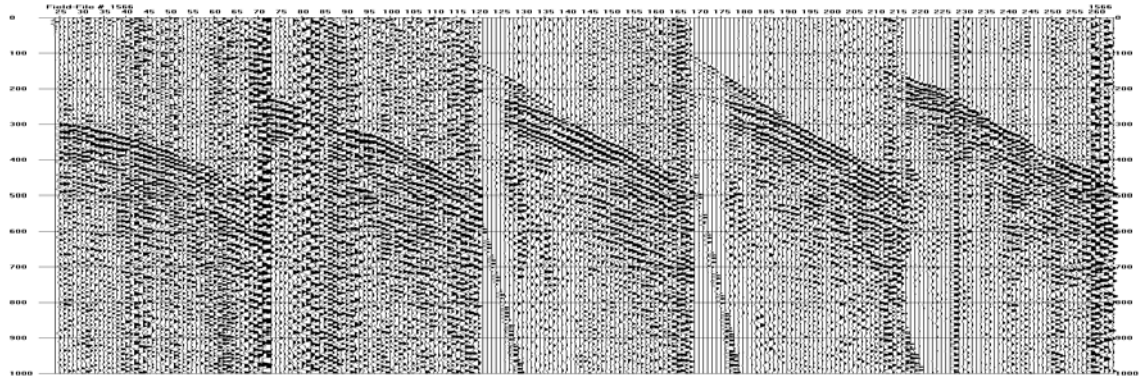

Figure 47. Correlated single sweep from station 13049 with no wind.

With a little over 400,000 gallons of CO_2 already injected into the ground, operators and engineers are expecting breakthrough soon. The volume of fluid injected (Figure 48) and recovered (Figure 49) are both monitored very carefully, and recovery of CO_2-enhanced oil is anticipated during the week of March 21, 2004.

Figure 48. Kevin Axelson measuring injected CO_2.

Figure 49. Kevin measures oil level in tank storing oil recovered from Colliver 12 and 13.

Shot gathers from the first three surveys, in general, were of very good quality (Figure 50). Repeatability of reflection amplitudes and source-wavelet characteristics was better than expected and clearly demonstrated the advantages of consistency in all aspects of the data acquisition on time lapse. This repeatability greatly reduced the importance of computational-equalization techniques that have been essential to time-lapse analysis on most other 4-D seismic surveys. Coherent energy arrivals with hyperbolic moveout, characteristic of reflections, were interpretable throughout the primary depth interval. More than a dozen individual reflections returning from between the Stone Corral Formation and Arbuckle were easily identifiable on the shot gathers with guidance from the downhole survey acquired in #16, the synthetic seismogram, and published data from this general area.

Meaningful correlation of the synthetic traces with traces from a shot gather requires estimates of reflection-arrival time based on source-to-receiver offset, time shifts that are compensated for on vertical incidence, and CMP-stacked sections using the NMO correction. Based on reflection-curve modeling, reflections from the L-KC should arrive at times ranging from 548 msec for vertical-incident traces to 610 msec for offsets of 900 m. Using this general relationship, the exact set of reflection wavelets returning from the injected interval can be identified on shot gathers.

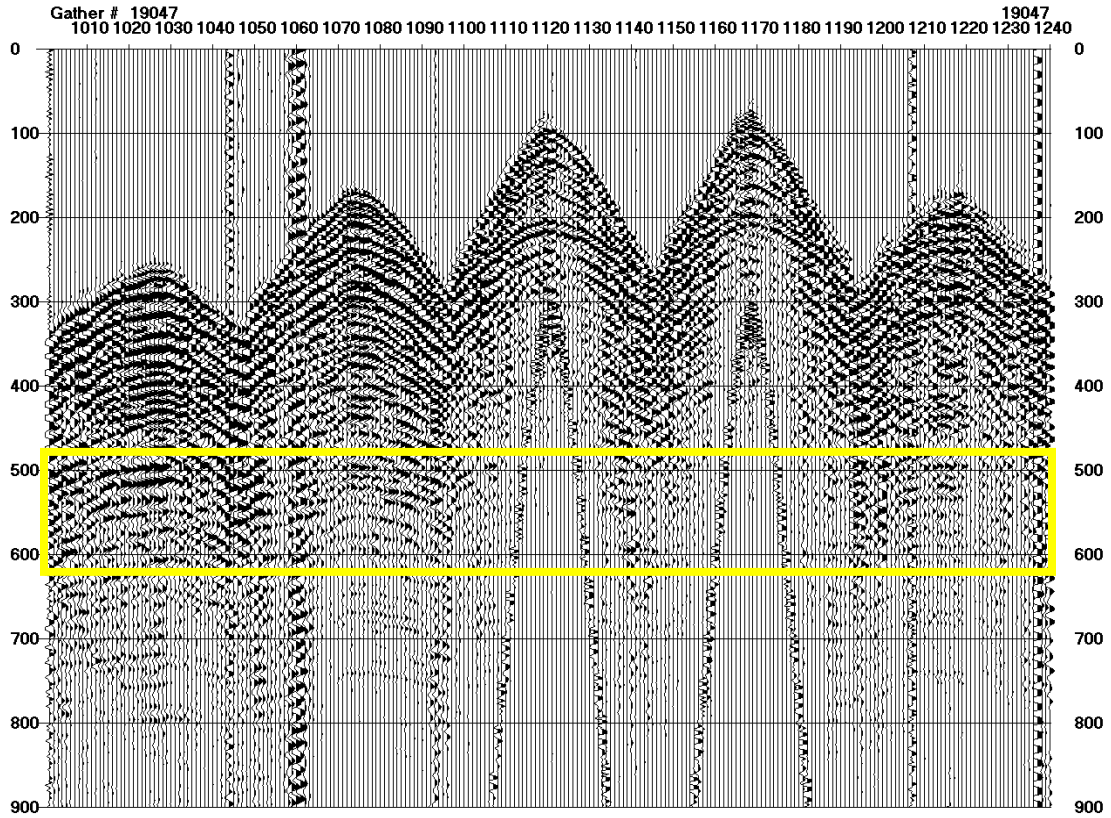

Figure 50 (figure continues next page)

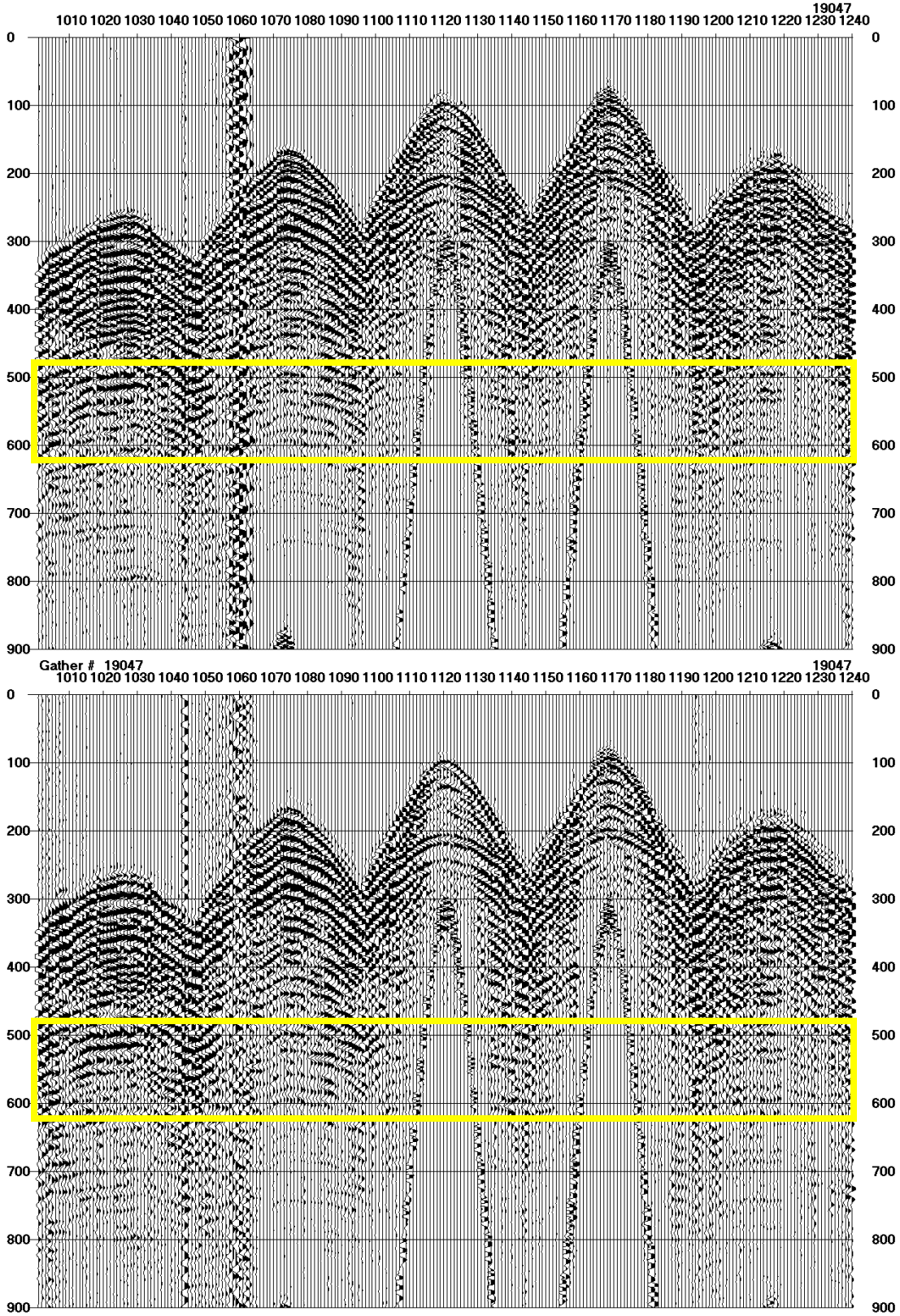

Figure 50. Comparison of shot gathers from three trips. Before CO_2 injection (top), after six weeks of CO_2 injection (middle, ~200,000 gallons), and then after slightly than three months of CO_2 injection (bottom, ~450,000 gallons). Reflections from the Lansing-Kansas City (L-KC) should be arriving between 550 and

590 msec, depending on source offset. Exact time depths are determined from VSP and synthetic seismograms produced from nearby sonic logs. The boxed area is enlarged in Figure 51.

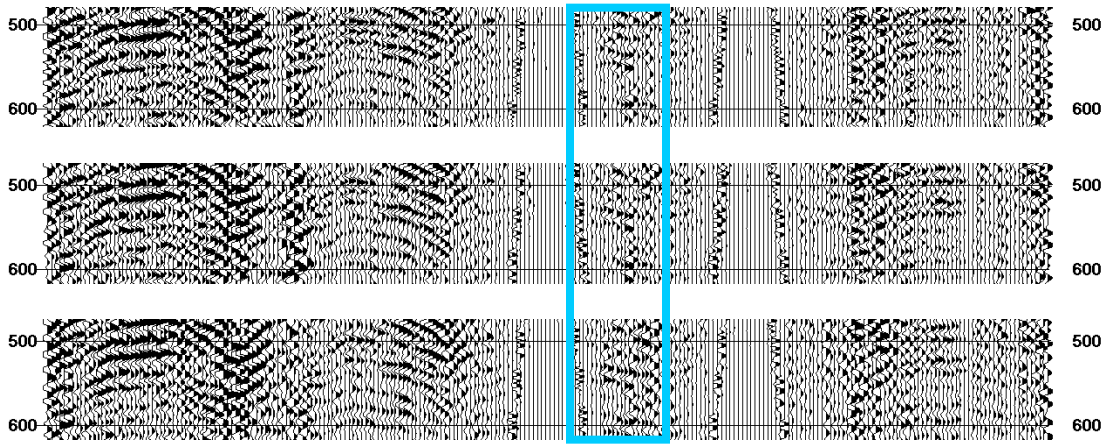

Figure 51. Time slice from the depth range of interest; baseline survey (top), first monitor survey (January 2004) (middle), and second monitor survey (March 2004) (bottom). Clearly with the passing of time and increased volume of CO_2—the reflection evident within the box at approximately the correct time for the L-KC—appears to possess steadily increasing amplitude. This increased amplitude could be indicative of increased reflectivity resulting from changes in layer characteristics.

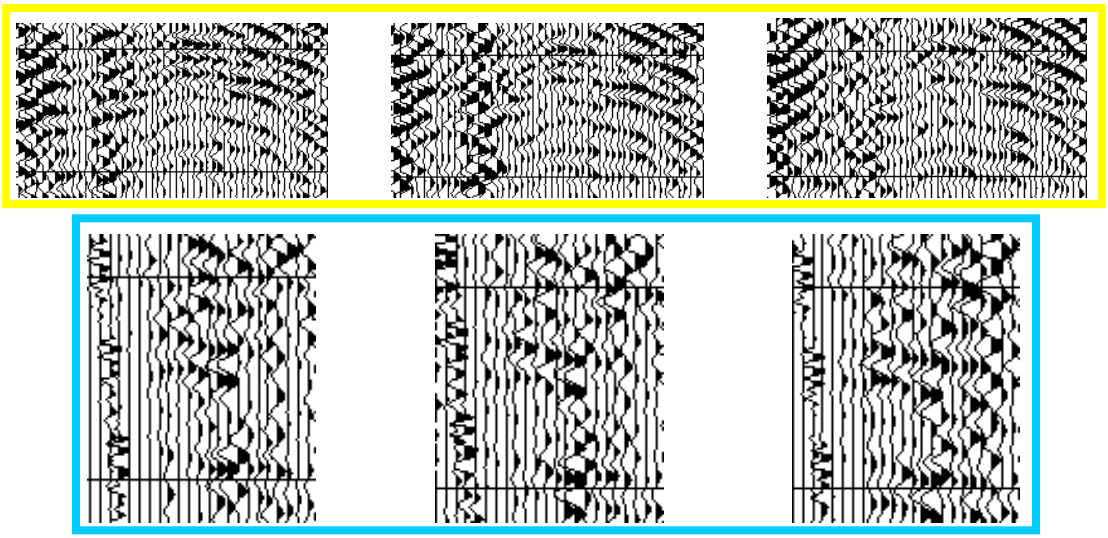

Figure 52. Magnified comparison of reflections within the time depth approximately correct for the L-KC interval. Blue and yellow highlights correlate to same zones in Figures 50 and 51.

Using the time-to-depth conversion extracted from the downhole survey conducted in #16 (Figure 53), it is possible to bulk time-correct the synthetic seismogram (Figure 54) for the normal inaccuracy in absolute time resulting from estimating overburden velocity. As usual, these errors range from less than a percent in areas with an abundance of ground truth to as much as 10 percent when no other information but the sonic log is available to help estimate replacement velocities. Using local well data only, the L-KC interval was estimated to be at a time depth of around 535 msec. Incorporating the VSP and manual wavelet-correlation techniques, the actual arrival time of the top of the L-KC on seismic data was around 548 msec. Using the VSP for the first-arrival information alone more than justifies the expense of getting these borehole data. Correlations

between borehole and surface seismic were critical to accurately defining the wavelet returning from the L-KC. Considering the producing interval, and therefore the interval the CO_2 is being injected into, is only 15 ft thick and equates to just a little more than 1 msec, it is imperative to identify the L-KC reflection within a few tenths of a percent.

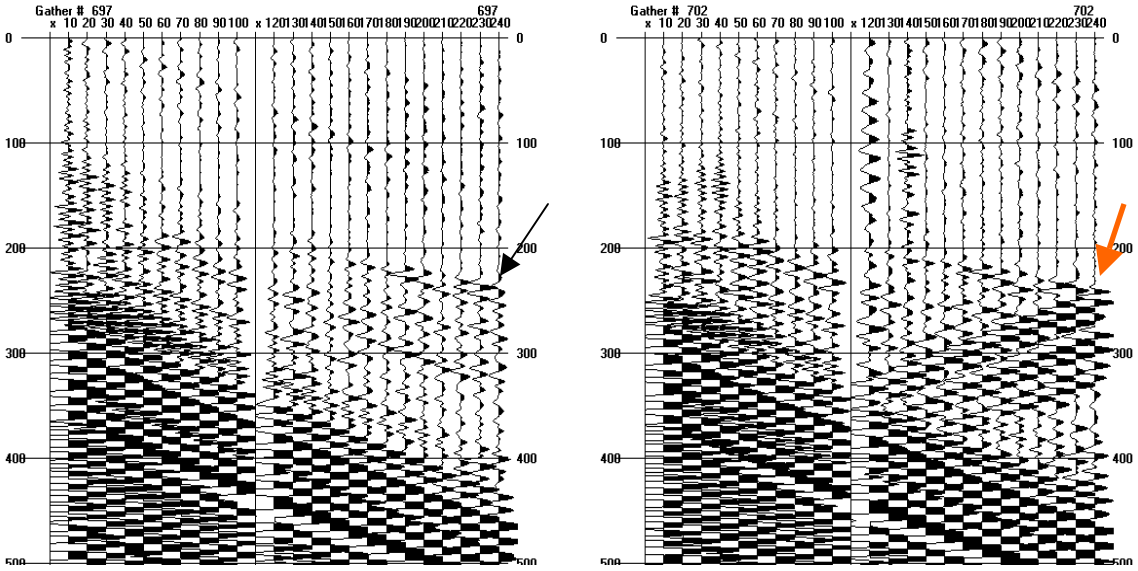

Figure 53. Uphole/VSP survey conducted in Colliver #16. → Indicates first arrival of seismic energy from source at hydrophone 2270 ft below ground. → Reverse energy is tube wave bouncing off weight hanging from bottom of cable carrying hydrophones.

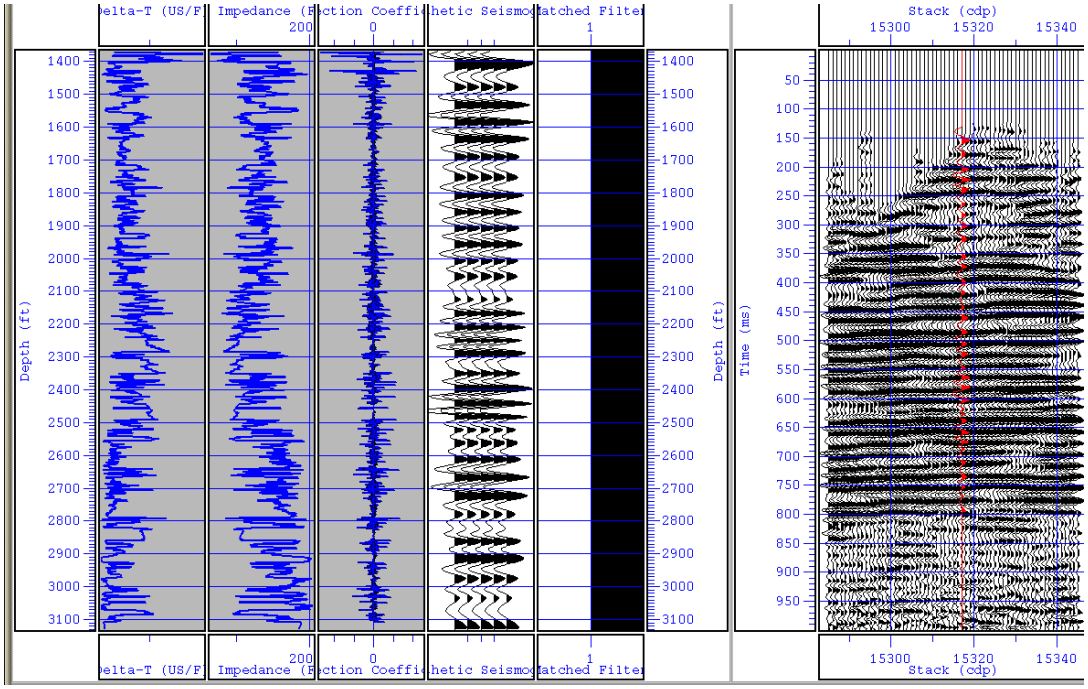

Figure 54. Synthetic seismogram generated from a sonic log from CO2I#1 convolved with a Klauder wavelet. The tie between the synthetic and real are outstanding at these lower frequencies. As spectral enhancements are complete the dominant frequency and resolution will increase significantly.

A 3-D seismic volume produced for the baseline survey provided an excellent look at preliminary data quality. At this very early stage of the data processing, reflection events looked quite good and only lack some of the sitewide coherency generally associated with seismic data from this depth interval and in this part of Kansas. However, considering the excellent data quality evident on shot gathers and with improved velocity analysis and statics, these data will provide the necessary quality to test the effectiveness of low-cost, minimal-deployment 3-D to monitor CO_2 injection from both the enhanced oil recovery and sequestration perspectives.

Using the time-to-depth conversion extracted from the downhole survey conducted in #16 (Figure 53), it is possible to bulk time-correct the synthetic seismogram (Figure 55) for the normal inaccuracy in absolute time resulting from estimating overburden velocity. As usual, these errors range from less than a percent in areas with an abundance of ground truth to as much as 10 percent when no other information but the sonic log is available to help estimate replacement velocities. Using local well data only, the L-KC interval was estimated to be at a time depth of around 535 msec. Incorporating the VSP and manual wavelet-correlation techniques, the actual arrival time of the top of the L-KC on seismic data is around 548 msec. Using the VSP for the first-arrival information alone more than justifies the expense of getting these borehole data. Correlations between borehole and surface seismic are critical to accurately defining the wavelet

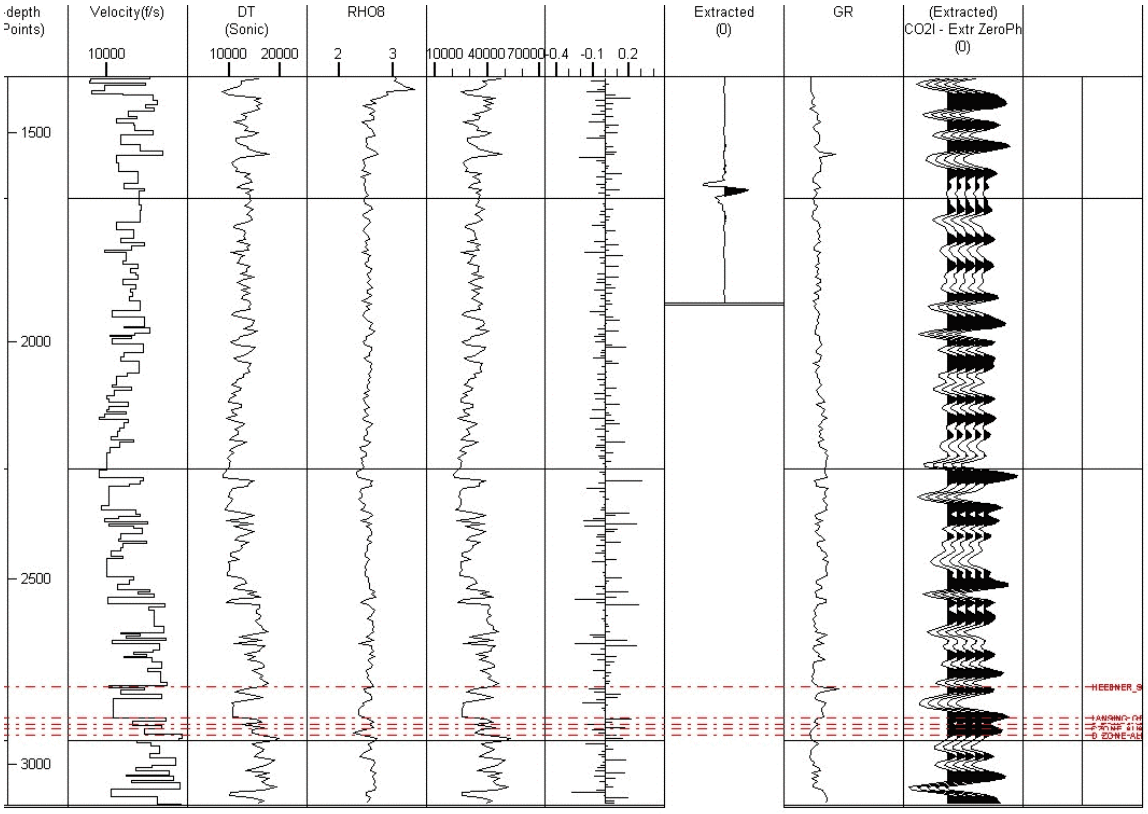

Figure 55. Synthetic seismogram generated by extracting source wavelet from cross-correlation of synthetic and ground force. L-KC interval is clearly indicated by complex doublet waveform. Once time-corrected the L-KC reflection will begin at around 548 msec.

returning from the L-KC. Considering the producing interval, and therefore the interval the CO2 is being injected into, is only 15 ft thick and equates to just a little more than 1 msec, it is imperative to identify the L-KC reflection within a few tenths of a percent.

A time slice taken at 560 msec possesses subtle variations in reflection amplitude around this site (Figure 56). These changes in amplitude are likely indicative of changes in properties within the interval imaged. Considering the 'C' zone is just a little more than 1 msec thick, an accurate velocity model was imperative to detailed analysis of subtle amplitude variations.

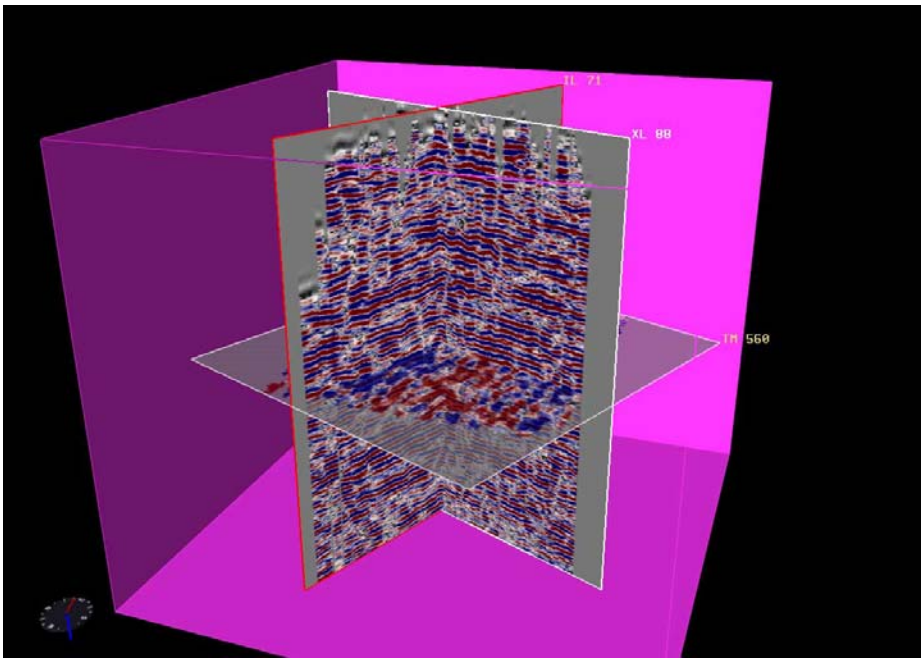

Figure 56. 3-D display with cross-line and in-line sections and a time slice at 560 msec.

Over the period June 23-July 1 the third monitoring 3-D seismic survey was conducted to obtain a snapshot before the flood began a WAG (water-alternating-gas) program.

Preliminary Processing and Interpretations of Baseline and First Two Monitor Surveys

Design of the receiver and shot grid was based on azimuth, offset, bin squareness, fold distribution, and equipment (Figure 57). Using the actual shot and receiver locations occupied, it was possible to improve slightly some of the grid characteristics. In particular, the fold distribution could be improved at the expense of centralization of midpoints within the bins. By rotating the grid slightly (Figure 58), the fold uniformity improved by almost 20% with only a minor increase in midpoint scatter within the bins as evidenced by the spider plots showing azimuthality and midpoint location (Figures 59 and 60).

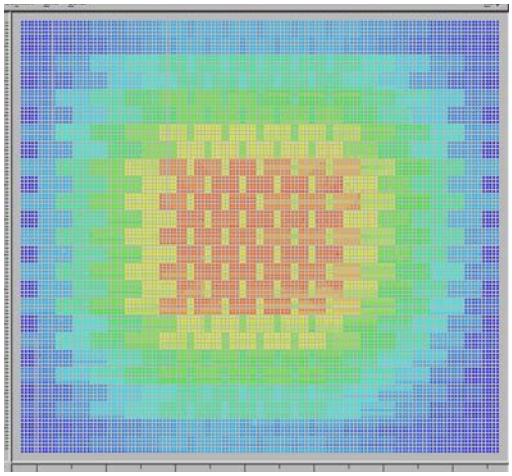

Figure 57. Fold map of grid (red-24 fold; yellow-20 fold).

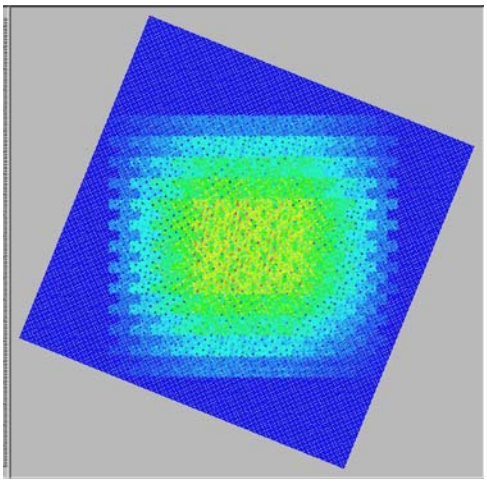

Figure 58. Grid rotated 112º.

Rotating the grid 112º (Figure 59) retained the squareness of the 10m x 10m bins and dramatically improved the fold distribution. With every compromise comes a negative and for this improvement in fold distribution, midpoint scatter within the bins increased. This scatter was evident in the spider diagram (Figure 60). Even though this increased scatter in midpoint centrality was not an improvement, its effect on the overall detectability of the CO_2 front should be negligible and therefore had no impact on the objectives of this research program.

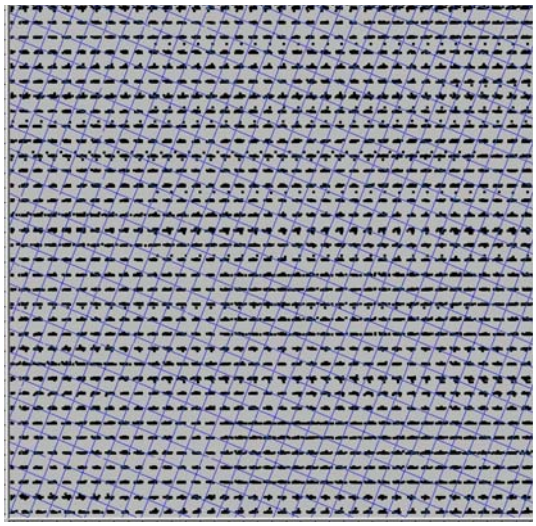

Figure 59. Midpoints and associated rotation.

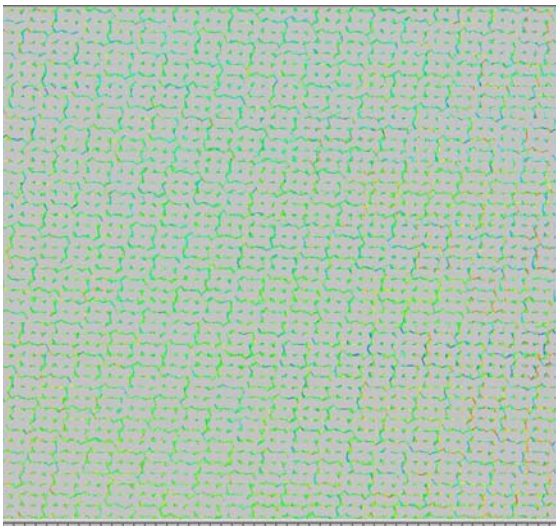

Figure 60. Spider diagram; midpoint azimuth.

Even at this early stage in the project, post-stack processing of the seismic volumes provided results that are both encouraging and somewhat unexpected. Significant early pre-stack processing problems related to long-offset NMO stretch, multiples, statics, and reduced resolution for far offsets have been, for the most part, overcome. CMP stacked volumes now possess excellent coherency, with a well defined and detailed velocity function, and near-surface static problems have been all but eliminated (Figure 61). Improvements in the processing flow and parameters are still being made, but the

data are ready for preliminary interpretations, including some first-order attribute analysis.

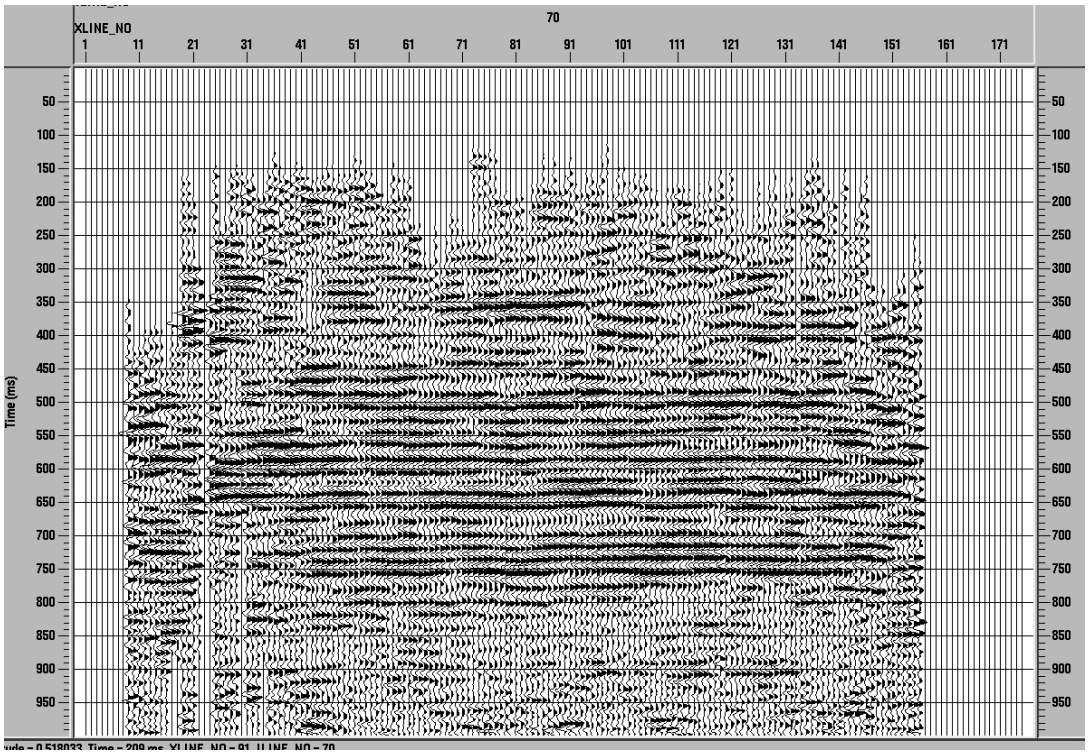

Figure 61. 2-D CMP stacked section extracted from 3-D volume of the second monitor survey. Reflection coherency is very good. Improvement in bandwidth and coherency of shallower reflections will be the primary focus of the next round of processing enhancements.

Synthetic seismic data derived from sonic logs taken in wells CO2I#1 and #16 provided essential ties between time on seismic sections and depth on borehole logs. Preliminary correlations between synthetics and real data have been excellent, with convincing matches between the real and synthetic seismic data in proximity to CO2I#1. Once the higher frequency reflections are enhanced and the dominant frequency moves over 100 Hz at the target depth, final synthetics will be produced allowing identification of the L-KC "C" to an accuracy of around one sample or 10 ft.

Key to many seismic analysis techniques and essential for attribute analysis is the preservation of amplitude, frequency, and phase of the reflected signature. All contributions from the seismic source and noise sources must be reduced as much as possible and ideally eliminated. The reflection signature left on CMP stacked sections must have characteristics that are as closely related to the reflected interface alone as possible without contributions from source, near surface, or background noise (both random and periodic). Considering the comparatively close offset range of interest for these relatively shallow reflections (by industry standards), a significant amount of ground roll and air-coupled wave was removed during processing, leaving some CMP bins with very low fold for some near offset ranges. Removal of multiples is also an important step for optimizing the analysis of these data, because changes in reflection characteristics related to the presence of CO_2 in comparison to reservoir fluids are small (~2-20% percent).

These data have undergone an extensive series of noise reduction steps to maximize the signal-to-noise ratio and statics/velocity corrections to improve coherency (Figure 62). More work needs to be done to verify that key attributes (phase, frequency, and amplitude) have been preserved up to this point in processing.

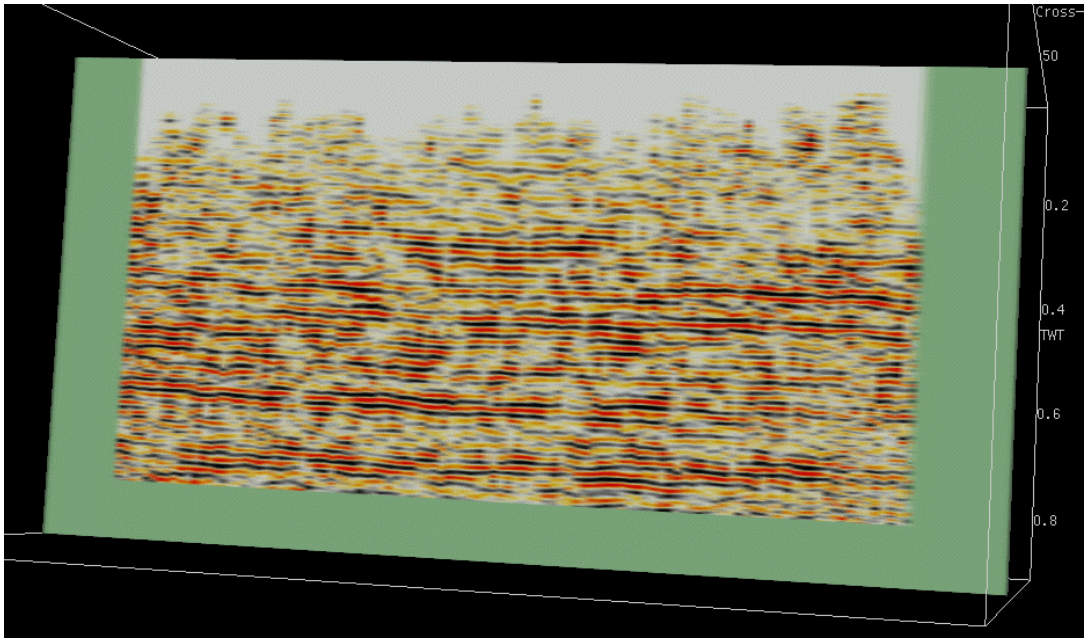

Figure 62. 2-D slice of 3-D volume with wiggle trace amplitudes represented in color. Coherency is quite good, but work is still underway to insure true amplitudes have been preserved through all processing steps. A few amplitude anomalies resulting from previous work eliminating noise can still be observed on this section.

Instantaneous attributes are measurements of specific seismic properties at an instant in time. Measurements of this type are only reliable and useful in extracting meaningful geologic characteristics if all phase and amplitude information is preserved during processing. Multiples and random noise limit the accuracy of interpretations derived from instantaneous attributes.

Given the areal size of the site, it is important to consider the horizontal resolution of the data in interpretations of map view representations of instantaneous attributes. Using the Fresnel zone as the basis for establishing horizontal sampling size on a layer, at 2,900 ft below ground surface for the observed frequencies the radius of the Fresnel zone (generally assumed to be the wavelet sampling size) is approximately 350 ft. Bin dimensions for these attribute data are approximately 30 ft x 30 ft with a unique value for each cell that includes variable contribution from the surrounding 50 or so cells or ~5 cells away in any direction. Therefore, even though the greatest contributions to each cell's value are from rocks within that cell area, nearby rocks outside the bin influence this value to some degree. Interpretations of patterns or textures must consider the overall sampling size of the wavelet and how far from the cell changes in rock property contribute to the overall signature.

In this document well locations are based on conversions from legal descriptions assigned during the permitting process when the wells were initially drilled. Therefore exact plotted locations relative to this DGPS (± 0.25 m) seismic grid could be in error by 50 ft or more (up to several cells). DGPS locations of the wells were obtained following the third survey and will be utilized in future analysis but are not shown in the figures here.

Interpretation of the seismic response, particularly for reservoir properties and fluid property changes, involves analysis of numerous attributes of the seismic waveforms returning from the subsurface and specifically from the single wavelet (peak and trough) that sampled the L-KC "C" zone. With only the uphole data from #16 available (synthetics and VSP are not fully developed yet) for time-to-depth correlation of reflections with reflectors, it is not yet possible to confidently identify the exact wavelet returning from the L-KC "C." When the synthetics are fully developed and confidently matched with the real data, the exact reflection horizon corresponding to the "C" zone will be mapped and attribute analysis will be performed specifically on the "C" zone reflection. Analysis to date has identified a zone or layer 24 msec (100 ft) thick, which includes the horizon of interest. Preliminary post-stack analysis of the seismic time-slice calculated to contain the "C" zone has been performed to investigate and uniquely identify any changes in response within this volume between the baseline and the subsequent two monitor surveys.

Instantaneous amplitude (amplitude constant-time slice) is the most intuitive of the instantaneous attributes; it provides a measure of reflectivity that represents a map view of seismic amplitude changes. In the case of these 3-D seismic volumes, an instantaneous amplitude time slice provides a general measure of layer structural/depositional topography more than reflectivity, assuming the velocity along the time slice does not vary significantly. From well data within the 4-D seismic area, the L-KC "C" zone exhibits approximately 35 ft of relief between a low near Colliver #6 and high near Colliver # 8. Structurally, Colliver #5 and #6 (west end of survey area) are drilled into lows and Colliver #16, #13, and #8 (eastern end of survey area) are all in a relatively high area. In general, these changes in elevation measured in the well bores are consistent with the amplitude trends on the 560 msec amplitude time slice (Figure 63). Considering this is a time slice and not a horizon map, variations in color are most sensitive to movement of the wavelet up and down in response to changes in reflector depth with only minor contributions from changes in layer reflectivity. Correlation between L-KC "C" elevation and amplitude values is excellent. Work continues trying to map geological/ rock-property discontinuities using seismic continuity/similarity volume attributes, which highlight geological discontinuities potentially affecting CO_2 movement through the reservoir.

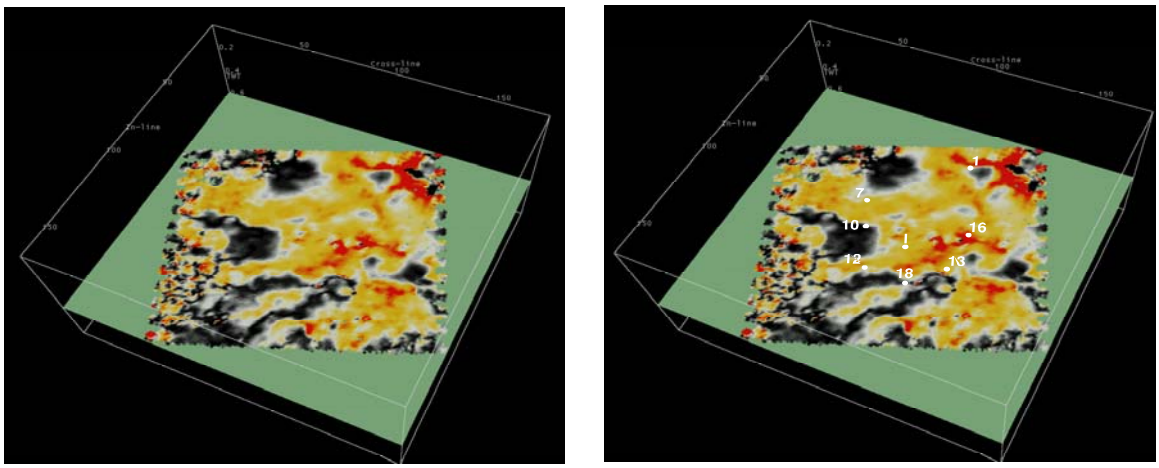

Figure 63. Color representation of amplitude values along the 560 msec time slice. Dark areas are relative lows and reds are structural highs trending into yellows representative of intermediate depths.

During final data analysis many different visualizations will be necessary to interpret the subtle changes expected from replacement of reservoir fluids (oil and water) with CO_2. In-line and cross-line seismic sections are used to calculate various seismic attribute volumes and provide the anchor for studying changes in key time slices and horizons throughout the volume. This analysis approach provides the 3-D visualization utilized to track CO_2 movement and geological spatial extent of structural, stratigraphic, and lithologic seismic signatures (Figure 64). Data coherency and uniformity in amplitude characteristics are excellent throughout the interval of interest. Processing to date has focused on the 400-to-700 msec time/depth window. As is evident on shot gathers, many reflections were recorded both shallower and deeper than this interval, and these extraneous reflections will be the target of enhancement processing once the preliminary analysis is complete on the principle zone of interest.

Preliminary processing of the first three surveys (baseline and two monitor) has provided crude time lapse analysis and shows changes between the baseline survey and the two surveys obtained after CO_2 injection began in December 2003. Some of these changes in seismic response can be interpreted to relate to changes in reservoir properties. As noted, with only the uphole data from #16 currently available for time-to-depth correlation of reflections with reflectors, it is not yet possible to confidently identify the exact reflection wavelet that has returned from the L-KC "C." However, a zone or layer 24 msec (100 ft) thick has been selected that includes the horizon of interest. Since the zone of interest (L-KC "C") is only 15% of the total thickness (15 ft of the 100 ft thick time slice) being analyzed, and the change in reflectivity associated with the fluid change from water/oil to CO_2 is expected to be less than 20%, changes in seismic properties resulting from the presence of CO_2 should be less than 4%. A change in the seismic response this small is at the detection limits of this thick slice analysis technique. It is therefore imperative for accurate interpretation that the exact horizon of interest be identified and analysis be focused on that interval.

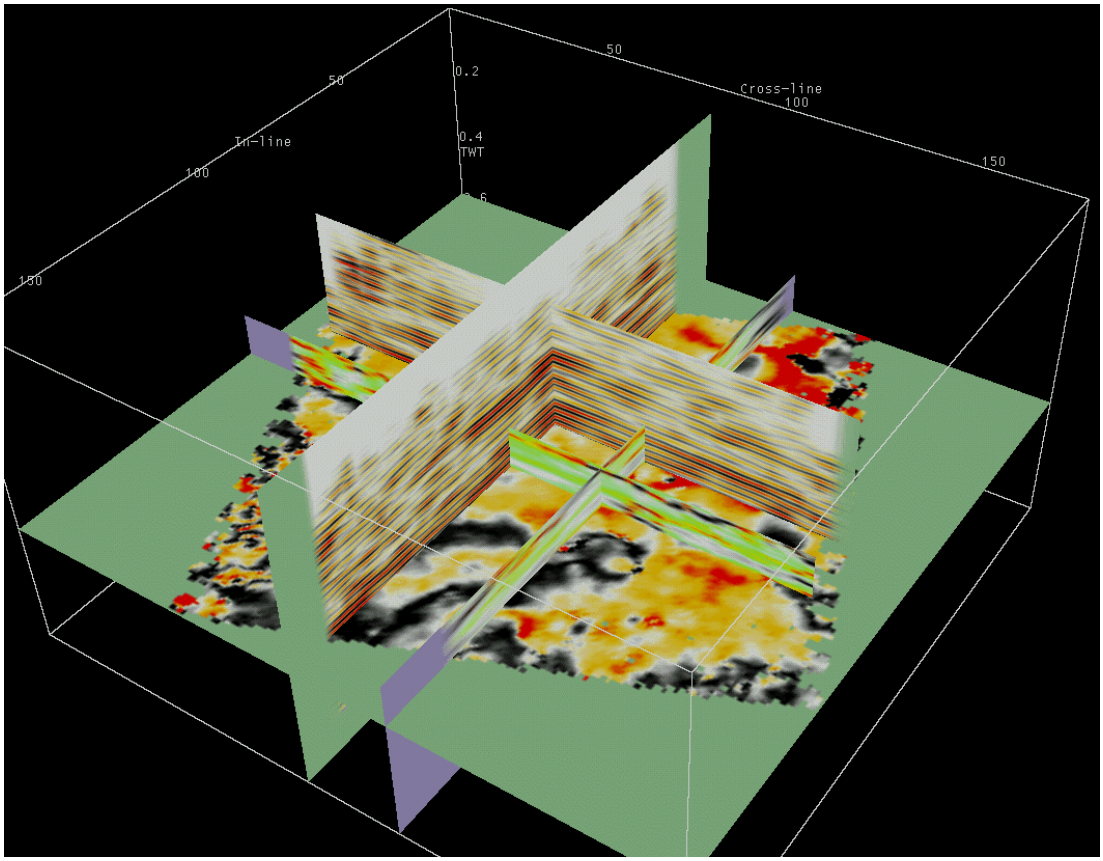

Figure 64. Vertical cross-line and in-line color wiggle trace displays intersected by the 2-D time slice from near the L-KC "C" interval. Correlating the time slice with reservoir tops as defined by well logs results in an excellent match between structure and amplitude. Reds are structurally higher than yellows, which are then higher than the blacks. Average instantaneous frequency in-line and cross-line sections (low is green and high is red) for a sub-volume around the target zone is shown.

A critical processing step that has yet to be performed on these seismic data is equalization. Ground conditions—and therefore coupling and velocity—change over time, resulting in data differences related to what is happening on the ground rather than in the ground. Even with the extreme care taken during acquisition to insure all equipment, parameters, and station locations were identical between surveys, minor changes in surface conditions between the different data acquisition campaigns affect each data set differently. Therefore, corrections unique to each survey data set must be made to reduce and hopefully eliminate surface effects that vary with climate from subsurface effects. After equalization, characteristics of resulting data sets can be directly compared and differenced data sets can be used to highlight CO_2 movement. It is important to note that since the data equalization processing has not been completed some of the differences observed between surveys are likely from changes in surface conditions and not changes that occurred in the subsurface.

Instantaneous frequency (IF) analysis was performed on the 24 msec-thick seismic volume. IF is an attribute sensitive to the temporal change in the continuity of seismic events, specifically; it is sensitive to waveform characteristic changes resulting from velocity and/or thickness variations in a thin layer. In general terms it can be

considered a measure of seismic spectral attenuation within a rock layer. IF plots by nature tend to have a high degree of variability. Although lateral changes in rock lithology are detectable using IF analysis, numerous different kinds of lithologic changes can produce IF features or anomalies and it can be difficult to interpret the nature of the lithologic change responsible. Because IF is more sensitive to noise and changing patterns of noise than most other seismic attributes, it is advisable to use the multiplicity/ redundancy of 3-D seismic sampling for a spatial averaging-extraction strategy, thus reducing the percentage of noise-related random variability in IF. This study has the benefit of multiple time-lapse images of the zone of interest. Changes in IF "texture," or the development of unique patterns on time-lapse images, may provide a good indication of small fluid composition changes within the layer itself, particularly when it is spatially continuous and consistent in a 4-D sense. As noted, these surveys are not equalized, and considering this analysis technique is especially sensitive to noise, changes in color patterns or textures on these plots can be partially a function of data equalization issues (changes in the near-surface not fully compensated for during processing or changing patterns of noise).

Parameters selected for displaying the IF plots were optimized for the baseline survey data (Figure 65). A specific color scale tuned to minimize the expression of variability while enhancing differences across the time slice was selected for all displays. Using this approach, coherent changes in IF that develop over time should be evident. Considering the expected change in seismic properties with the 24 msec time slice as a result of a change in fluid composition from water/oil to high-pressure CO_2 for the seismic volume being analyzed is less than 4%, as much visual enhancement as possible is important. Again, noting that some differences may be related to equalization and pressure changes in the pattern, development of consistent patterns or local changes in texture are likely indicators of CO_2.

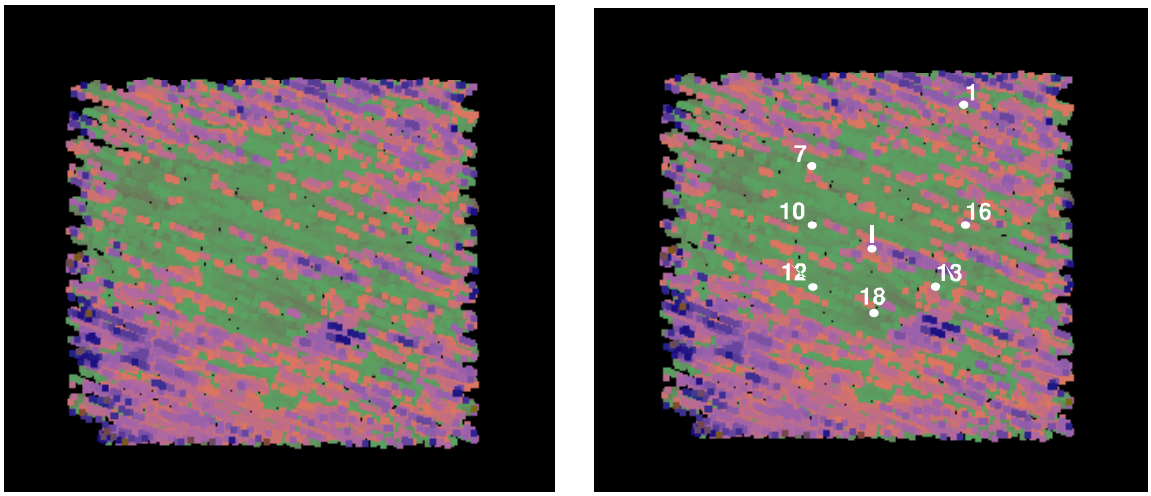

Figure 65. Baseline Survey—Color representation of instantaneous frequency for a 24 msec-thick slice at a depth of around 560 msec for the baseline 3-D survey conducted when the field was fully pressurized with water and just prior to the first injection of CO_2. Well locations (coordinates based on conversions from legal descriptions) are placed to improve spatial awareness of the key locations around the field.

An obvious northwest to southeast grain is evident in the IF plots. This grain is the result of rotating the grid 120° during processing to improve the distribution of subsurface samples. Values in each cell are independently calculated from CMP traces within that cell only and are in no way influenced by CMP traces gathered within adjoining cells. Therefore, the discrete, blocky character of the displayed data is a result of the receiver line orientation (trends along inline direction) and rotation of the seismic bins.

Some sense of the lithologic trends potentially influencing the performance observed at the various wells can be gained by comparing and contrasting apparent boundaries and changes to the texture of specific seismic properties across the site. In making these observations keep in mind that both the amplitude and frequency attribute plots (Figure 66) show response changes for seismic volumes representing an interval of rock over 100 ft thick that includes the subsurface interval of interest. Thus some of the data characteristics observed may be from overlying and underlying beds, or changes in the "C" zone may be subdued by consistent seismic response from overlying and underlying beds. A prominent feature evident in both plots is a contrast in properties north and south of an east/west trending line (A) lying immediately south of well #18 (Figure 66). This trend (A) marks a substantial change in seismic character on both amplitude and frequency plots and may indicate the presence of a structural feature or an abrupt change in rock properties. Another lineament (B) follows a high (red) trend on the amplitude plot and an anomalous group of cells on the frequency plot. This feature, though subtle on both plots, is interpreted to exhibit sufficiently high contrast to represent a marked change in rock properties of some kind. A third more subtle northeast/southwest trending lineament (C) marks a change in texture on the frequency plot and an apparent alignment of anomalies on the amplitude plot. Because of the greater sensitivity of instantaneous frequency to lateral lithologic changes in comparison with instantaneous amplitude, it seems likely this (C) lineament may be related to a lithologic change. It is unlikely the (C) lineament would have been interpreted from amplitude plots alone.

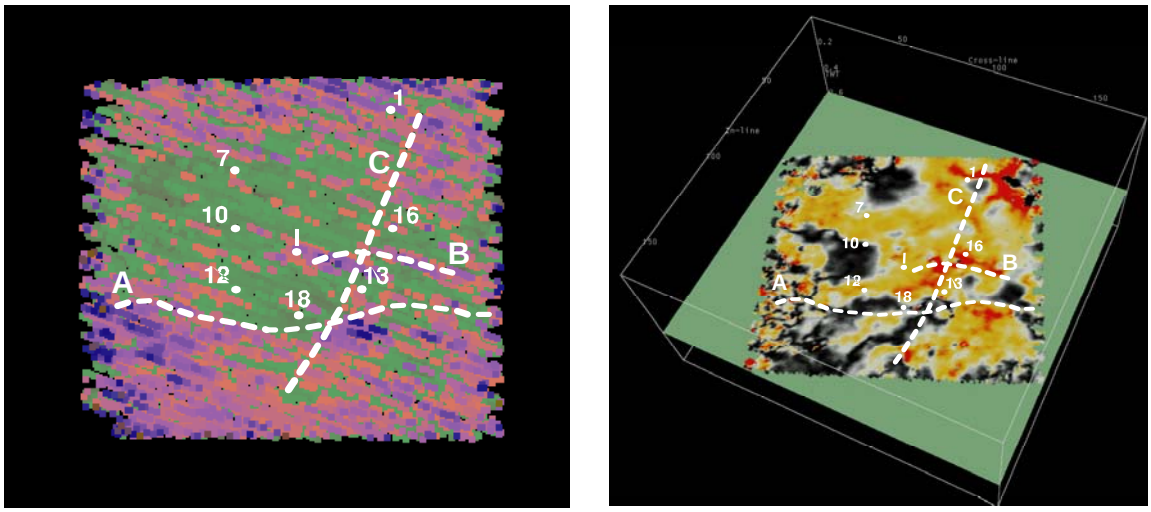

Figure 66. Baseline Survey—Lineaments based on changes in data character or texture were interpreted on baseline data from 24 msec time slices at around 560 msec. These lineaments are interpreted identically on both lines—instantaneous frequency (left) and amplitude (right).

Analysis and comparison of the baseline and first and second monitoring surveys show changes in instantaneous frequency within the study area (Figures 65, 67, and 68). Because of the thickness of the seismic volume, equalization, and IF response issues, interpreting these data at this stage will be limited to identification of areas where changes occur between surveys. All significant changes observed in these data are generally within an area defined by wells number 12, 18, 13, 16, 7, 10, and 1 (Figure 69, "b" or right side). Comparing and contrasting the two monitor surveys with the baseline survey, changes in IF can generally be grouped in one of four ways: 1) similar change in both monitoring surveys, 2) change in the first survey not evident on the second survey, 3) change in the first survey and a different change in the second survey, and 4) no change in the first survey but change in the second survey. The third monitoring survey obtained June 23-July 1 will provide a further examination of the consistency of changes in different areas. Definition of the LKC "C" zone wavelet will also refine changes.

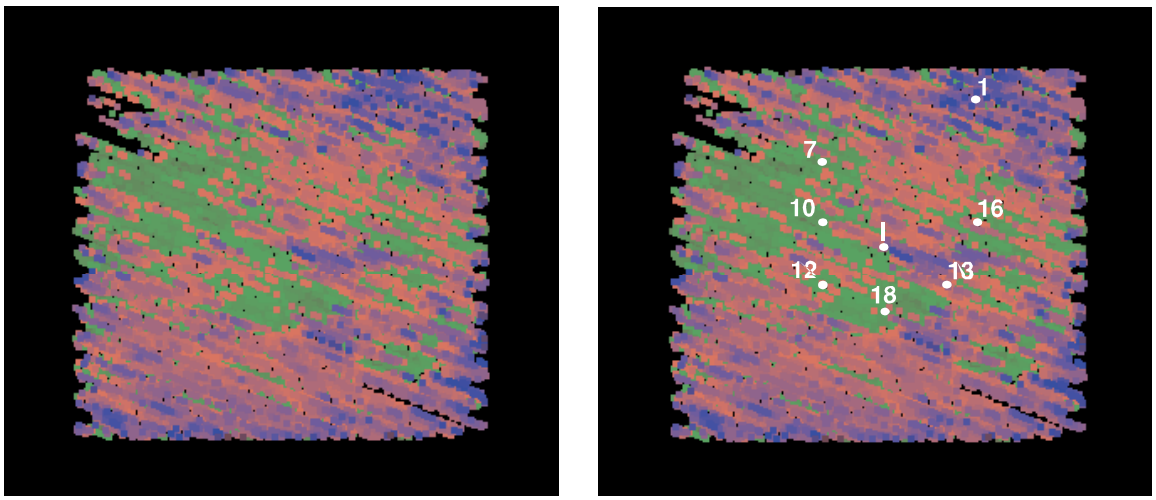

Figure 67. First Monitor—Instantaneous frequency plots of the first monitor survey using an identical color scale as used on the baseline (left). Well locations are estimated from conversion of legal descriptions, so some inaccuracy exists in their locations (right).

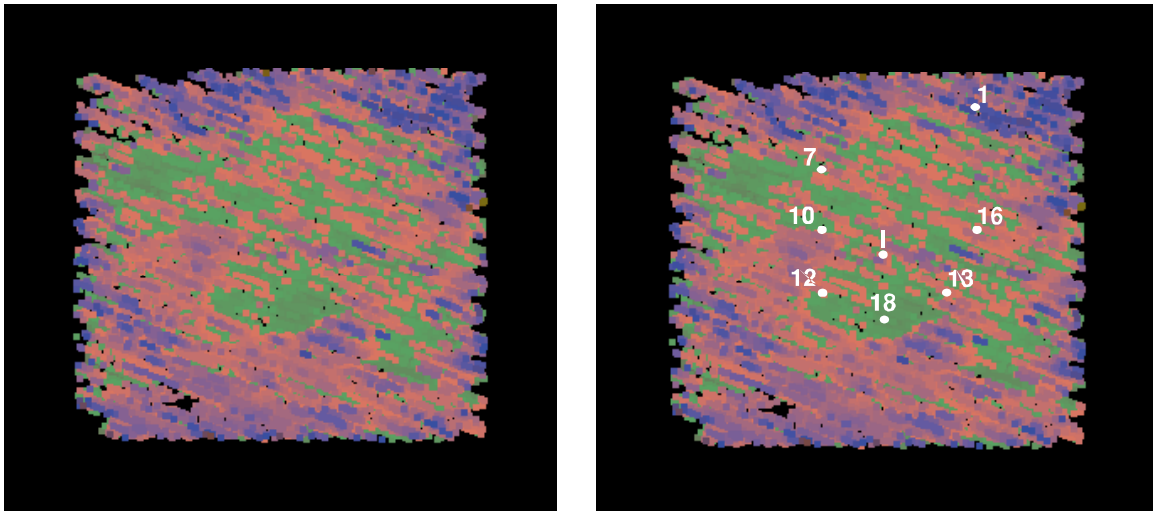

Figure 68. Second Monitor—Instantaneous frequency plots of the same 24 msec time slice as displayed for monitor survey one and the baseline survey. Color scales and well locations are identical for all IF plots.

The evident changes in texture for the general CO_2 pilot region compared to outside the flood region lend support to the idea that changes are being detected. However, interpretation of the causes for the differences observed between the monitor surveys is not yet clear nor is the size of the area of change in the subsurface compared to the seismic response fully resolved (Figure 69). Volumetric analysis precludes the possibility that change observed in the entire region shown in Figure 69 represents significant CO_2 invasion. Assuming CO_2 was flooding only a 1-foot thick interval with the CO_2 displacing only 33% of the oil/water in the pores, the change observed only in the northeastern quarter may be due to CO_2 invasion at the time of the first monitor survey (Figure 69 Bb). However, this would require that CO_2 moved along a focused region or arc and did not move radially out into the formation from the CO2I#1. Insufficient CO_2 volume was injected at the time of the first monitor survey to affect the entire area simultaneously. However, seismic response will noticeably change with a small percentage change in saturation of CO_2. As well, considering the size of the Fresnel zone, "fingering" will appear enlarged on seismic data. Depending on the geometry of the "fingering," seismic images could easily represent thin zones of higher CO_2 saturation that are moving through the reservoir.

In general changes on the monitor surveys relative to the baseline survey are predominantly north of CO2I#1 (Figure 70). Changes are evident south of CO2I#1 but they appear less coherent as a mass and seem to generally increase in areal extent on the second survey relative to the first. When considering the extremely small percentage change expected in seismic properties of the L-KC "C" for this study, changes from one monitor survey to the next on these particular preliminary analyses might not be numerically consistent. Areas consistently changing rather than consistent change relative to the baseline survey are the targets of the seismic attribute analysis at this point in the interpretations.

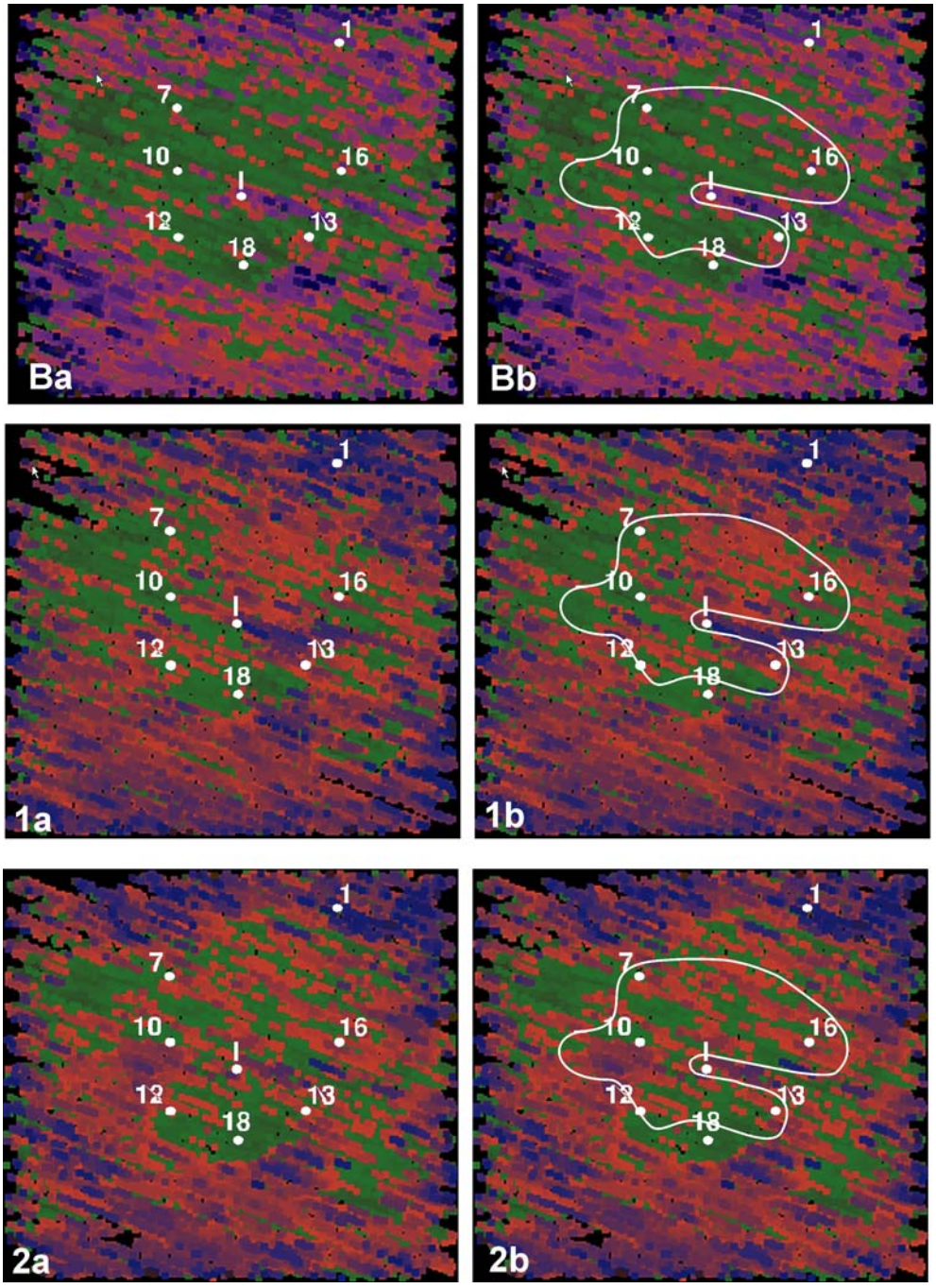

Figure 69. Comparison of baseline (B), monitor 1 (1), and monitor 2 (2) IF plots with wells located (a). The area highlighted possessed notable changes in data character, intensity, and/or texture between the three surveys. Changes between surveys are not necessarily consistent due to a variety of reasons (equalization, changes in reservoir, etc.), but the changes observed within the highlighted area seem to suggest that as the CO_2 has progressed the subsurface in proximity to the injector is experiencing changes.

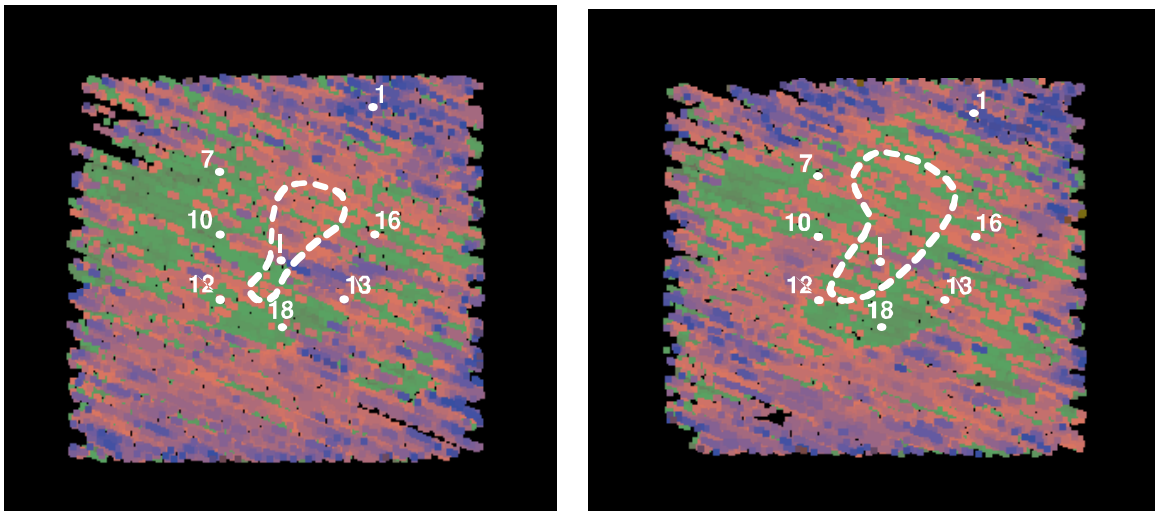

Figure 70. Monitor survey one (on left) and monitor survey two (on right) with the areas possessing the greatest and most consistent change relative to the baseline survey outlined with a dashed line. These areas of greatest change are not necessary numerically consistent with each other, but they do, from a relative perspective, contain the set of cells that define the greatest overall relative change.

Seismic Data Acquisition: Monitor Survey Three

With initial CO_2 detected in Colliver #12 near the end of May, this third monitor survey provided an important snapshot for reconstructing the time-lapse path CO_2 has taken through the field from injector to producer. Based on pre-injection models, progression of CO_2 from injector to producers as well as the volumetric expansion of the CO_2 slug was expected to preferentially move toward Colliver #12.

This third survey was delayed a few weeks until after wheat harvest, avoiding significant damage to the wheat crop being grown on about one-third of the survey area. On June 25 the wheat harvest was completed. An unusually rainy June also delayed acquisition by several days. Ground conditions were ideal for receiver coupling immediately after harvest with only wheat stubble left in the fields (noise from wheat moving with the wind was all but eliminated) and because of the 3+ inches of rain that fell the week before the start of the third monitor survey (Figure 71). A negative aspect of these ideal receiver conditions was the softer-than-previous ground conditions, which with a vibrator source reduces the efficiency of the energy transfer process.

Surface conditions changed between the end of March and end of June surveys. Geophone planting conditions were very similar while surface activity and associated noise was quite different. Noise from cattle and farm equipment provided new challenges to data acquisition and processing. Cattle were penned away from the receiver lines but we were still close enough to be a source of noise on the northernmost receiver line (Figure 72 left). This third monitor survey was scheduled as soon as possible after the second monitor survey while avoiding wheat harvest, rain, and the plugging of Colliver #2 (Figure 72 right).

Figure 71. View looking west showing vibrator sweeping in the wheat stubble field surrounding the CO_2 injection well. Colliver #12 is visible on the horizon to the left of the vibrator in this picture. The CO_2 injector is enclosed in a yellow steel protection fence and can be seen immediately behind the vibrator, in the distance. Combines completed cutting wheat from this field just days before this picture was taken.

Figure 72. Noise sources and unique acquisition obstacles change with each survey and the seasons. (left) Cattle in the pasture immediately north of the CO_2 injector. (right) Colliver #7 pumping in the foreground and Colliver #2 being plugged in the background.

Ground and weather conditions were ideal during the first several days of acquisition. With over three inches of rain falling days prior to the deployment of receivers, planting and coupling conditions were very good and better than expected for this area during this time of the year (Figure 73 left). Geophone locations were DGPS surveyed to be within a few centimeters of previous geophone locations. Because the wheat had just been harvested the cables could be laid quickly through the stubble with ATVs, reducing the extra care necessary on previous surveys to minimize damage to growing crops (Figure 73 right).

Figure 73. Geophones were planted (left) in a 0.3 m equilateral triangle centered on the DGPS-located station. Weatherproofed reinforced Ethernet cables stored on spools (right) connected the eleven 24-channel Geometrics Geodes to the NZC seismic controller. These cables were deployed using a custom cable handling system.

Shot gathers from this survey were of similar quality to those from the previous three surveys (Figure 74). Wind was light and variable with speeds not exceeding 15 mph. Noise from the fixed sources (pump jacks, pipelines, and power lines) is evident as on previous surveys. Vehicle noise on county roads was random, but was overall equivalent in volume and frequency to previous surveys as well. Unique to this survey was the noise from cattle movement near line 1 and the combine harvesting wheat on June 25 near the east end of lines 3 and 4. Contributions by both these noise sources, new to this third monitor survey, were minimized due to their non-stationary nature and the collection of four-sweep vertical stacks at each station.

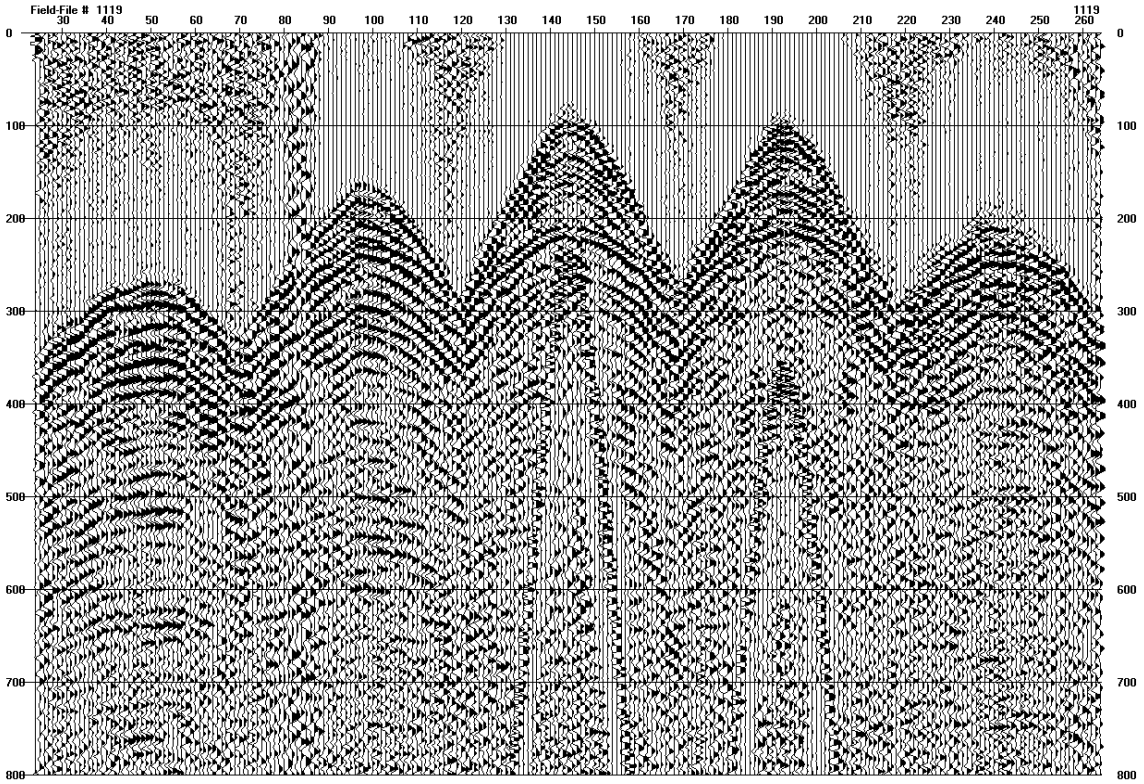

Figure 74. A single sweep from near center of the receiver spread. This shot gather has been scaled to enhance reflections within the 2500 to 3500 ft depth range. Reflections from the L-KC "C" zone will arrive

between 550 and 650 msec across this spread. This range of arrival times is directly related to source-to-receiver offset and associated non-linear increase in travel path with source-to-receiver separation.

An apparent dominant frequency of around 120 Hz at 1,000 ft and 60 Hz at 3,000 ft was increased by 50% at 1,000 ft and doubled at 3,000 ft during processing using spectral balancing techniques (band-limited spiking deconvolution). Vibrator ground force was around 12,000 lb at 60 Hz, decreasing linearly to around 6,000 lbs at 200 Hz. Spectral properties of the recorded data were controlled by the source energy spectrum (power as a function of frequency) and the natural attenuation of higher frequencies by the earth. With large dynamic range recording systems and minimal background noise, low amplitude signal at higher frequencies were enhanced to some degree relative to the more dominant lower frequency recorded energy.

Data quality on this fourth survey (third monitor survey) was not quite as high as on the previous two monitor surveys. Considering the efforts taken to insure exact duplication in equipment and parameters, this difference was clearly related to the ability of the ground surface to accept and propagate seismic energy (Figure 75). The noticeable enhancement in coupling between receivers and the ground was likely due to the substantial rainfall that preceded the survey. Unfortunately the softer ground conditions that resulted from the rain adversely affected energy transmission by the source into the ground. Ground force curves, as calculated using the baseplate and mass accelerometers, were consistent with previous surveys, while the recorded energy levels at the receivers were down. The difference was clearly related to the saturated nature of the upper 1 ft of soil in this area.

Figure 75. November survey (upper left), January survey (upper right), March survey (lower left), and June survey (lower right).

Data acquisition for this third monitor survey required eight days with an additional two days of land surveying to relocate receiver stations after wheat harvest was completed and cattle were put out to graze across part of the survey area. An additional day of surveying was necessary to exactly locate the wells within the survey grid. With another almost two inches of rain falling the night after the final sweeps were recorded for this survey, small footprint, low ground-pressure vehicles kept the equipment free of excessive mud and avoided damage to farm fields and pastures (Figure 76). Equipment was picked up and the site secured in a day.

Figure 76. With almost two inches of rain the night after acquisition was complete, the six-wheel drive ATVs were instrumental in picking up and transporting cables and phones back to the semi-trucks where they were loaded for transport back to Lawrence without "rutting" the farmer's fields and pastures.

Data Processing

Processing data from each of the different surveys followed as near the same procedures as possible, only changing parameters as necessary to accurately compensate for surface changes and equipment performance. No standardized equalization approach was used, the only changes unique to each survey were in response to variations in statics related to changes in soil conditions. A standard 3-D processing flow was used, minimizing applications that were influenced by data characteristics, and focused on processes that act more uniformly on the different data sets. In general, the last four sweeps at each station were correlated, noise unique to each sweep removed, geometry assigned, and vertically stacked to provide the greatest signal-to-noise enhancement possible. These four-shot vertical stacks at each shot station were then muted to remove first arrivals, air-coupled wave, and ground roll. Prior to binning, these shot gathers were spectrally enhanced through deconvolution and digital filtering. Next the traces from each shot gather were sorted into their assigned bins, corrected to vertical incidence as a result of the different source-to-receiver offsets, and adjusted for trace-specific static irregularities. A variety of other processing operations were tested and some proved beneficial and will be used during final processing. Once the data were appropriately processed, they were CMP stacked to produce a seismic volume.

After production of a suitable seismic volume, any 2-D line can be extracted and viewed as a seismic cross section (Figure 77). In a 2-D format subtle differences in wavelet character can be recognized both horizontally (trace to trace) and vertically (as a function of depth). Because time-lapse techniques are being used on these data, subtle changes in wavelet characteristics are also readily recognizable over time (survey-to-

survey). Changes appearing consistent throughout the time-depth interval on a single survey are likely related to the near surface. However, if changes are observed in reflection wavelets across a limited number of traces and within a small vertical time-depth window on different surveys, it is reasonable to suggest those changes are in response to variation in the rock properties somewhere within the subsurface volume. In some cases changes in seismic signature can be tracked to anomalous zones elsewhere in the section; shadow zones or dim outs are a common example.

Comparing and contrasting 2-D cross line 87 from both the baseline and third monitor (June 2004) surveys, changes in seismic character are evident (Figures 77 and 78). Clearly with a dominant frequency of only around 60 Hz, much is still needed to enhance the higher frequency component of these data present on shot gathers. However, even with this preliminary lower resolution data, a change in the reflection wavelet amplitude is likely related to reflectivity, and therefore the presence of CO_2 is evident. This change in amplitude and wavelet character between the baseline and third monitor survey can be observed across a zone approximately centered beneath X-line 71 and near the top of what is interpreted as the Lansing-Kansas City (L-KC) reflection at around 560 ms. This difference is quite pronounced considering that there has been no interval-specific processing done to these data specifically targeting the L-KC interval and this type of anomaly. Other changes in amplitude can be distinguished between the two surveys, but they are not consistent with theoretical expectation nor do they have a geometry that would lend itself to this kind of change in rock properties.

Careful study of differences between the two vertical slices through the seismic volume reveals other differences below the interpreted top of the L-KC that are not directly related to the CO_2 (there is some possibility that a few of these could be indirect indicators of changes in fluid properties). For example, differences such as beneath X-line 81 at about 650 to 700 ms appear different between the two data sets. However, the depth of this anomalous zone beneath the L-KC (almost 100 ms) and its apparent isolation (that is, vertical connectivity as would be the case for a “shadow zone” related to increased attenuation or reflectivity due to the CO_2) rule out this relative difference between the two surveys as related to the CO_2 invasion. As well, intervals with differences in amplitude between the two surveys such as that visible between about 650 ms and 730 ms beneath station 111 are related to differences in source energy, coupling, cultural and natural noise, and other acquisition mismatches between the two surveys. Some data processing operations will effect slight changes in data characteristics unrelated to reservoir-specific change, as might be the case when noise levels change or soil conditions result in altered reflected wavelets.

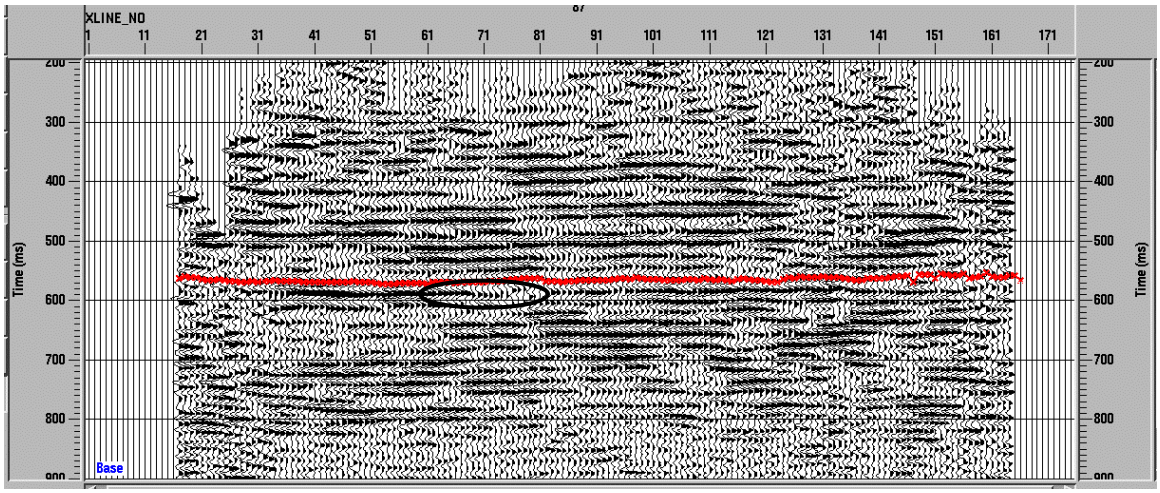

Figure 77. A 2-D slice from the baseline survey during November 2003 with the approximate top of the L-KC interval interpreted in red and an ellipse defining the area immediately below the L-KC appearing to change most dramatically when contrasted with the same 2-D cross line slice of the June 2004 survey.

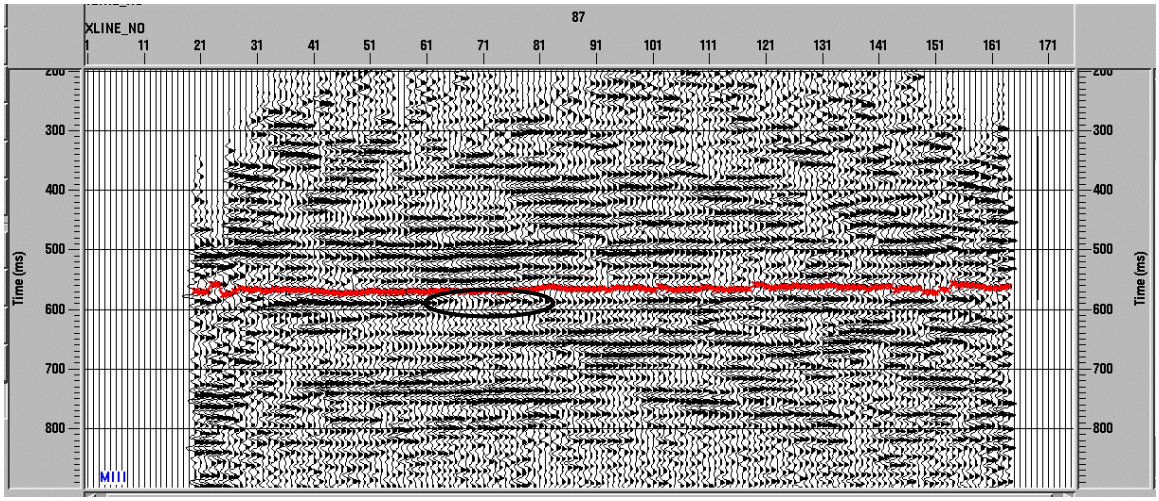

Figure 78. The same 2-D slice as Figure 77, except from the third monitor survey acquired in June 2004. As with the equivalent 2-D cross line slice, the approximate top of the L-KC interval is interpreted in red with an ellipse defining a zone where a marked change in reflection character can be observed between the baseline and third monitor survey.

Analysis

Seismic Modeling and Rock Physics

In this thin-layer pilot case study, it is essential to take into consideration that complex seismic responses to change in seismic velocity introduced by variations in pore fluid composition and therefore rock properties are similar to the apparent "velocity change" due to thickness change. Seismic modeling of a thinning layer (Figure79) indicates that seismic amplitude may increase or decrease depending on whether thickness increases render layer thicknesses less than or greater than half the dominant seismic wavelength. We therefore took notice that the CO_2-related amplitude dimming might be weakened or enforced by thickness-related effects, depending on the region of thickness variability.

Nonuniform pore-fluid acoustic-property changes resulting from associated changes in reservoir pressures and facies within the pilot study area (pressure changes ranging from 11.7 - 106 N/m2 [1700 psi] at the injection well to 2.7 - 106 N/m2 [400 psi] near wells 12 and 13) and the associated continuum of CO_2 proportions in the pore-fluid composition significantly complicate calculations of the effective pore-fluid properties, generalized over the entire flood-pattern. Consequently, we have attempted to get an approximate bulk snapshot of the effects of pore-fluid composition changes.

Gassmann's relations can be used to estimate rock-bulk modulus change for the two (effective fluid) pore-fluid compositions in proximity to the injection well. For our case, the two-fluid composition includes the combination of oil-water and miscible CO_2-oil-water (Figure 80).

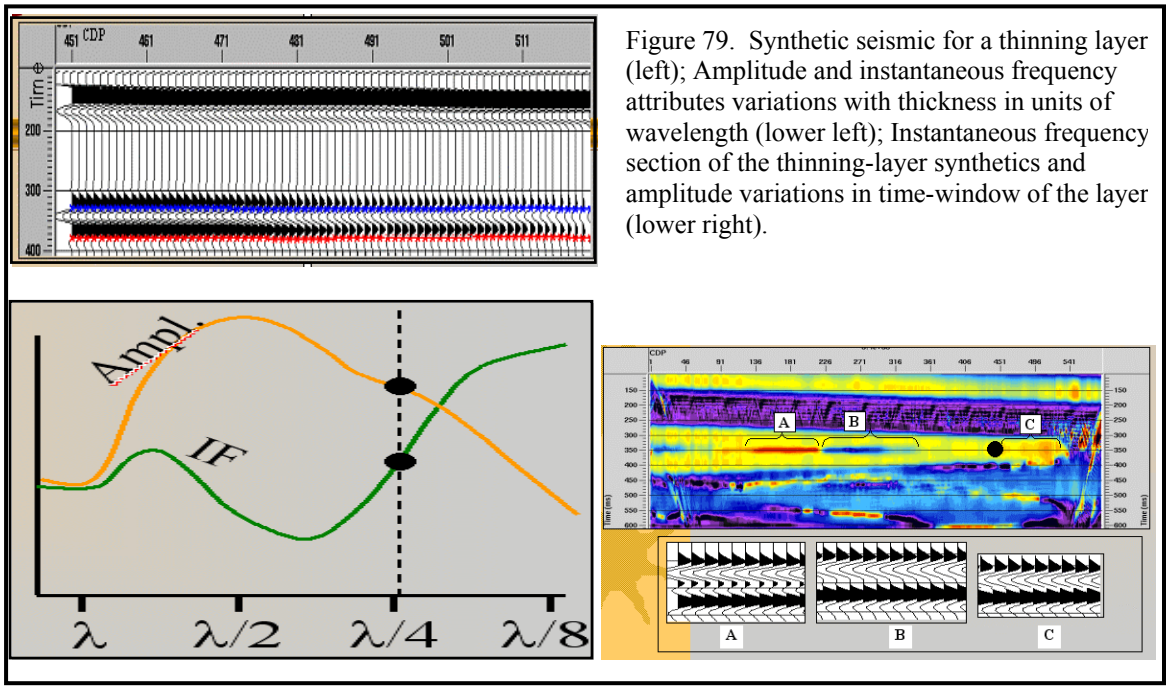

Figure 79. Synthetic seismic for a thinning layer (left); Amplitude and instantaneous frequency attributes variations with thickness in units of wavelength (lower left); Instantaneous frequency section of the thinning-layer synthetics and amplitude variations in time-window of the layer (lower right).

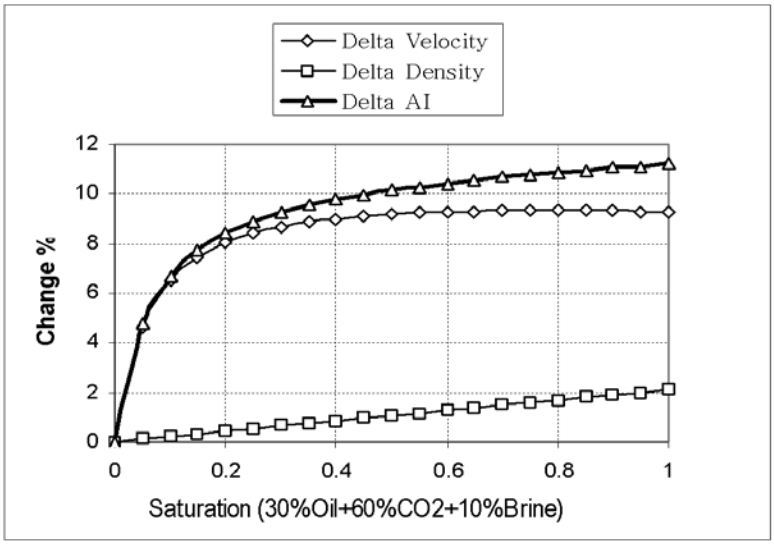

Figure 80. Gassman modeling. Percentage of property change equivalent to effective fluid (30% Oil + 60% CO_2 + 10% Brine) compared to 100% (30% Oil + 70% Brine) (pressure of 11 Mpa and temp. of 35°C).

Unlike many carbonate reservoirs where significant facies changes can occur over very short distances, the relative lateral uniformity of petrophysical and lithological properties in the target oomoldic limestone interval should allow the use of Gassmann's type of fluid-replacement modeling. CO_2-induced acoustic-impedance changes of up to 11% are expected based on these calculations.

Amplitude Envelope Attribute Analysis

Instantaneous frequency attributes provided a gross image of the areal extent of the CO_2 early in the program (previous web updates). With the need for horizon-based interpretations and a higher resolution image of the CO_2 plume as it expands across the site, a more detailed processing flow involving reflection specific enhancements and amplitude analysis was initiated. After the horizon interpreted as the L-KC "C" was identified on all 3-D seismic cubes (baseline and first three monitor surveys), the amplitude envelope attribute was calculated for the L-KC horizon. Amplitude envelope or reflection strength seismic attribute was selected because of its insensitivity to small phase shifts. This is especially important for this data set because the vibrator used for this study was not phase locked; minor variations in wavelet phase should be expected from survey to survey and shot to shot. Seismic reflection data for this study are all recorded uncorrelated, providing the opportunity during the later years of this study to apply phase compensation filters prior to correlation. This will allow defensible comparison of phase-sensitive attributes in the future.

Amplitude envelope falls in the category of instantaneous attributes, which are based on the complex trace concept. A complex trace *F(t)* is given by:

$$F(t) = f(t) + jf_{\perp}(t) = A(t)e^{j\theta(t)}$$

Where $f(t)$ = Real trace data, $f_{\perp}(t)$= Hilbert transform of real trace (quadrature trace), $A(t) = |F(t)| = \sqrt{f^2(t) + jf_{\perp}^2(t)}$ = Amplitude Envelope or reflection strength, and $\theta(t)$= Instantaneous phase. Those complex trace attributes provide instantaneous and quantitative description of seismic waveform.

Average amplitude envelope is phase and frequency independent and more stable in terms of susceptibility to noise contamination when compared to many other seismic attributes. Those characteristics, besides the intrinsic property of being instantaneous, suggest that the average "median" amplitude envelope may be a robust candidate for time-lapse studies and enable a higher level of tolerance to imperfection in cross-equalization practices. For our application we used a "median value" of five samples around the time horizon. From analysis of synthetic examples, amplitude envelope has proven to be one of the most tolerant and robust properties to noise-effects and phase fluctuations.

PPB Interpretation Technique

Considering the necessity to image a weak (in the vicinity of background noise) EOR-CO_2 change, it was essential to apply an interpretation approach that avoided differencing time-lapse (TL) data or attribute with the corresponding baseline data or attribute. Our approach uses parallel progressive blanking (PPB), color balancing and

color focusing of both baseline and TL amplitude envelope attributes, and analysis of resulting textural differences (Figure 81). With the PPB method of interpretation, no differencing is applied; PPB is applied to both the baseline and the TL-amplitude envelope maps, and a comparison/search for TL-textural reservoir signature is carried out. We applied the PPB method to balanced and normalized amplitude envelope maps of one baseline and three monitor amplitude envelope maps.

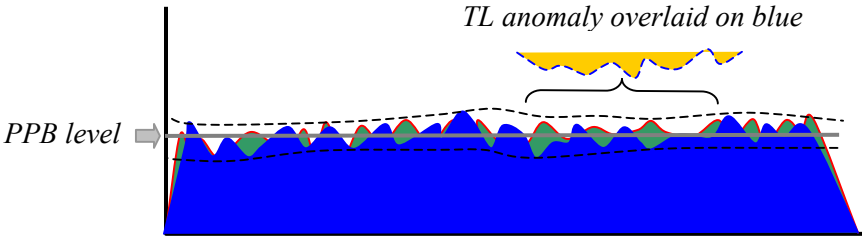

Figure 81. Schematic of the PPB approach of revealing below-background TL anomalies.

The PPB concept is based on the observation that differencing alone does not highlight reservoir anomalies if the change in magnitude of the seismic response is less than the amplitude of non-repeatable background noise. A background color is assigned to all values outside a narrow range within which the full color spectrum is focused to increase the sensitivity to fine details (Figure 82). In so doing, spatially significant textural differences can be enhanced at the highest level of resolution where otherwise the coarseness of the scale would have made these differences indistinguishable from noise. Using PPB, the sensitivity of the seismic signature to changes in the reservoir appears to be far greater than has previously been demonstrated using more conventional approaches.

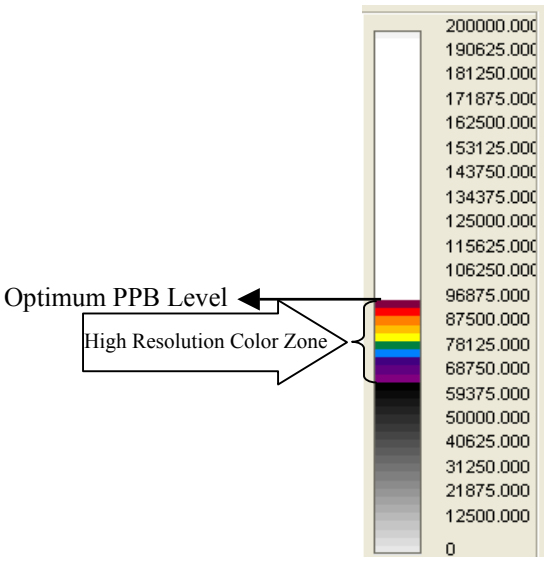

Figure 82. Sample color bar demonstrating how the fine sampled zone of data values can be presented in the highest resolution format possible.

The PPB approach can be illustrated (Figure 81) by placing a very weak TL attribute anomaly over a TL attribute profile from a seismically innocuous area (blue). Based on modeling, the expected change in amplitude from the incursion of CO_2 is very low (below noise fluctuations). A textural interpretation approach is a much more

effective way of distinguishing areas with such small changes in amplitude compared to differencing approaches (baseline survey [green] with a TL dataset [blue]). Delineating weak reservoir signatures by their textural characteristics is effective because of the inherent reduction in sensitivity to background noise and heightened resolution potential of the data.

For this seismic imaging program, PPB proved sensitive to weak time-lapse signatures that otherwise would have been concealed by noise and remnants of balancing/ cross-equalization techniques. These textural differences are relatively stable over a range (two-three color steps) of scanned levels, suggesting their origin is production and/or EOR effects. These observations were verified with production simulation, production data, and consistency in multiple surveys.

As applied here, this newly developed 4-D-seismic interpretation approach allows better focusing of color scales within the critical textural-difference range on time-lapse attribute maps, thereby enhancing apparent resolution within the critical range. Below the temporal resolution in thin heterogeneous stiff reservoirs, signatures of reservoir change are encoded in and interfered with by main events. Contribution of small changes in fluid saturation will manifest themselves as subtle spatial changes in texture rather than monotonically increasing or decreasing horizon attributes.

The PPB method is an alternative to TL-map differencing when targeting low S/N TL anomalies and can be described succinctly using the following expressions:

$$B(x, y) = S_T(x, y) + N_b,$$

where *B(x,y)* is the baseline survey attribute horizon map and a monitor survey (acquired at some later time) attribute horizon map, and

$$M_1(x, y) = S_T(x, y) + S_{TL}(x, y) + N_m,$$

where N_b and N_m are random noise in baseline attributes and TL attributes respectively, and S_{TL} is the change in attributes due to a change in physical properties. The anomaly (S_{TL}) is not distinguishable over the background signal/noise levels on difference maps (B-M_1), when N_b - N_m is equal to or greater than S_{TL}. The extremely subtle S_{TL} imprinted on the S_T, combined with the non-geologic, highly variable N_m results in textural differences between baseline and monitor horizon attributes at "optimum" PPB-level. This textural change is only observable when PPB-levels for the baseline horizon are selected near background levels. Intrinsic with this approach is the need to suppress background noise so a larger color range is available within this critical variability range of TL and baseline attribute maps.

Preliminary Interpretations of January, March, June 2004 Surveys (M1, M2, M3)

With the expected small change in seismic response relative to the change in fluid during the CO_2 flood at the Hall-Gurney field, the utilization of the PPB method for interpretation of the presence of CO_2 is believed to provide accurate results (Figure 80). Because this method does not involve differencing, PPB can be applied to amplitude envelope maps of baseline and monitor data without equalization operations. Unlike differencing, PPB allows more control (determining the PPB range and scale segmentation) on the part of the interpreter, placing a more significant emphasis on matching display characteristics with the geologic setting.

Most data were of good quality, providing an excellent match between seismic cross-sections and synthetic traces (Figure 83). The target seismic horizon (gray) is at about 570 ms two-way travel time and for this project is defined as represented by a peak amplitude value.

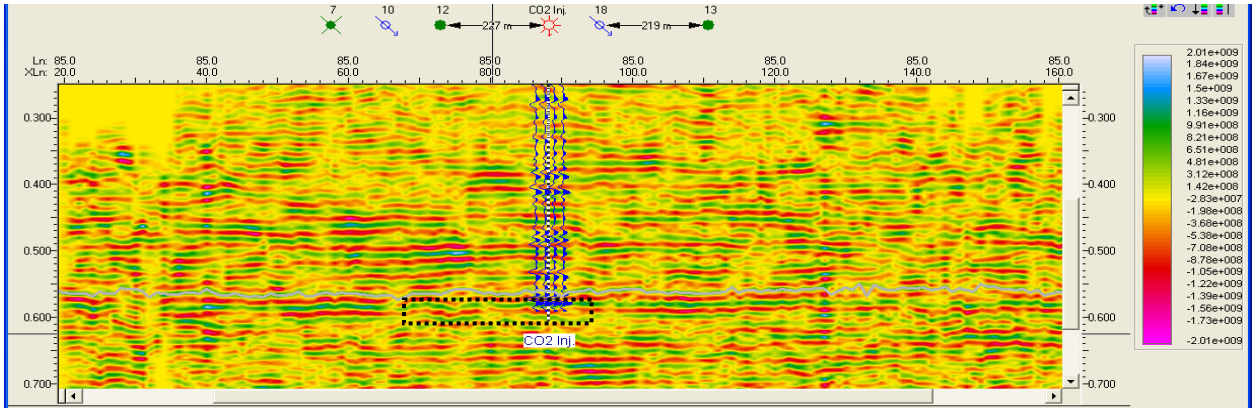

Figure 83. Seismic amplitude section, interpreted target top horizon (gray), and seismic synthetics at well CO2I#1. Gas shadow effect is evident below time horizon in the vicinity of the injection well.

Expansion of the CO_2 plume within the pilot area was successfully monitored seismically and tested against field production data (Figure 84a, b, c, d). Amplitude envelope attribute for the L-KC "C" was extracted from the horizon interpreted independently throughout each seismic volume. Synthetics generated from the sonic log of the CO_2 injection well were a principal guide in consistently identifying the appropriate wavelet. Comparison of the four different amplitude envelope attribute maps of data acquired over an eight-month period clearly shows the subtle nature of the anomaly associated with the CO_2 plume. However, using reasonable constraints on interpretations the affected area can be identified with reasonable confidence for each of the unique TL images.

Flood pressure distribution and consequent CO_2 movement are strongly influenced by the presence of boundaries interpreted to exist in the pilot region. These have been discussed in previous progress reports. Previous field performance and modeling had indicated the presence of a permeability barrier south of well 18. Seismic data clearly show the presence of an anomaly consistent with this production response. A N-S seismic anomaly has also been identified to the east of CO2I#1 and lying between CO2I#1 and well 13. This is discussed below.

Due to the weak signal-to-background seismic response, the boundary of the region identified as having CO_2 is not precise or unique. Given that CO_2 originates from a single location (CO2I#1), it is logical to assume that areas indicating consistent seismic response change, and interpreted to exhibit the presence of CO_2, would be connected with the injection source and exhibit a continuous invasion path from any CO_2-occupied area back to CO2I#1. Regions not exhibiting a continuous connection to CO2I#1, but that exhibit what might be interpreted as a change in seismic response and the presence of CO_2, are assumed to not contain CO_2 but are noted (Figure 84). For the most part, the

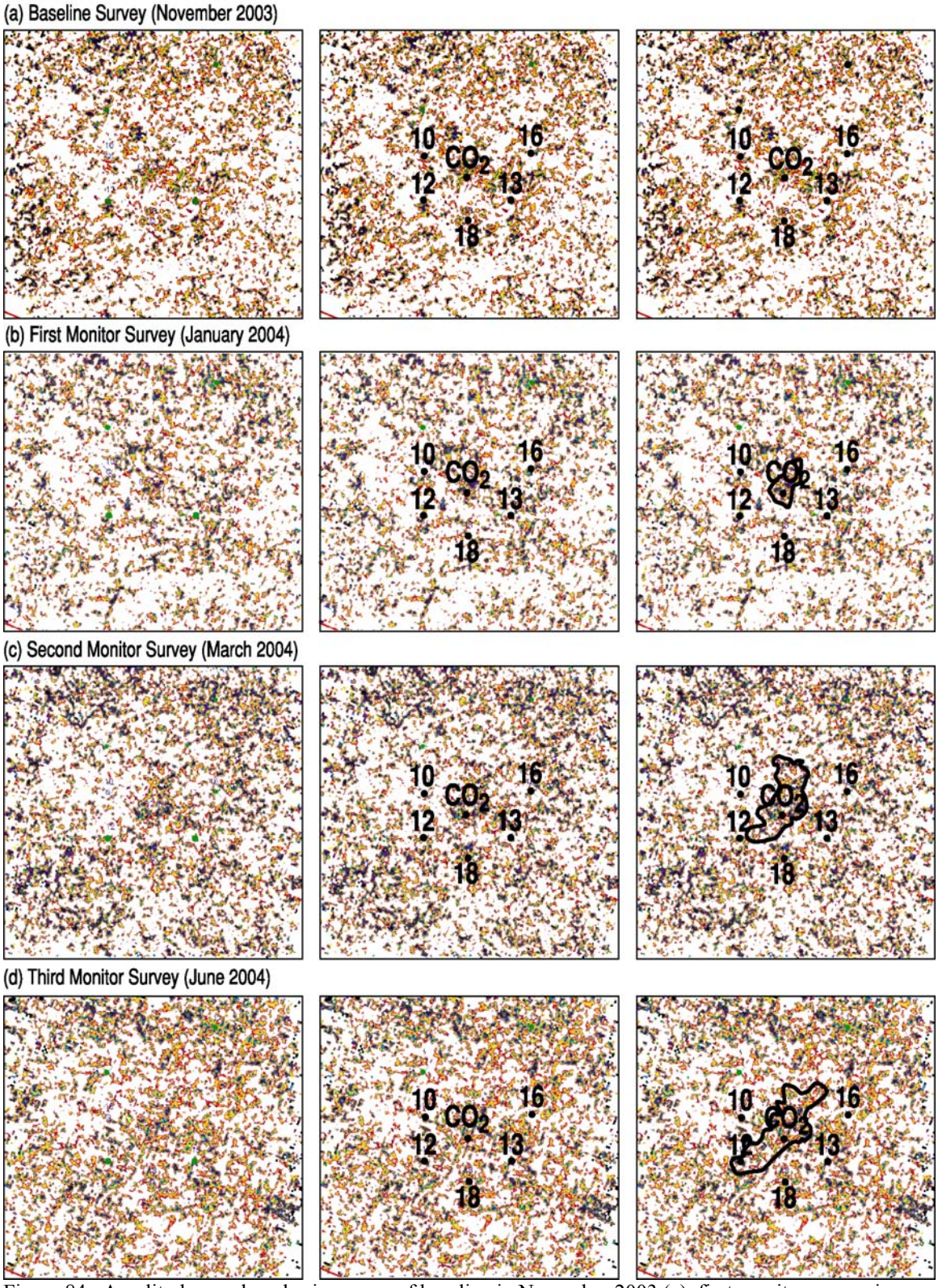

Figure 84. Amplitude envelope horizon map of baseline in November 2003 (a), first monitor survey in January 2004 (b), second monitor survey in March 2004 (c), and third monitor survey in June 2004 (d).

anomalous seismic region interpreted as having CO_2 has exhibited a continuous and contained shape through all the time surveys. To verify how the region identified as containing CO_2 agreed with the material balance of CO_2 volume injected, volumetric analysis based on total injected fluid and mapped reservoir properties was performed to determine the reservoir conditions necessary to obtain the interpreted CO_2 plume size and distribution. Volumetric analysis indicates that insufficient CO_2 has been injected to have CO_2 sweep through the entire thickness of the L-KC "C" zone for the areas defined seismically. However, the interpreted areal extent of CO_2 is consistent with a volumetric model where CO_2 migration is restricted, in some portion of the flood area, to a thin (1-2 ft thick) higher-permeability interval within the "C" zone. This was premised on assumed three-phase relative permeability relationships. This model for L-KC "C" zone permeability distribution vertically is consistent with permeabilities observed in CO2I#1.

Production data are consistent with the interpreted change in the CO_2 plume area. The January 2004 and March 2004 surveys are interpreted to indicate that the CO_2 plume reached well 12 very near the time of the March 2004 survey. Production data recorded increases in CO_2 concentration in well 12 in March 2004. The June 2004 survey interpretation indicates CO_2 approaching well 13 but not reaching the well. Production data show traces of CO_2 reaching well 13 in October 2004.

Seismic mapping of the progression of the CO_2 plume away from the CO2I#1 injector provides a consistent picture of plume development. In addition, observed changes in the CO_2 plume through time are consistent with changes in field injection and production rates (Figure 85).

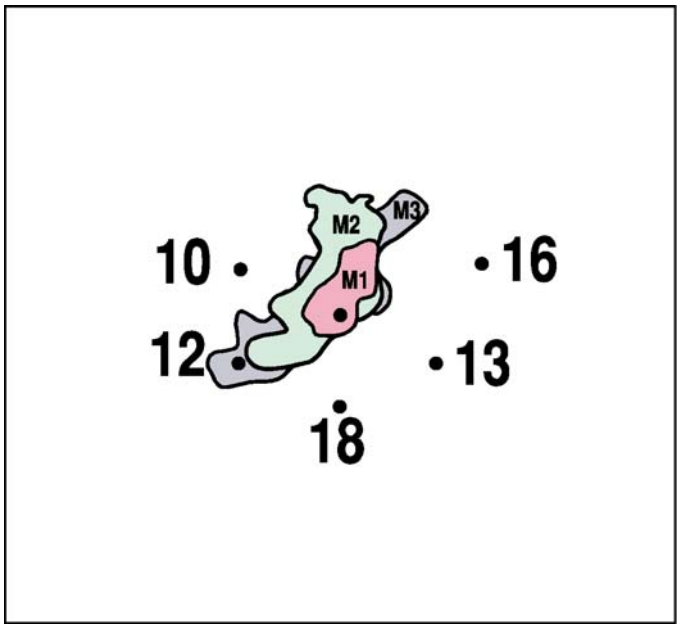

Figure 85. Interpreted boundary of the CO_2 plume based on the first three monitor surveys (January, March, June 2004). Note CO_2 movement toward well #13 only began to occur between the March and June surveys in response to increased water injection in well 7. Also note the northwest appendage evident on the March 2004 survey has receded in response to the increased water injection in well 10.

It is unlikely the area of the reservoir involved in the flood has uniform rock properties considering the geology as interpreted from seismic and well data. Based on ooid shoal geometries, it is not unreasonable to postulate that the seismically interpreted boundaries represent shoal boundaries and a possible tidal channel on the east and therefore, potentially, restrictions to CO_2 flow. Within the flood area vertical and horizontal changes in reservoir porosity and permeability within and between bedsets would be expected to result in non-uniform migration both horizontally and vertically. The interpreted bounding anomalies could be expected to influence areal pressure distribution and CO_2 flow. Differences in permeability within bedsets could be anticipated to result in vertical differences in permeability, as observed in CO2I#1, and CO_2 movement along thin higher-permeability intervals for the distance that the high-permeability bedset extends.

Monitor surveys were acquired at gradually increasing time intervals following the pre-CO_2 injection or baseline survey, acquired in November 2003, with injection of CO_2 starting December 2003. Seismic monitoring of CO_2 movement began with the first monitor survey 6 weeks after starting injection (M1), followed by the second monitor survey about 12 weeks after start of CO_2 injection (M2), then a third monitor survey at 26 weeks (M3), and fourth monitor 42 weeks after start of CO_2 injection (M4; Figure 85).

Movement of CO_2 is a function of injected CO_2 volume and pressure in CO2I#1, injected water volumes and pressures in wells 10 and 18, the production rates and bottom hole pressures in wells 12 and 13, and the distribution of reservoir properties in the flood area. Expansion of the CO_2 plume appears to be predominantly in a northeast/southwest direction (Figure 85). Some CO_2 flooding to the north of CO2I#1 was modeled in reservoir simulations prior to initiation of the flood. However, the northward extent of the CO_2 area defined by seismic response is greater than reservoir simulations predicted. This may reflect more focused CO_2 movement than modeled due to several factors including: 1) restriction of movement to the east in response to the observed barrier; 2) decreased pressure drop to the southeast toward well 13 due to the presence of the barrier; 3) possible enhanced permeability to the north, as indicated by good reservoir properties in wells 8 and 1; 4) under-production early in the flood resulting in movement of CO_2 away from producing wells; and 5) under-injection in well 10 for the actual reservoir properties compared with those modeled resulting in less containment to the north than modeled.

As expected, changes in injection and production rates impacted the movement of the CO_2. An apparent recession of the CO_2 plume between monitor surveys M2 and M3 in the northwest is consistent with the response expected from an increase in water injection rate in well 10 initiated during that time interval (Figure 85).

Seismically, trends in lithologic relationships may be observable on a lineament attribute map of the horizon interpreted as the L-KC “C” (Figures 86 and 87). A strong northeast/ southwest series of lineaments are evident across the entire area. The most pronounced of these lineaments lies between CO2I#1 and well 13 and extends across the entire survey area. Another notable northeast/southwest-trending lineament bounds the

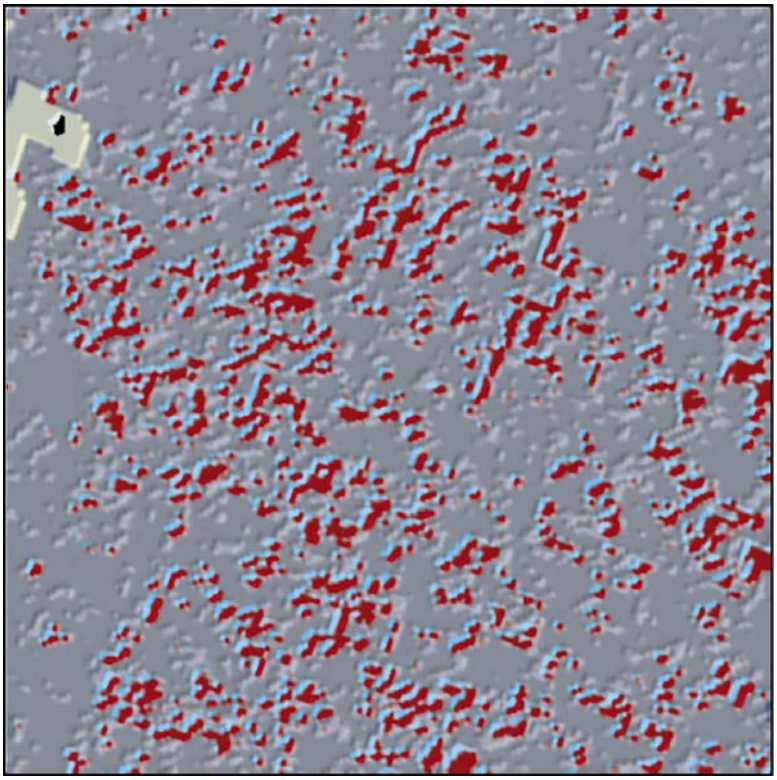

Figure 86. Lineament attribute map. The principal trend is northeast/southwest with secondary trends oblique to the principal trend with an orientation around west-northwest by east-southeast. The principal trends can be traced across the survey area, while the secondary trends are much more discontinuous.

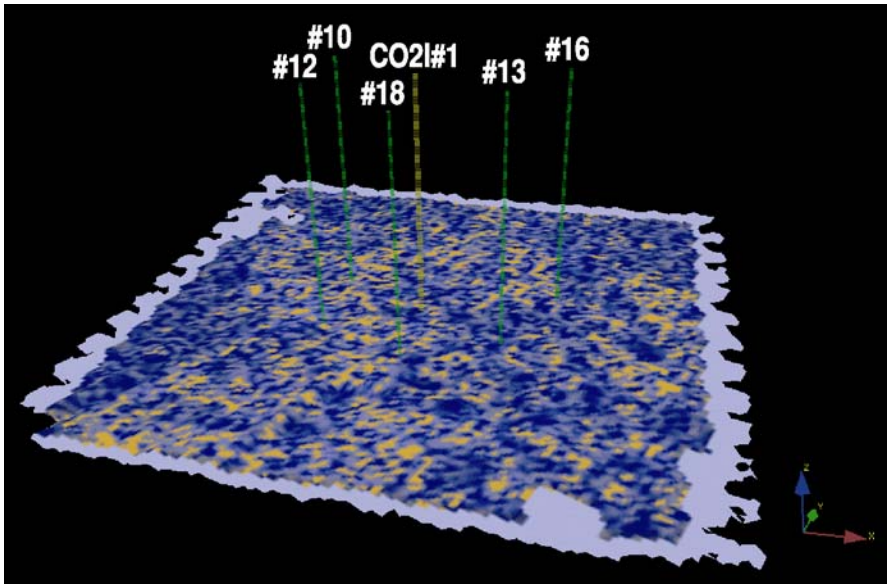

Figure 87. Seismic lineament maps rotated and annotated with well locations. The main trend of lineaments, shown in gold, is NNE-SSW.

western edge of the pilot area. Also evident is a secondary trend of much smaller and more discontinuous lineaments with a more east northeast/west-southwest trend. These are especially pronounced in the northern half of the survey area. The possibility was investigated that these lineaments are a processing artifact representing a byproduct of the receiver and shot lines orientation that after grid rotation during the binning process would have a bearing consistent with that rotation. The orientation of the primary and secondary seismic lineaments is not consistent with the 22° grid rotation. Therefore, these lineaments are interpreted to not represent artifacts of processing or acquisition.

A strong correlation exists between the preferential movement of the CO_2 through this reservoir and features evident on the lineament attribute map. Overlaying the lineament attribute map with the amplitude envelope attribute image provides added support for the suggestion that orientation of rock properties might be influencing fluid movement through this reservoir (Figure 88).

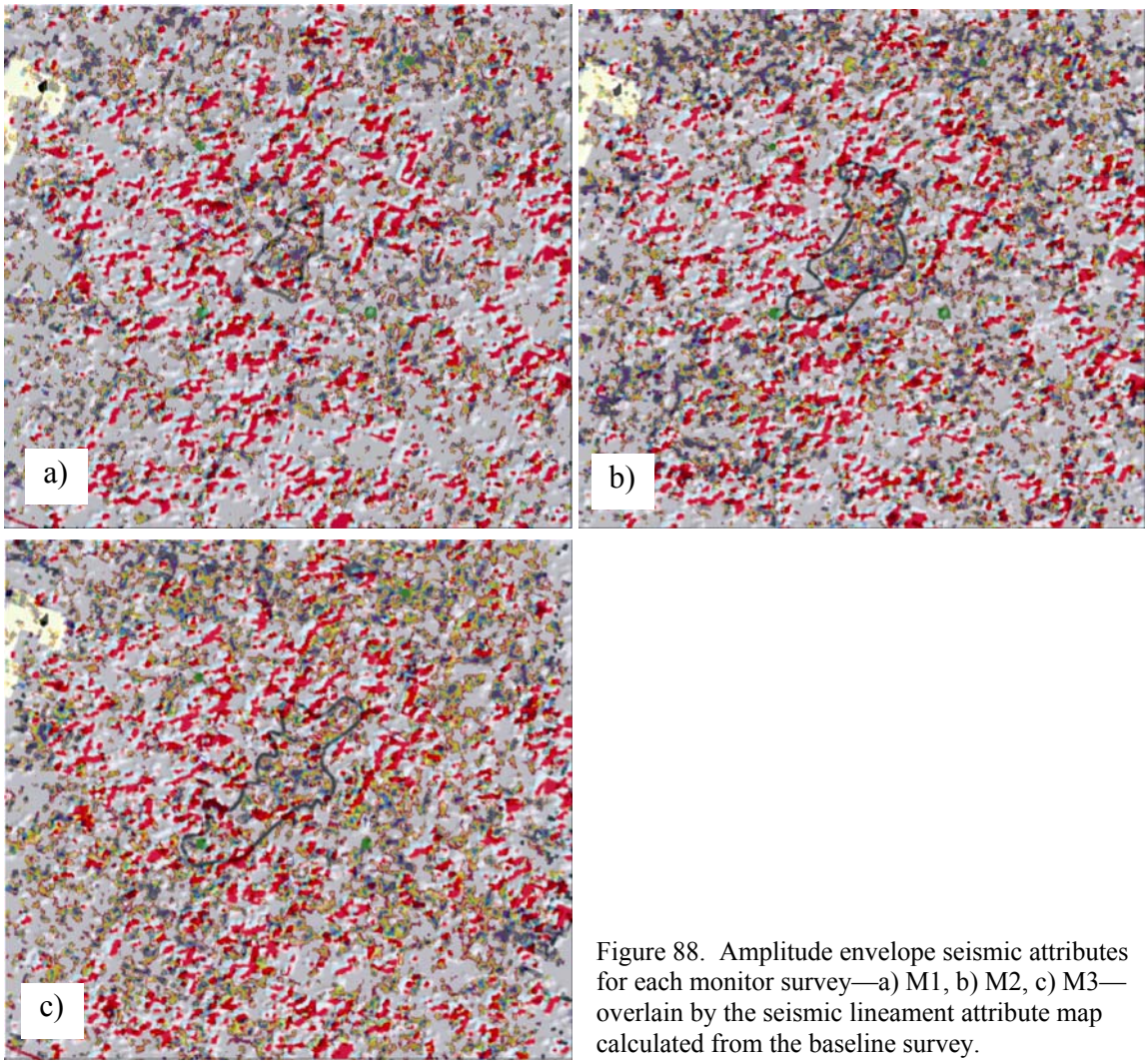

Figure 88. Amplitude envelope seismic attributes for each monitor survey—a) M1, b) M2, c) M3—overlain by the seismic lineament attribute map calculated from the baseline survey.

Of particular interest are the two lineaments that appear to be influencing the expansion of the CO_2 plume at the time of the second 3-D survey (Figure 88b). A generally west-to-east lineament running immediately south of well 12, in conjunction with water injection in well 18, can be interpreted to be diverting the southernmost "tail" of the CO_2 plume from northeast to southwest to move westerly. Under the pressures and fluid present along the southern edge of the CO_2 plume at the time of this survey, this lineament might represent a change in permeability and therefore is effectively channeling the CO_2 in more of a southwesterly direction. A second dominant lineament runs approximately northeast to southwest between CO2I#1 and well 13 and was previously identified on the lineament-only attribute map. At the time of the second survey, the CO_2 plume had only just contacted this lineament southeast of CO2I#1.

Clearly development of the CO_2 plume is strongly influenced by features enhanced on the seismic lineament attribute maps (Figure 89). Comparing each interpreted amplitude envelope map for the three monitor surveys overlain by the lineament map it seems that growth of the CO_2 plume is consistently influenced by several key lineaments it encounters through time and lateral expansion. The two dominant lineaments are easy to identify, but of particular importance are the apparent breaches in the "barrier" as defined by the northeast/southwest lineament. These offsets could represent pathways through this northeast/southwest barrier and would provide CO_2 access to well 13.

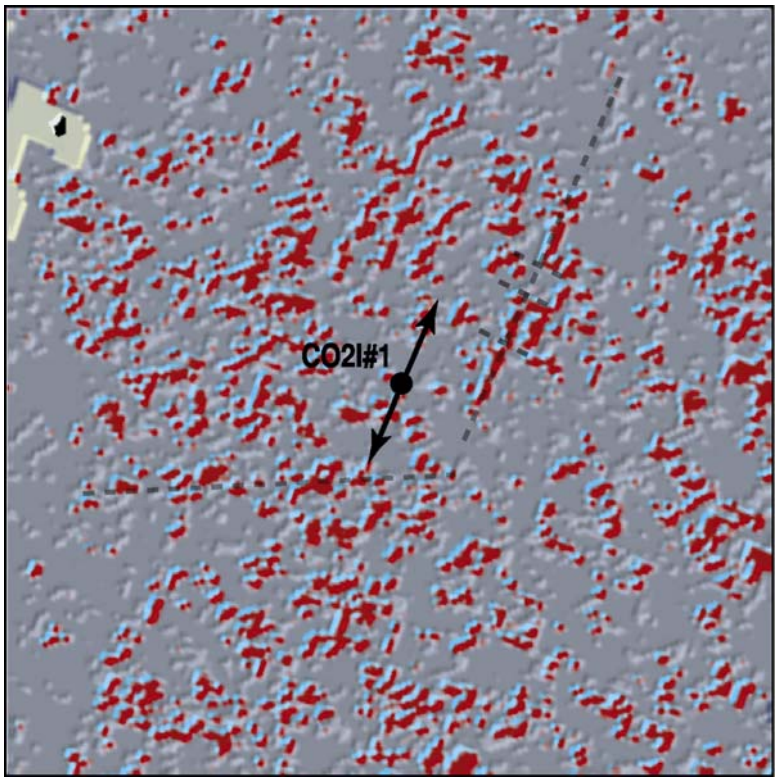

Figure 89. Major lineaments that appear to be influencing fluid movement away from CO2I#1.

The similarity facies attribute map overlain by the L-KC horizon structure map provides a deeper look into possible lithologic explanations for the rate and path of the CO_2 (Figure 90). From the facies map the northeast/southwest directionality of the lithology is evident. Detailed examination shows that the area near well 13 appears both topographically and lithologically different compared to the areas around wells 12 and CO2I#1. This difference may account for the delayed response of well 13.

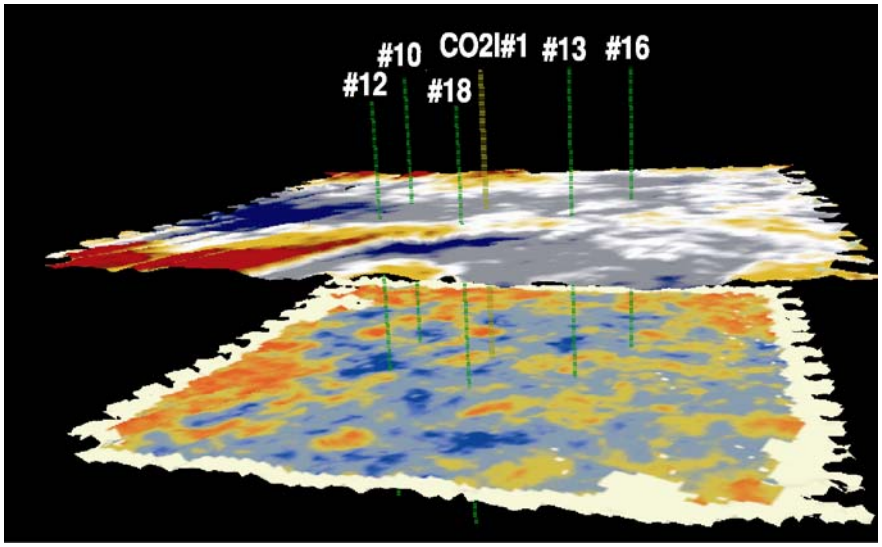

Figure 90. Similarity "seismic facies" map on bottom of diagram. Highest similarity is shown in blue and lowest similarity shown in red. The better reservoir properties occur in blue areas as demonstrated by preferred (faster) EOR-fluid movement in those areas and generally in a SW-NE trend. Well 13 has had delayed response as a result of being separated from a CO_2 injection well (yellow) by lower (golden-red) quality reservoir properties. The distribution and geometries associated with similarity seismic facies patterns are suggestive of a complex ooid shoal depositional motif, which is supported by oolitic litho-facies being the known reservoir in this interval (image ~ 0.75 mi. square). Upper map in diagram is a time structural map showing highest areas in red and lowest areas in blue.

Seismic Data Acquisition: Monitor Survey Four

Over 790 shot stations were recorded during the October 2004 monitor survey. Data quality overall was good with a slight increase in signal-to-noise ratio that was attributed to a decrease in the average wind speeds over the recording period and increased soil moisture conditions as a result of a wetter than normal fall. Average daily production was around 150 shot stations.

Figure 91. David Thiel operating the IVI minivib2 with GPS tracking and guidance system. A two to four times increase in power was obtained after installation of an Atlas rotary style servo valve in comparison to the factory Moog valve.

Equipment and parameters used during the October 2004 survey were as nearly identical to those used during the previous four surveys (baseline and three monitor surveys) as possible. The IVI minivib2, outfitted with a GPS tracking system, occupied the designed source stations with the exception of three on sandbars (too wet and represented an elevated equipment risk), six in a milo field ready for harvest, and one due to construction of a new pond (Figure 91). All shots were recorded with a Geometrics StrataVisor NZC controller operating ten 24-channel Geodes deployed along five 48-channel survey lines (Figure 92). An eleventh Geode was used to record the pilot, which was sent via radio to the recording vehicle from the vibrator. Three 10-Hz Mark Products Ultra geophones were planted in a triangle measuring about a half-meter on a side centered on the GPS-located station.

Figure 92. Sunset during October 2004 survey. Some data were collected at night to avoid wind noise that increased during the afternoons.

Figure 93. Weather was very pleasant most days with highs in the 70s to 80s and lows around 40. The seismic recording vehicle housed the Geometrics NZC controller and one Geode used to record the vibrator ground force. All data were transmitted to the recording vehicle from the other ten Geodes via ruggedized Ethernet cables. Graduate student Theresa Rademacker of Lincoln, Nebraska, recorded data and performed initial data quality control monitoring of the 240-channel uncorrelated vibroseis data and ground force pilot trace.

With no moisture and daytime temperatures in the 70s to 80s, data acquisition progressed rapidly (Figure 93). The one-square-mile survey area was covered in just over six days. More than 60 Gigabytes of data were recorded during this acquisition period. Data were transferred each day from the hard drive on the controller to the computers located in the mobile processing vehicle via Ethernet. Once the data were transferred to truck-mounted computers, the data were checked for quality and analyzed to determine if the overall data set would benefit from the reoccupation of any shot stations. In general about 15% of all stations were reoccupied in an attempt to improve the signal-to-noise ratio (S/N).

Reduction in wind noise was routinely possible during night acquisition in comparison to during the average day at this site. Clear nights with light and variable winds were the rule, allowing large time windows without interruptions and stoppages due to weather noise. During night shooting, the increased safety and productivity actualized by using the DGPS route and tracking system was dramatic. Even with the very rough and sometimes treacherous terrain around the Smoky Hill River on dark nights (no moon luminance or cloudy), production rates exceeding 15 shot stations per hour were easily maintained. Once the vibrator operator became accustomed to using the computer/DGPS route and tracking system, the only reason to look outside the cab was to make sure obstacles such as tree limbs or ditches dug, appearing since last survey, were not in the vibrator's path.

Surface conditions, especially the vegetation, changed noticeably throughout the first year. Soil moisture conditions changed as evident in slight changes in weathering velocity calculated from first arrivals. Only during the January 2004 survey was the ground frozen. Little change in data quality was observed that could be directly related to that particular ground condition. The normal crop cycle for dryland wheat grown in this part of the Midwest is two years long and includes a growing year and a fallow year. During the fallow year, volunteer vegetation (grasses and weeds) grow rapidly.

An increase in the S/N was observed on data from the October 2004 survey (Figure 94). As previously noted, this increase in signal is likely related to increased soil moisture and reduced average wind speed during the recording of these 790+ shot stations. Reflection events are very coherent and possess a reasonably broad bandwidth. Reflections arriving at 850 msec and deeper at source offsets in excess of 1 km have excellent signal strength and sufficient coherency to estimate velocity.

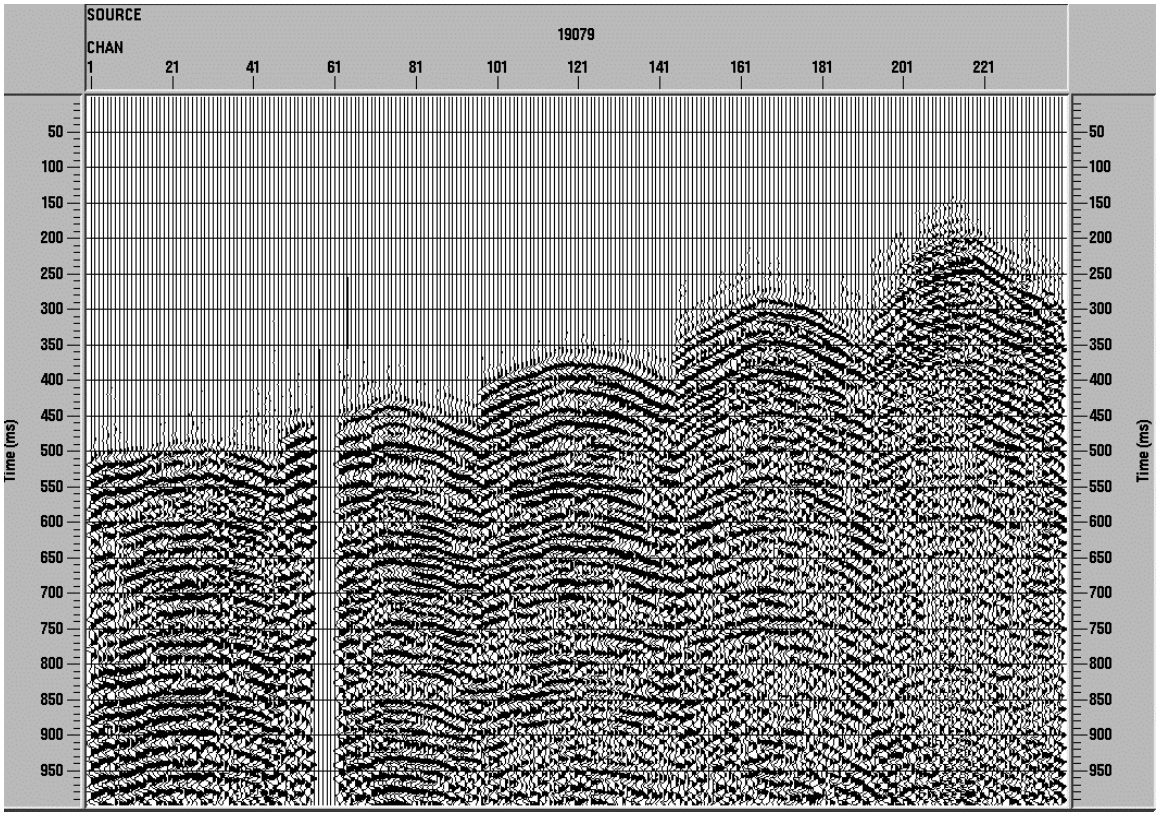

Figure 94. A 240-channel shot gather from station 19079. Reflection events dominate the four-shot vertically stacked shot gather. Coherency of events is excellent and the dominant frequency of this un-filtered shot record is around 80 Hz. After spectral balancing the dominant frequency easily exceeds 100 Hz.

Preliminary Processing and Interpretation—Fourth Monitor Survey

Preliminary interpretation of the October 2004 3-D survey suggests increased "fingering" in the CO_2 migration (Figure 95). Considering the lateral resolution of these data, small objects (sub-wavelength) will be smeared to appear much larger. Therefore a narrow higher permeability zone may possess a seismic signature several times larger than the actual affected area. With that in mind, the fingers from the main CO_2 body may be representative of regions that are several times smaller than they appear on the amplitude attribute data. These fingerlike features have all the necessary characteristics to suggest that this seismic response is based on changes in fluid composition.

One obvious consideration is the volumetrics of a feature this large and the apparent growth since the June 2004 survey. Basic volumetric balance with injected CO_2 and the CO_2 area shown by seismic requires that the defined area of CO_2 represent movement of CO_2 in a thin interval and not through the entire C-zone pay section. Volumetrics would also support the interpretation that the fingers may be narrower than they appear on the seismic data.

Overlaying the four monitor surveys is preliminary due to how early the October 2004 data are in the processing phase (Figure 96).

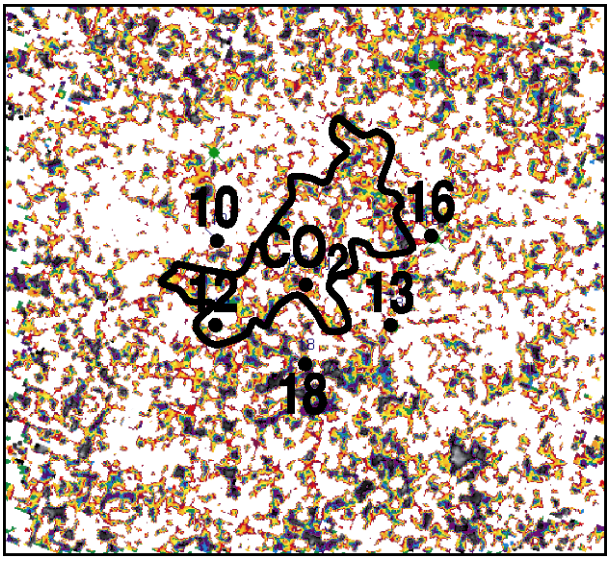

Figure 95. Amplitude envelope attribute for a very preliminary processed October 2004 survey. Fingering is becoming much more pronounced with the general trend of those accelerated migration paths consistent with the secondary lineament orientations previously identified.

Interpretation of the areal pattern change can be interpreted to show that growth toward well 13 appears to be accelerating between June 2004 and October 2004, but the path of the CO_2 is not direct. If this interpretation is correct and movement toward well 13 is following narrow, directed pathways, then gradual breakthrough might be anticipated as exhibited by field production.

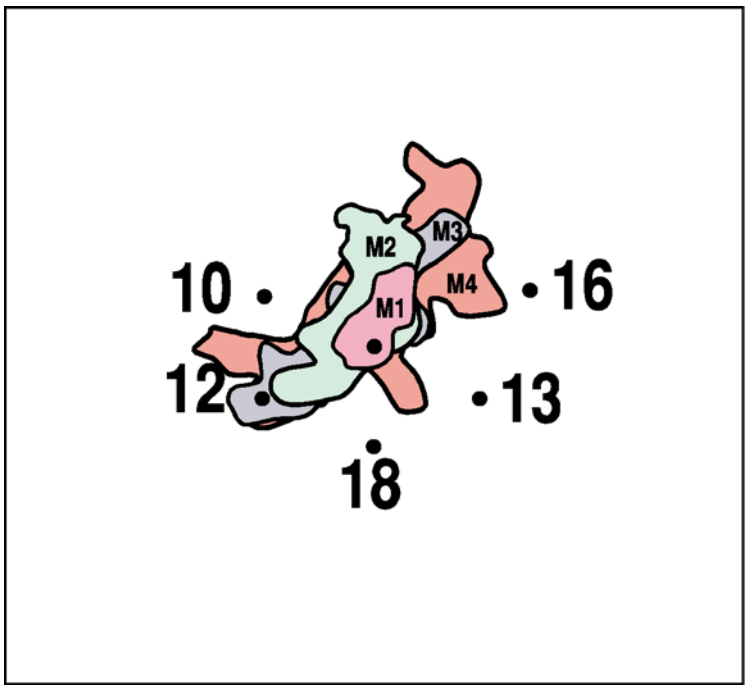

Figure 96. Overlay of monitor survey 1 (M1), monitor survey 2 (M2), monitor survey 3 (M3), and monitor survey 4 (M4). Apparent fingering along the secondary lineament orientations is quite pronounced.

Small concentrations of CO_2 began to appear in well 13 at very low levels (0.49%) in August 2004, but may have represented pre-flood natural CO_2 in reservoir water. By October 2004, CO_2 concentration had increased (3.09% of total gas) but was still below levels suggesting breakthrough. In December 2004, CO_2 concentrations increased to 6.44%, suggesting limited breakthrough had occurred. With low production and delay in oil or gas arrival at well 13, the field operations team decided that well stimulation should be performed. A process known as Huff-n-Puff (injection of CO_2 directly into well 13 to modify the relative permeability around the well) was initiated. Following this treatment, concentrations of CO_2 are no longer reliable measures of the progression of the main CO_2 body.

This gradual increase in concentration of CO_2 in well 13 is consistent with a possible fingering scenario. The seismically mapped progression of CO_2 between CO2I#1 and well 12 exhibited a more uniform flood front, consistent with the observed increase in CO_2 concentrations in well 12. The different response in well 13 suggests either a different migration pattern and/or migration mechanism at work between CO2I#1 and well 13.

Comparing the interpretation of the preliminary processed October 2004 survey with the seismic lineament attribute map, the general trends of the fingering and main body are still consistent with the interpreted "barriers" associated with the major lineaments (Figure 97). One of the more interesting observations is the location where the CO_2 appears to have moved east through this northeast/southwest "barrier." Looking at the lineament attribute map only (Figure 23), this location exhibits anomalous seismic response along an otherwise relatively continuous expanse of this feature. Considering the pressure field established around well 13, once the CO_2 has moved through this "barrier" it should move more quickly toward well 13. If this interpretation is correct, the volume of CO_2 moving to well 13 may be controlled by the nature of the "break" in the possible barrier.

This preliminary interpretation of the October 2004 (Figure 95) data will be further examined with processing and interpretation. Throughout the pilot study it has been known that well 13's response to injection in CO2I#1 was complex and potentially indicative of some form of restriction between wells CO2I#1 and 13. The present interpretation of the 4-D seismic data supports this conclusion.

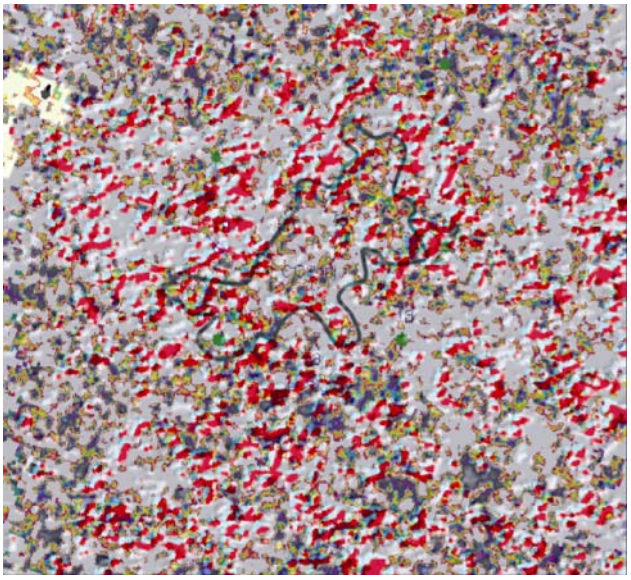

Figure 97. October 2004 survey amplitude envelope attribute map with interpretations of the CO_2 "front" overlain by the lineament attribute map.

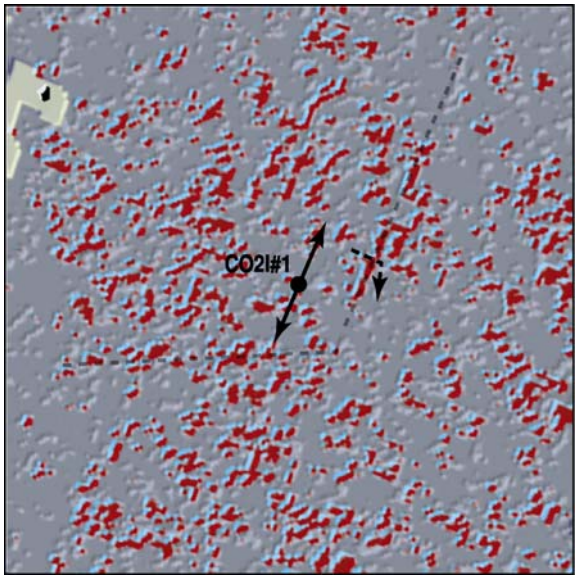

Figure 98. Major lineaments that appear to be influencing fluid movement away from CO2I#1, including the possible route the CO_2 took to breach the barrier associated with the northeast/ southwest lineament.

Seismic Data Acquisition: Fifth Monitor Survey

To date the seismic data from the baseline survey and first three monitoring surveys in January, March, and June 2004 have been first-pass processed and preliminary interpretation completed. Over the period of October 21-29, 2004, the fourth monitoring 3-D seismic survey was conducted to obtain a snapshot of the CO2, more specifically to provide clues to better understand why well #13 was not producing at the expected rate. Because of the sluggish response in #13 and the lower-than-expected yield in #12, the WAG (water alternated with gas) program was delayed. A noted increase in production in

well #13 and an upward overall production trend from both the demonstration wells (#12 and #13) was reported just prior to the fifth 3-D monitor survey, which began in early March 2005. This report includes field activities for March 2005.

Petroleum Production Overview at Time of Fifth Monitor Survey

The general appearance of the site and operational aspects of the equipment have changed little in the 18 months since the project began (Figure 99). As of March 2005, CO2 is being injected at a rate varying between 2.5 g/m and 3.0 g/m, or about 20 tons a day. With just over 7,500 tons of CO2 injected through CO2#1, at a bottom hole pressure between 1800 psi and 1900 psi since December 2003, the rate of oil production from #12 and #13 has been averaging between 2.0 and 5.0 b/d since the beginning of 2005.

Figure 99. CO2 storage tank, oil stock tanks, CO_2 pumping station, and seismic support vehicles in this picture taken looking northeast. Wind sock and American flag are good indicators of wind speeds exceeding 15 mph.

Site Conditions

For the most part the spread geometry has been unchanged from the initial survey, however a few physical changes on-site have required slight modifications to a few source stations. The ground conditions and land access for the March 2005 survey was consistent with previous surveys with the exception of a new drill pit and changes in the location of a brush pile, requiring skipping two points while two new points were accessed. Ground temperatures were significantly above freezing.

Changes in site conditions that affect data between the October 2004 survey and the March 2005 survey are subtle but will be noticeable on seismic data. Since these changes are both natural (soil moisture, wind, and vegetation) as well as mechanical (all pumps must remain on, more pumps currently working, and duty cycles of water injectors almost continuous), with the exception of wind noise, little can be done during acquisition to compensate for the noise.

Weather during the two most recent 3-D surveys was as expected during late fall and late winter, variable. During the October 2004 survey temperatures were near perfect ranging from 40s at night to 80s during the day. Winds were consistently very acceptable with no data recorded when sustained winds were above 10 mph. Acquisition rates exceed 150 shot stations per day for a continuous 5-day period. During the March 2005 survey, wind conditions changed dramatically. With sustained winds exceeding 20 mph

for days on end, maintaining a shooting threshold of < 15 mph required a significant number of down days and night shooting. Temperatures ranged from 20s at night to 70s during the day. Several days temperatures never exceeded 40°F with accompanying winds greater than 30 mph.

With the clear dependence of data quality on wind noise, an anemometer was used to quantify wind speeds during the March 2005 survey where previously wind speeds had been judged using a windsock (Figure 100). Data were not collected when average wind speeds exceeded 15 mph. On several occasions wind gusts exceeded 40 mph during the March 2005 survey.

Figure 100. An anemometer to allow accurate measures of wind speed correlated to those previously judged using a windsock and National Weather Service reports. When average wind speeds exceeded 15 m/h (approx. 25 km/h), the survey was halted.

To ensure accurate repeat placement of receivers and sources, a Trimble DGPS 4800 and 4700 model system was set up and operated any time data were being acquired or the spread was being deployed (Figure 101). A survey pin, cemented in place immediately south of CO2I#1 prior to the baseline survey over 18 months ago, was established as the "permanent" marker for the entire six-year duration of this study. With winds exceeding 25 mph expected during the March 2005 survey, sand bags were used to weight the tripod legs, ensuring a rigid placement throughout the two weeks expected to complete this survey.

Fortunately, ground conditions were good for laying out the receiver spread (Figure 102). After three months of winter the vegetation was minimal, the ground was not frozen, and the soil and sub-soil moisture was quite high relative to the norm in this area (based on discussions with local farmers and construction workers). These conditions allowed quick geophone planting while providing excellent coupling to the earth.

Figure 101. Electrical engineer Brett Bennett and geologist David Laflen level and align the DGPS tripod base prior to installation of the satellite receiver and ground plane.

Figure 102. Engineering technician Andrew Newell carrying a partial hasp of geophones to the next station along the receiver line. Flags were used to mark the receiver stations. Once the three geophones were seated into the soil, the flags were removed, avoiding noise resulting from the flag flapping in the breeze.

Receiver stations in areas not disturbed by seasonal agricultural activities were marked with wooden stakes that should remain in place throughout the duration of this study (Figure 103). Three Mark Products 10 Hz U2 geophones on 5-inch spikes and wired in series were firmly seated into the soil centered on the station location and separated by around 0.5 m. With receiver lines traversing soils in fields used for wheat or milo, pastures, roads, waterways, wooded areas, and sand dunes, coupling will be variable as will weathered layer velocities.

Receivers deployed in the perennial grasses required more clearing around the geophone area to minimize the noise from grasses blowing in the wind. The sand dunes along line 5 provided some of the very best receiver coupling in comparison to the other

Figure 103. Set of three geophones planted along line 5 (southernmost receiver line) in an area with thick grass cover not routinely farmed.

Figure 104. Engineering technician Nicky Proudfoot secures geophones to the analog seismic cables. With receiver stations separated by 20 m, each east/west receiver line is just less than 1 km in length.

four lines in tilled fields, pastures, and road ditches (Figure104). However, the sand dune topography did provide its own set of static problems that needed to be overcome during processing.

Geodes used on this survey were 24 channels per unit with all eleven Geodes connected to each other and the controller via ruggedized Ethernet cables (Figure 105). These Ethernet cable runs have very stringent length limitations and minimum coil radius to remain within the seismograph manufactures transmission specifications and to avoid cable damage, respectively. A weatherproof covering and military-grade connectors make this Ethernet cable extremely field rugged. On this project, 1900 ft of this cable in 10 separate segments were necessary to network all the seismographs with the controller.

Even these "ruggedized" Ethernet cables are sensitive to very small crush pressures. To avoid damage at the various road crossings, the cables were housed in PVC pipe and either buried into the unimproved roads or slid into culverts or drain tiles under roads (Figure 106). On several occasions it was necessary for the vibrator to drive over these lines. For those crossing a piece of PVC pipe was moved around and the Ethernet cable was inserted through a slit cut the length of the PVC.

Figure 105. A six-wheel-drive Polaris ATV with two Ethernet cable reels on a four-reel customized bracket.


Figure 106. Engineering technicians Andrew Newell and David Thiel prepare the Ethernet cable shield for for insertion into a culvert under the east/west county road.

With the temperatures dipping several degrees below freezing at night, the seismic recording vehicle was outfitted with a thermal boot (Figure 107). A propane heater was used to keep the inside temperatures above 65°F. Digital lines (Ethernet) from the four electronic lines were connected to the controller's four network ports. The ground force signal calculated using the vibrator mass and baseplate acceleration measurements were transmitted real time to the seismograph via radio. This ground force signal was used as part of the QC process to verify vibrator operations were consistent with design sweep parameters.

The seismic recording vehicle has enough 12-volt battery power for more than 24 hours of continuous operation (Figure 108). Besides the seismograph, vibrator controller, and VHF radio, the lights and furnace fan (propane furnace) are operated on 12-volt power. Running without a 120 VAC generator reduces noise. Each pair of Geodes positioned along the five analog receiver lines shared a 12-volt deep cycle marine battery that required recharging about every 36 hours of operation.

Figure 107. John Deere Gator outfitted with cold weather cover. Propane heater keeps operator's area at room temperature when outside temperatures are well below 0°F.

Figure 108. Graduate student Theresa Rademacker operates the seismograph and coordinates the night-time acquisition from the enclosure on the back of the John Deere Gator 4 x 6 ATV.

As on previous surveys, the IVI minivib2 with the Atlas Rotary Servovalve provided the energy (Figure 109). The vibrator was guided from station to station using a customized computer mapping system incorporating DGPS technology with digital terrain maps. Five 10-second linear upsweeps were delivered at each shot station across a frequency bandwidth from 20 Hz to 250 Hz. The first sweep was designed to seat the pad thereby improving the uniformity in pad coupling and sweep consistency on the last four shots, which were vertically stacked to enhance signal strength relative to noise.

Figure 109. IVI minivib2 on station, immediately south of the CO_2 injection well, and DGPS base station. Receiver line 3 crosses near the CO_2 injection well where two Geodes also recorded 24 channels in each direction east and west from this central location.

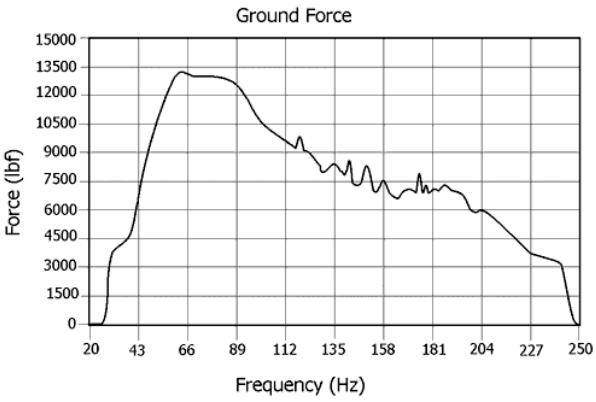

Figure 110. Average force diagram for vibrator operations at the Russell County site for the IVI minivib2.

The 14,000 lb vibrator was set to deliver a maximum of 12,500 lb-ft of power to the ground across the design frequency band. Ground force power plots are calculated from base plate and mass accelerometers and represent an estimate of the force being applied as a function of frequency (Figure 110). More than 6000 lb-ft was imparted to the ground across the 50 Hz to 200 Hz frequency range. Based on the these ground force plots the predominant frequency range on seismic reflection data should be between 45 Hz and 180 Hz with the dominant frequency around 90 Hz (Figure 110). For the most part this force curve is relatively smooth. Some minor "chatter" is evident between about 120 Hz and 180 Hz. This is an artifact of driving the vibrator at its limits through this range of frequencies.

Continuous recording over time periods in excess of 15 hours resulted in a sustained production rate of around 15 shotpoints per hour. Downtime for mechanical or electronic failures never exceeded 30 minutes throughout that the acquisition period with just one exception. A servovalve failure near the end of the second night of recording required operations to be temporarily suspended for a period of four days while the vibrator was shipped to Tulsa, Oklahoma for repairs. Data acquisition was completed within an eleven-day window.

Windy conditions in central Kansas during late winter and early spring are the norm rather than the exception. With the winds diminishing in the evenings, at night, and in the early mornings, most data for this March 2005 survey were acquired during darkness (Figure 111). With vibrator routes preprogrammed in the DGPS guidance system, the vibrator operator could move the source from station to station and line to line without looking outside the cab. All routes were DGPS choreographed to sub-meter accuracy, allowing extreme precision in the track followed by the vibrator between surveys. Because of the necessity of recording data after dark, lighting on the vibrator was significantly enhanced over standard factory.

Figure 111. IVI minivib2 working in a field of winter wheat in total darkness. Auxiliary lighting has been installed on this machine providing an enhanced view of the mass and baseplate system as well as the ground around the vibrator cab.

As previously indicated, wind noise necessitated night operations. During the eleven-day field campaign production acquisition was only possible on four nights (due to wind and mechanical issues). Over those four nights the crew averaged about 200 shot stations per night. With the exception of a new and quite significant noise source (pumping oil wells within the receiver spread), the data quality was high and consistent with previous surveys.

Noise from pumping oil wells within the receiver spread (oil wells that had been shut off during data acquisition on previous surveys) was extreme. Noise amplitudes on uncorrelated QC plots were at levels equivalent to those observed from 15+ mph winds on previous surveys (Figure 112). Correlated records from this survey possessed the most significant data quality problem so far during this monitoring program. These extremely elevated noise levels were the result of well operations and included both cyclic noise (pump cycle approximately 4 seconds to 6 seconds for a stroke) and a more random noise from motors powering the pump jacks. Five wells within the 1 square mile source grid that were shut down during acquisition of seismic data on previous surveys were pumping during the March 2005 survey.

Reflections evident on correlated shot records possess characteristic hyperbolic curvature (Figure 113). The actual geometry of the reflection curves is related to the source-to-receiver offset of adjacent traces and the rate and linearity of the incremental change in that source-to-receiver offset between those adjacent traces. Signal-to-noise ratio is clearly lower on this single sweep shot gather than has been observed on gathers from previous surveys. Background noise is a more dominant component of these

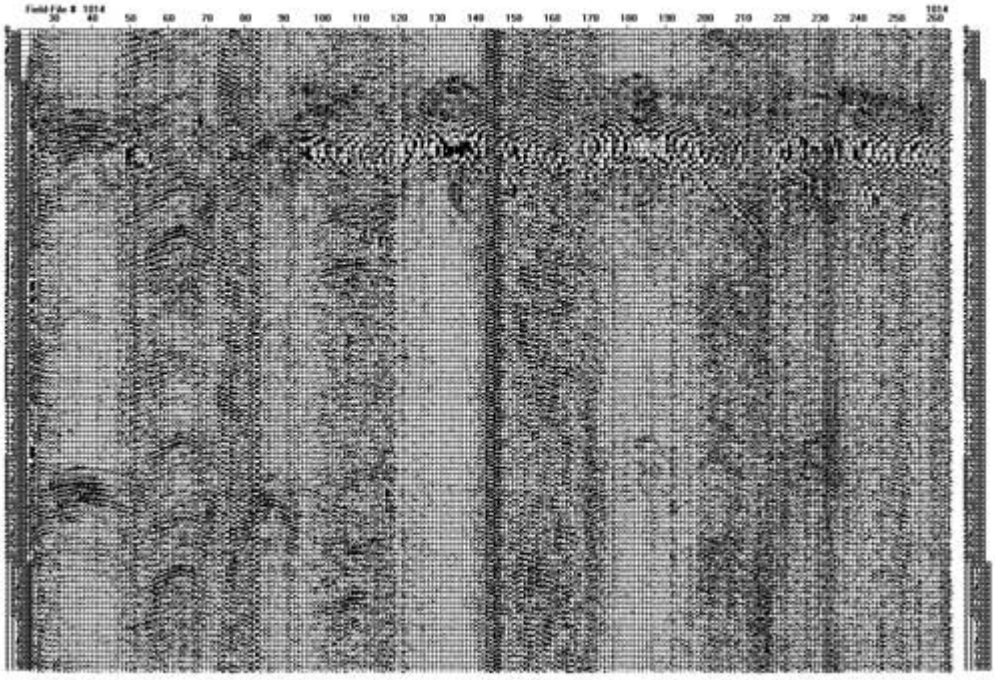

Figure 112a. Uncorrelated shot records near center of patch recorded with seven production wells and four injection wells operating during March 2005 survey.

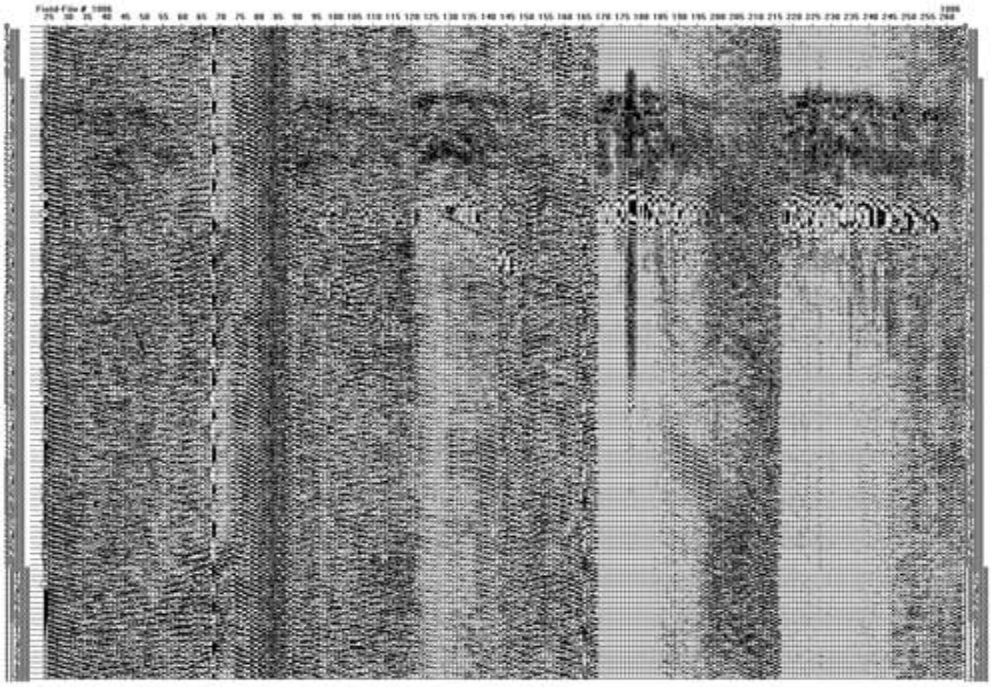

Figure 112b. Uncorrelated shot records near center of patch recorded with two production wells and three water injection wells operating during January 2004 survey.

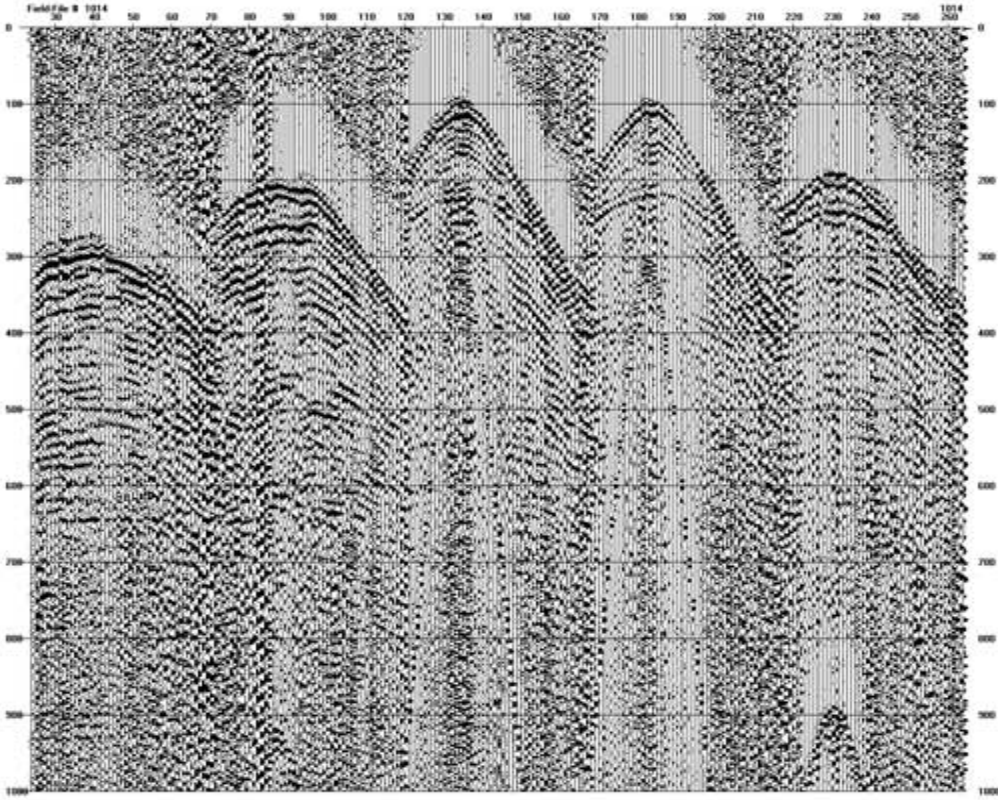

Figure 113. Correlated, single-sweep shot gather from near the center of the patch. Background noise is much more pronounced on this record than has been the case on most gathers from previous surveys. Reflections are easily interpretable to depth in excess of 900 ms and offsets exceeding 3000 ft.

records, but even with the elevated noise levels resulting from pumping units, reflections with dominant frequency in excess of 70 Hz can be interpreted at depths in excess of 700 ms directly off these raw records.

Changes in near-surface conditions and surface noise have impacted the recorded data in different ways on each of the six 3-D surveys completed over the last 18 months. Fortunately none of the changes in data quality and/or character has been sufficient or significant enough to surpass the expected and observed differences that have occurred as a result of fluid displacement with the reservoir. With changes in weather, surface noise, and ground conditions all playing supporting roles in the overall signal quality, it would be difficult to ascertain which seasonal influence enhanced or degraded the data quality and/or resolution the most.

Seismic Data Acquisition: Sixth Monitor Survey

The first five monitor surveys were acquired during the first 16 months of this project while CO_2 was being injected. The next and seismically more challenging component started on June 21, 2005, with initiation of water injection (Figure 114). The sixth 3-D survey was acquired during the first two weeks of July 2005.

Figure 114. Sun setting over the site with well 7 pumping in the background.

Processed data from all five monitor surveys give good indications that CO_2 was imaged, reservoir heterogeneities are relatively consistent from one survey to the next, and images from each monitor survey show consistent expansion of the CO_2 plume.

Data from the sixth monitor survey represent the last data acquired that might not be affected by the injection of water designed to chase the CO_2 and, depending on how the water affects signal response, may be the last survey that provides a clear image of the complete CO_2 plume. As water injection pressures change in the field, the saturations of the various components change. Less than two weeks of water injection separates the end of CO_2 injection on June 20, 2005, and the acquisition of the sixth monitor survey in July 2005. Given the size of the horizontal sampling window at the reservoir depth and the volume of water injected, and the corresponding radius of water invasion, the influence of the injected water on seismic imaging of the CO_2 plume at the time of the survey is considered negligible and limited to the single imaged pixel containing the CO2I#1 well.

Petroleum Production Overview

Over the 18 months between start of CO_2 injection on December 4, 2003, and the end of continuous CO_2 injection and initiation of the first water injection on June 21, 2005, CO_2 was generally injected at a rate of 2.5-3.0 gallons/minute (~20 tons/day) at bottom-hole pressures of 1,800-1,900 psi. By June 21, 2005, approximately 8,500 tons of CO_2 were injected into CO2I#1. The rate of oil production from wells 12 and 13 has averaged between 2.0 and 5.0 barrels/day since the beginning of 2005.

Site Conditions

With higher-than-average rainfall during the early part of the summer, the seismic acquisition characteristics, such as source and receiver coupling, near-surface attenuation, and unconfined water table depth, are much more conducive to the propagation of high-frequency seismic body waves than is normally observed during July. As is normally the case in this part of Kansas, the midday and afternoon/evening winds are challenging for high-quality, high signal-to-noise recording of the low-amplitude high-frequency signals necessary for high-resolution surveying. Unlike previous 3-D surveys over the past 18 months at this site, no attempt was made to record during the middle portion of the day or during afternoons. All data were recorded between 6:00 pm and 9:00 am. As has been clearly shown on previous surveys, the improvement in data quality is significant and justifies the additional acquisition expense.

More rainfall also resulted in an increase in night-flying insects, which presented a problem for operating the seismograph at night. To avoid enclosing the seismograph operator and equipment, which would have involved climate control (air conditioner and generator) and increased noise, mosquito netting was draped over the seismograph vehicle (Figure 115). This kept the air temperature equivalent to the outside air, allowed a breeze at the operator station and across the equipment, and kept insects away.

Data Acquisition

Data were acquired at over 790 shot stations with a location accuracy of better than 0.5 m (Figure 116). All receiver stations were deployed within 0.2 m of previous locations using DGPS. To avoid environmental noise, the data were acquired between 6:00 pm and 9:00 am over a 7-day window between July 7 and 13. For this survey, as with the March 2005 survey, the operator of the field was not in a position to shut down

Figure 115. Mosquito netting was draped over the seismograph vehicle to keep the air temperature equivalent to outside air, allow a breeze at the operator station and across the equipment, and keep insects away.

Figure 116. Data were acquired at over 790 shot stations with a location accuracy better than 0.5 m. All receiver stations were deployed within 0.2 m of previous locations using DGPS.

the peripheral pumping units during the seismic data acquisition and therefore noise from those pumps resulted in notable deterioration in signal-to-noise ratios on raw data.

Overall data quality was consistent with the five previous monitor surveys. Ultra-near-surface conditions have changed with crop rotation and farming practices. These changes are noticeable on shot gathers from some areas. However, they are predominantly evident in subtle reductions in the amplitude of the higher portions of the reflection bandwidth. Balancing these frequencies reduces the spectral differences and to a limited extent reduces the signal-to-noise ratio. Fortunately, less than 20% of the survey area has seasonal crop rotation issues.

Data acquisition in most areas around the site has been consistent throughout the almost two years of recording (Figure 117). For the most part, the water table in the river valley areas of the site has been consistent, and stations with the highest data quality in seasonally consistent areas (not affected by farming practices) have routinely provided the highest quality data. It is likely these better-than-average data locations have stiffer soils, higher water tables, shallower bedrock, etc., relative to the other lower-quality areas around this site.

Figure 117. Data acquisition in most areas around the site has been consistent throughout the almost two years of recording.

Data Processing of First Seven 3-D Surveys

Based on the results of the first year of seismic monitoring of the CO_2 injection process, results suggest that seismic reflection methods have been effective at providing data that can be used to image the movement of CO_2 across this 3000-ft-deep, 15-ft-thick reservoir interval. Based on present processing and interpretation methods, CO_2 movement is best imaged by extremely low amplitude changes in the amplitude envelope attribute and subtle variations in instantaneous frequency.

To extract as much information as possible from the data, stacked sections must be produced that fully capture and enhance the relevant information content of the data. The focus of this enhancement activity is on coherency, signal-to-noise ratio, and resolution. Stacked sections produced to date have been preliminary and intended to satisfy the need for quick turnaround at the expense of identifying the best processing and interpretation methods. The rapid development of interpreted seismic sections was necessary to provide seismic imaging of the flood for the on-going CO_2 flood management. Dynamic adjustment to injection and withdrawal management and flood design is likely to be a future application of the method as an EOR monitoring/evaluation tool.

To enhance the image quality for interpretation and image resolution, several aspects of data processing must be addressed. Enhancement of coherency can be achieved by improving uniformity of source wavelet properties and statics. In addition, optimized velocity corrections can improve wavelet consistency from trace to trace. Signal-to-noise ratio is always an important characteristic when dealing with high-resolution seismic reflection data. Improvements in signal-to-noise ratio require optimizing the frequency bandwidth, ensuring consistency in phase, elimination of as much noise through muting and filtering as possible, and pre-stack statics. Finally, to extract the highest resolution interpretations possible, the upper corner reflection frequency must be identified and the focus of spectral shaping (keeping in mind the need for a broad bandwidth) must be determined, as well as resolving statics issues and balancing amplitude characteristics.

Enhancement processing began midway through the second year of the program. All data will undergo the optimized enhancement flow in a consistent fashion. Initial analysis suggests phase correction pre-correlation and pre-vertical stacking results in a better than 20% increase in bandwidth and in data coherency (Figure 118). Spiking deconvolution improved the reflection bandwidth and provides improved wavelet characteristics, but decreases the apparent signal-to-noise ratio. This is a tradeoff that is necessary and turns out to be all positive based on downstream processing.

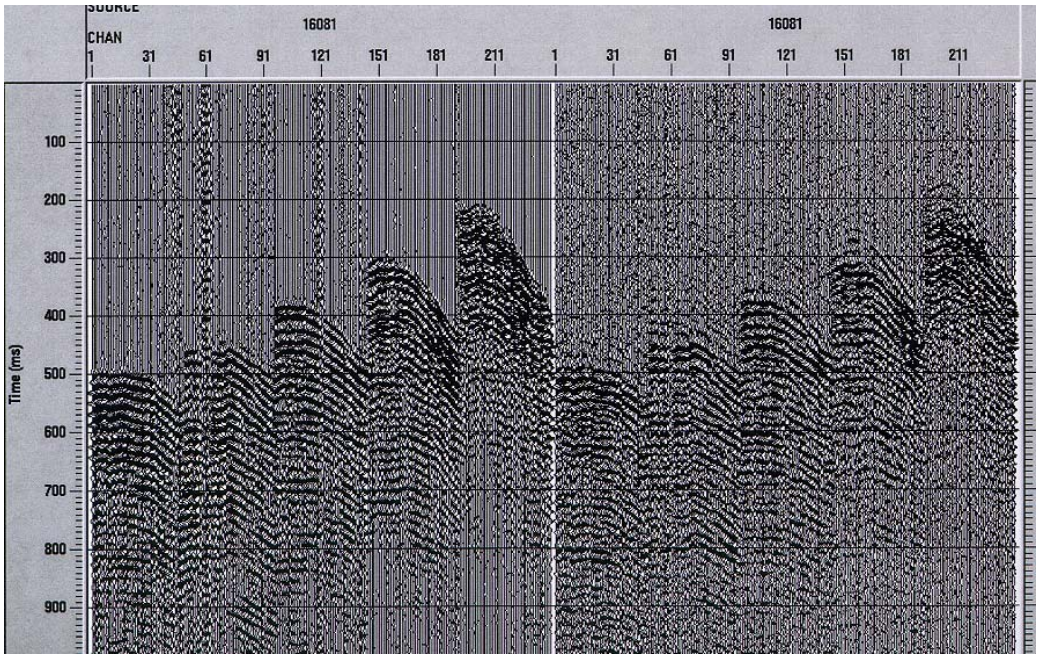

Figure 118. Raw correlated shot gather (right) compared to the same shot gather after phase filtering and spiking deconvolution shot gather (left).

Amplitude attributes provide important information about where CO_2 is present within the pattern. Based on the acquisition design, the amplitude distribution within the grid has natural artifacts associated with the pattern (Figure 119). Correction to this non-uniform distribution in amplitudes will eliminate the shadows evident on the amplitude envelope attribute consistent with the receiver grid. After amplitude distribution corrections only minor linear artifacts remain, predominantly inline and crossline to the imaged space (Figure 120).

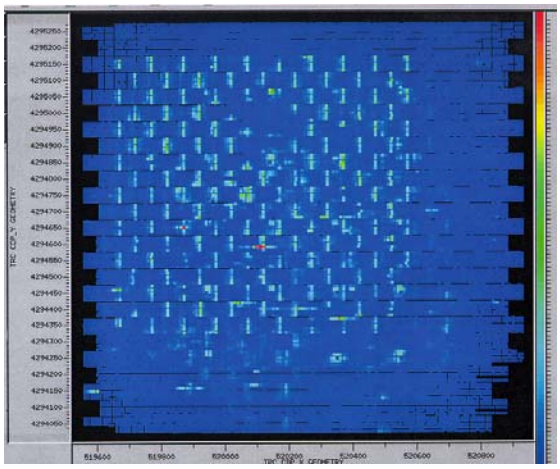
Figure 119. Seismic trace root-mean-squared amplitude map *before* surface consistent amplitude balancing.

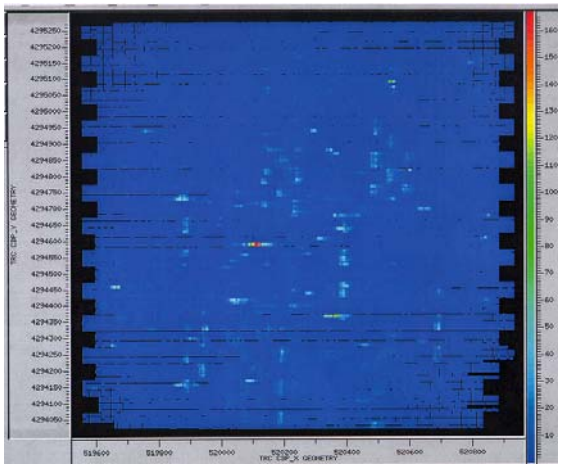
Figure 120. Seismic trace root-mean-squared amplitude map *after* surface consistent amplitude balancing; acquisition footprints have been largely eradicated.

During preliminary processing, source and receiver statics were corrected for using surface-consistent correlation statics routines (Figure 121). These corrections were adequate for general stacked sections, but lack the station-specific accuracy necessary for high quality image construction. After the application of residual statics focusing on a 500-msec window surrounding the target reflection, a significant improvement can be noted in the coherency of the unstacked, moved-out shot gather (Figure 122).

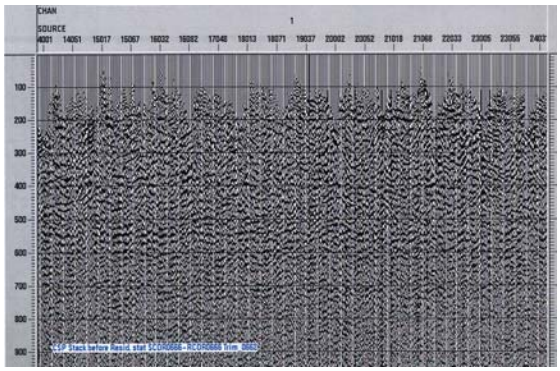

Figure 121. Common-shot-point stacked seismic data after surface-consistent correlation statics, but before residual statics.

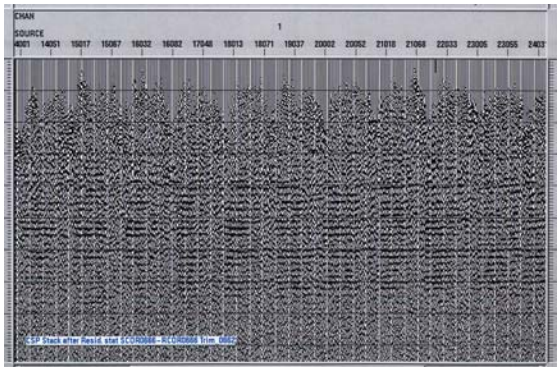

Figure 122. Common-shot-point stacked seismic data after both surface-consistent correlation statics and residual statics.

After gathering the data into common receiver bins, and applying residual statics in a fashion consistent with application of the same statics routine on common shot gathers, reflection coherency improves dramatically and the spectral (therefore resolution) also makes a marked improvement. Common receiver stacks possess good signal-to-noise ratios but lack the sitewide coherence and consistency in arrivals indicative of a section with all near-surface effects removed (Figure 123). In the middle of the seismic volume, the data are higher amplitude and seem to possess better shallow continuity in comparison to the lower-fold data near the ends of the spread. This is consistent with the CMP stacked volumes interpreted during the preliminary stages of processing. After a residual statics operation was applied to the receiver gathers, problems associated with coherency, bandwidth, and amplitude all seem to dramatically reduce (Figure 124). The pre-residual statics data are the same data that were used to produce the stacked volumes that were interpreted and suggestive of differences related to the presence of CO_2.

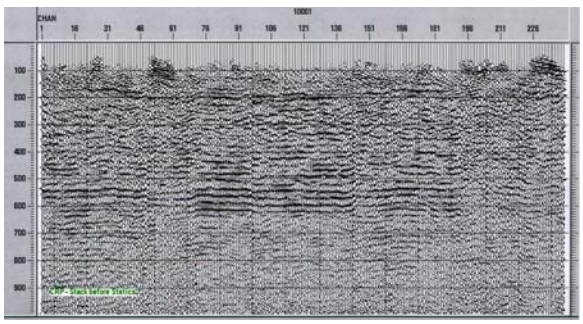

Figure 123. Common-receiver-point stacked seismic data after surface-consistent correlation statics, but before residual statics.

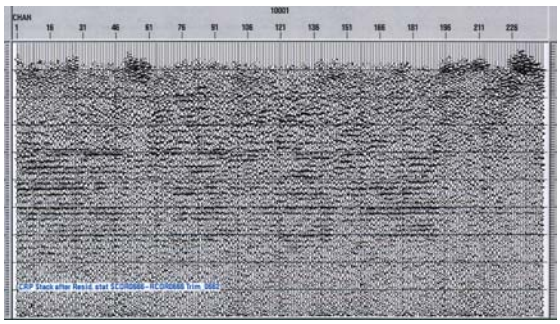

Figure 124. Common-receiver-point stacked seismic data after both surface-consistent correlation statics and residual statics.

RESULTS AND DISCUSSION

Processing and Data Properties

Accurate data analysis starts with a representative velocity function defined at intervals considered spatially subspread length and temporally at a frequency consistent with the dominant reflection sequence or stratigraphic cycles. Consideration must be given for the fact that subtle changes in near-surface conditions can significantly alter the average velocity. High amplitude reflections within each shot gather and for each repeat survey were analyzed for velocity based on the NMO curves prevalent throughout the upper 800 msec on most records (Figure 125). High resolution velocity analysis was accomplished using both common velocity stacks and semblance techniques (Figure 126). To insure laterally consistent and meaningful velocity function developments, each automatically selected high correlation velocity value was inspected with some degree of manual fine-tuning necessary for a very small (< 10%) number of gathers.

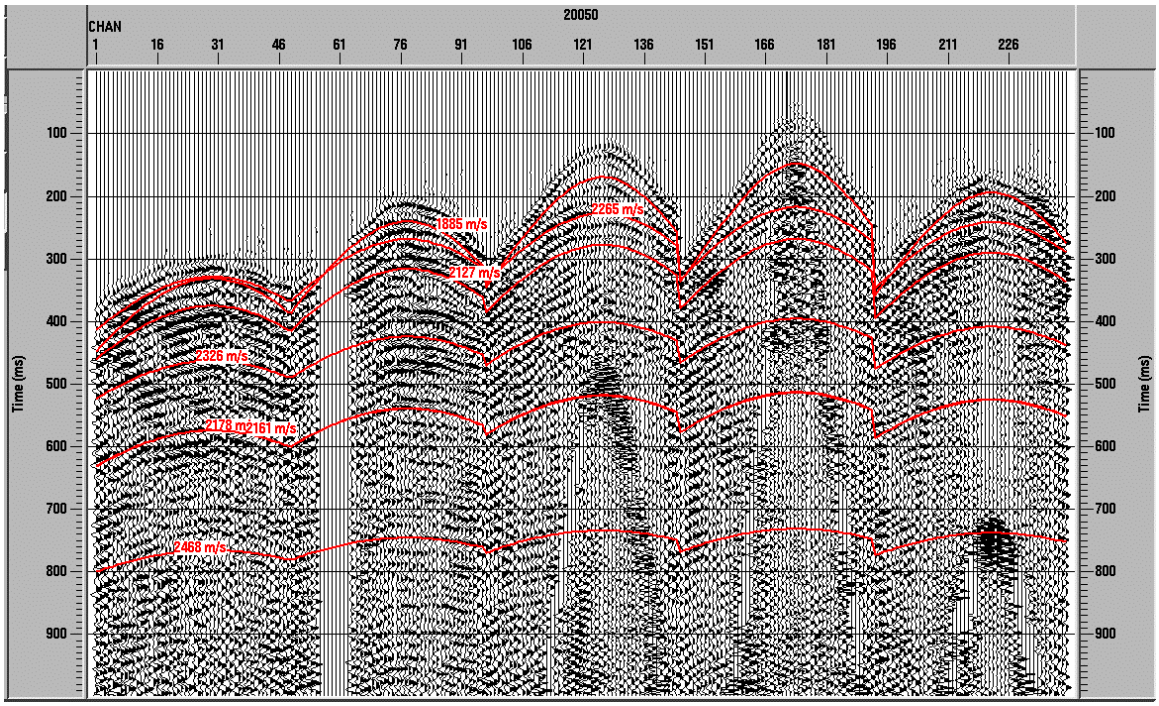

Figure 125. RMS velocities calculated using curve-fitting routines.

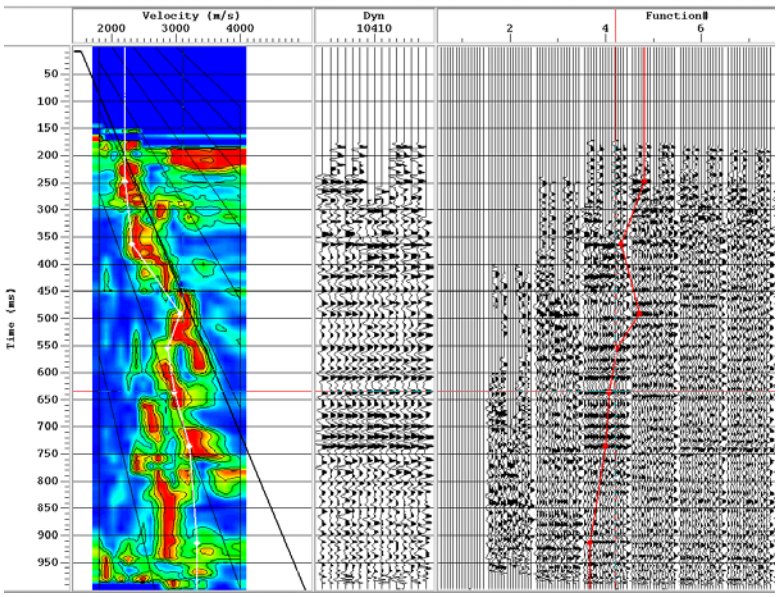

Figure 126. Horizon velocity analysis increased lateral resolution of velocity analysis.

Critical for multi-survey correlations and evaluation of change based on time lapse surveys is repeatability of background data characteristics. With the high degree of attention and expense focused on identifying change in the reservoir over time consistent with the volumetics of CO_2 injection, repeatability in data quality and characteristics was essential. RMS amplitude differences between the various surveys across key over-burden layers provided a measure of repeatability (Figure 127). Most surveys resulted in stacked sections with better than 80% repeatability in wavelet properties.

To further minimize the variability between surveys due to difference in acquisition and processing a cross-equalization adjustment was performed on all the data sets to boost the survey repeatability to better than 90% for most intervals (Figure 128). Changes observed between baseline and monitor surveys that are visible on stacked sections within the reservoir are almost exclusively related to the influence of CO_2. Some amplitude variability outside the pattern can be observed in the section that is related to low-fold and variability after muting operations to remove noise.

The target interval correlates extremely well with synthetics generated from nearby sonic logs (Figure 129). Coherent reflections are prominent within the L-KC reservoir interval with uniformity in wavelet characteristics and event continuity indicative of this producing horizon. Matching the log synthetics with the seismic reflection data provides a high degree of confidence to interpret subtle changes in wavelet attributes suggested to be a direct result of fluid exchange.

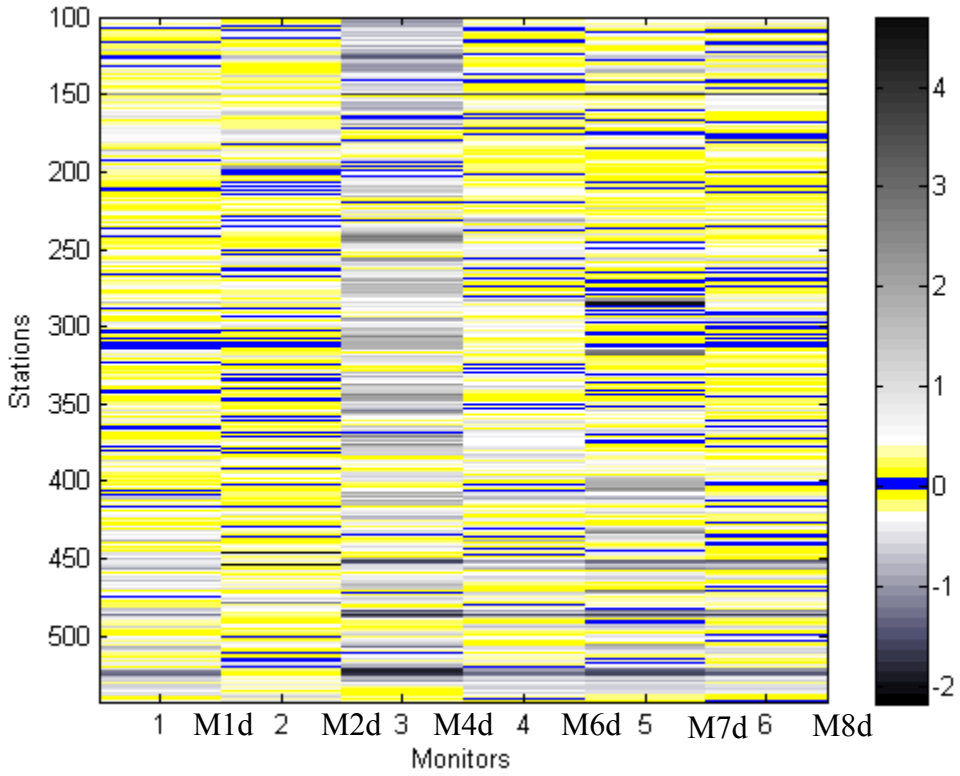

Figure 127. Quantitative measure of repeatability: blue (near perfect repeatability), yellow (70-80% repeatable), and grey tones less than 70%. Monitor Survey Four had the least repeatable data characteristics.

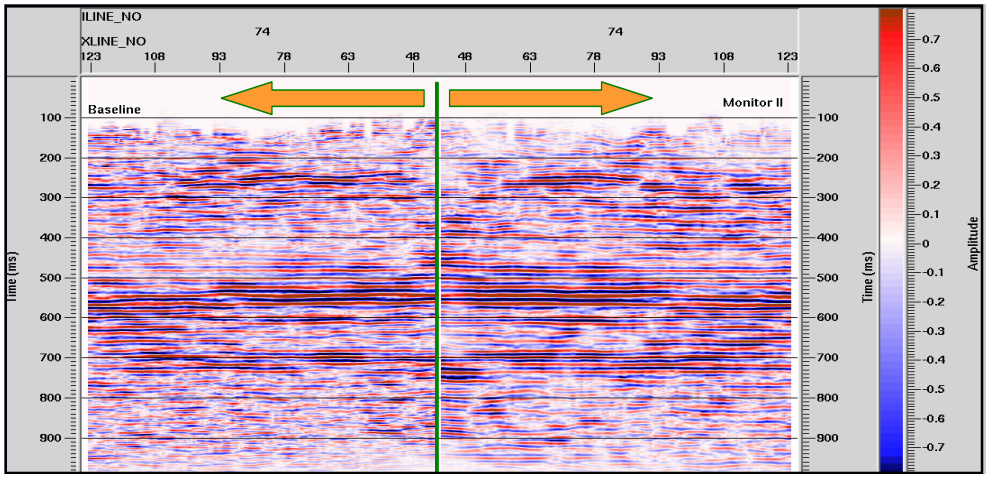

Figure 128. Baseline to second monitor survey tie and viewed in book format after processing tune-ups.

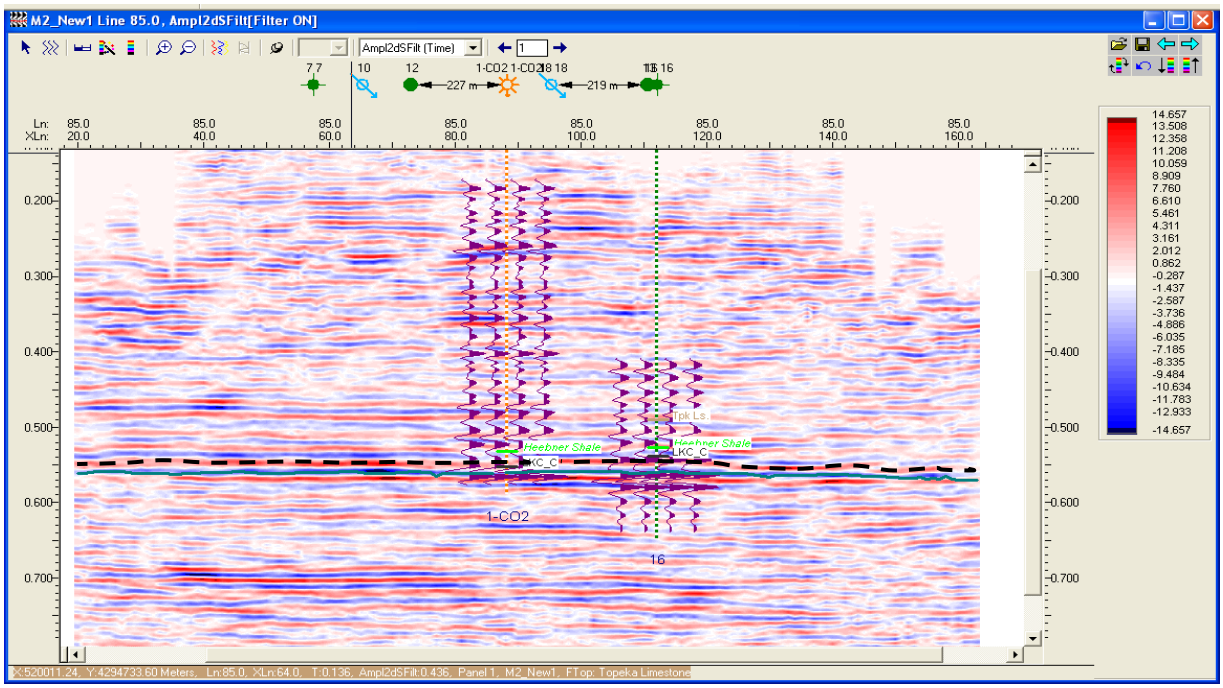

Figure 129. The target interval correlates extremely well with synthetics generated from near-by sonic logs

Comparisons of character on time slices from five of the eight monitor surveys at the interpreted top of the injection interval is sufficient to identify zones where CO_2 is influencing the reflection wavelets returning from the top of the 'C' zone (Figure 130). Changes in the intensity of these amplitude attribute slices suggest an increased reflectivity associated with the presence of CO_2. The ever-growing main body of the CO_2 plume through the nearly two years of injection is very evident in these data. However, with the resolution of these data and the extremely low (~10%) change in reflectivity

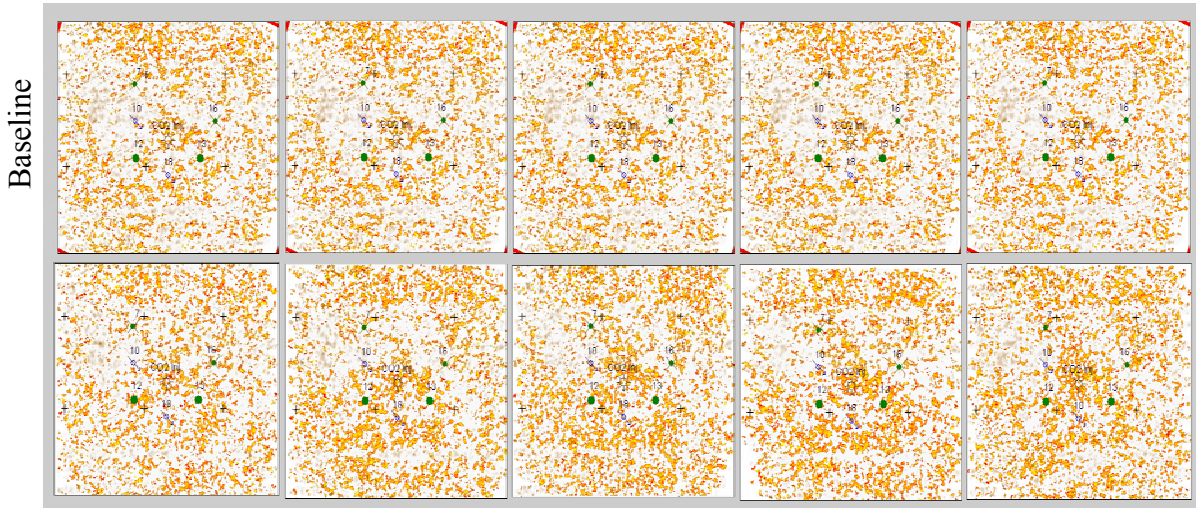

Figure 130. Comparison and contrast of each monitor survey below a repeated baseline survey.

associated with CO_2 replacement of reservoir fluids (brine/oil mix), high permeability zones that are sub wavelength in width would not be detectable on these data. This is an important fact when considering the detectability of CO_2 pathways responsible for production fluids in wells significantly north, outside the injection zone.

Seismic attribute analysis provides outstanding support for the suggestion that time lapse monitoring of a CO_2 miscible flood using the approach described previously as applied to this shallow carbonate reservoir is possible with a reasonable degree of confidence. Time structure (target interval reflection time 2-D map) of the seismic facies attribute correlated to well data can be interpreted to correlate to changes in lithologies or rock textures that seem to relate to preferential flow patterns (Figure 131). Overlaying the curvature attribute and the amplitude envelope highlights a lineament patterns within the reservoir with a northwest/southeast trend (Figure 132). This trend if related to permeability would explain the unexpected arrival of the CO_2 plume more than ¼ mile outside the pattern to the north.

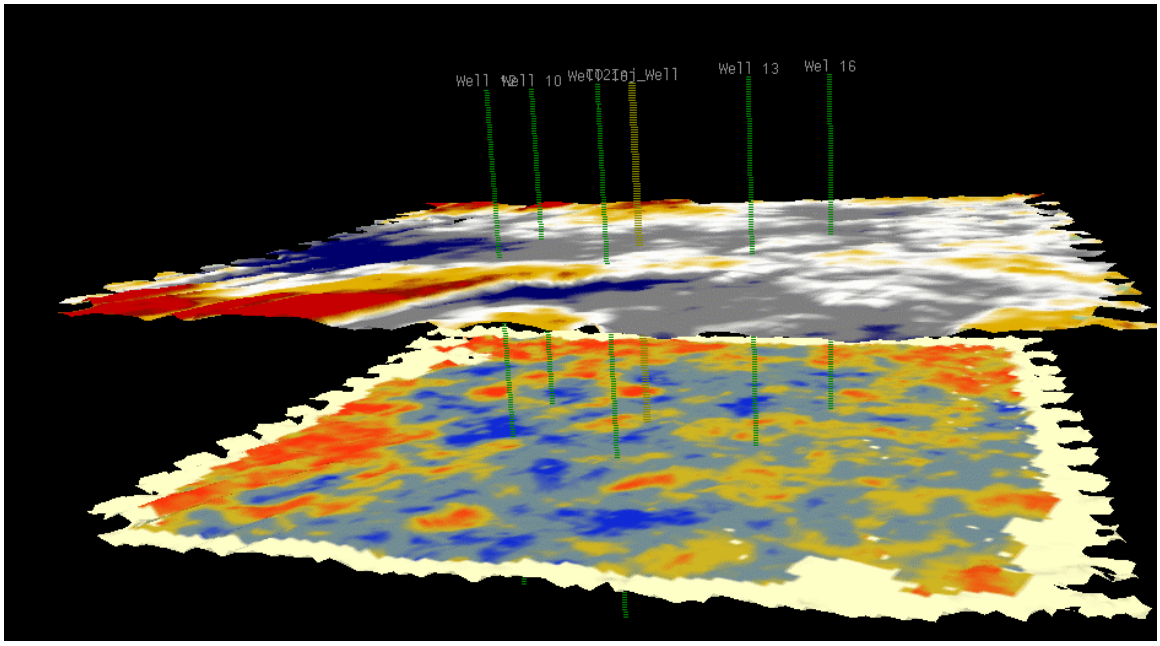

Figure 131. Time structure seismic facies map over coherency map.

Of all the attributes evaluated it appears spectral ratio maps possess a high sensitivity to the presence of the miscible phase of CO_2 (Figure 133). This monitor survey data is consistent with model location of CO2 and appears to provide strong evidence in support of a somewhat meandering northerly trend or texture to the rocks outside the pattern. Early in the study instantaneous frequency appeared to be a key data property with a lot of evidence supporting a high sensitivity to changes in wavelet characteristics from reflections near the top of the injection interval.

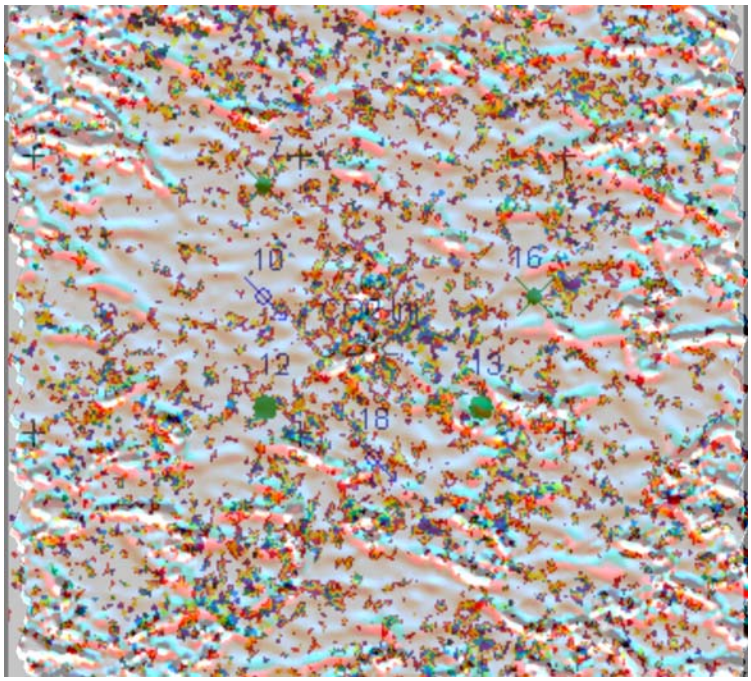

Figure 132. Curvature attribute overlaid on PPB result.

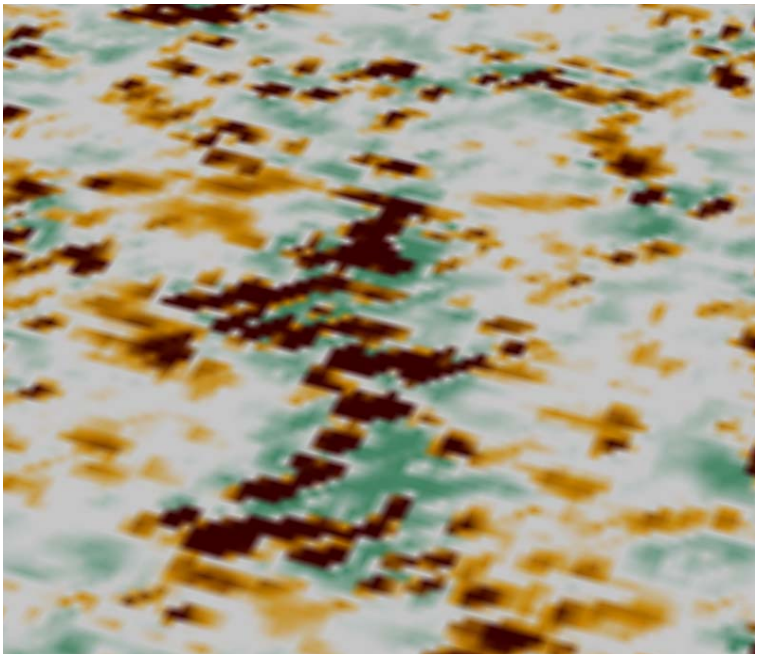
Figure 133. Spectral ratio attribute expanded at the CO_2 injection well and including nearby production wells that define the pattern.

CONCLUSION

- Time-lapse seismic monitoring of EOR-CO_2 revealed weak anomalies in thin carbonates below temporal resolution and is successful after moderate cross-equalization and attention to consistency in acquisition and processing details. Most of all, methods applied here avoid the complications associated with inversion-based attributes and extensive cross-equalization techniques.

- Shortness of turnaround time of time-lapse seismic monitoring in the Hall-Gurney field provided timely support for reservoir-simulation adjustments and flood-management requirements across this very short-lived pilot study.

- Spatial textural, rather than spatially sustainable magnitude, time-lapse anomalies were observed and should be expected for thin, shallow-carbonate reservoirs. Non-inversion, direct seismic attributes proved both accurate and robust for monitoring the development of this EOR-CO_2 flood.

- After differencing, amplitude residual data provided more pronounced anomaly contrast than previous instantaneous frequency or amplitude envelope data. Extensive and thorough equalization proved valuable in distinguishing very small percent changes between presence and absence of CO_2.

- Seismic data acquisition and preliminary processing on the nine 3-D reflection surveys (one baseline and eight monitor) has been completed within three years as planned and budgeted.

  - Preliminary data processing on the nine seismic volumes is complete with secondary processing halted due to project termination. This secondary processing would have enhanced data resolution and interpretations beyond any documented studies at these depths and for beds this thin.

  - Various interpretation approaches have produced images with strong agreement to production models, volumetrics, and observations that provide the essential ground truth for this study.

  - Interpretations are still very crude, but work with processed data to optimize consistency, resolution, and signal-to-noise has been halted prematurely.

- Several unique approaches to data equalization have allowed differencing and interpretations consistent with previous approaches, enhancing confidence in the image and growth pattern suggested from preliminary processing and interpretations.

  - A variety of unexpected data and reservoir characteristics have been identified and explained, providing engineers with detailed scenarios of fluid movement unlike any reservoir study in the literature.

- Unique and consistent anomalies in both amplitude and frequency data suggest the presence of CO_2 in the rock can be imaged at these depths and reservoir characteristics and if key aspects of the data could be identified and enhanced with specialized processing flows images of the CO_2 plume would have become even more vivid.

- After extensive equalization of reflection data to minimize and eliminate noise and balance data signal characteristics inconsistent from survey to survey and not related to changes in the reservoir, time slices from the reservoir interval were differenced. These differenced images provided interpretable patterns consistent with previous analysis.

- After differencing, amplitude residual data provided more pronounced anomaly contrast than previous instantaneous frequency or amplitude envelope data. Extensive and thorough equalization proved valuable in distinguishing very small percent changes between presence and absence of CO_2.

- Distribution and geometries associated with similarity seismic facies and seismic-lineament patterns are suggestive of a complex ooid shoal depositional motif, an interpretation consistent with an oolitic lithofacies reservoir type. Oolitic facies are imaged on these seismic data at a resolution significantly greater than previously documented.

Key Observation Consistent with Seismic and Completely Unexpected Based on Production Data and Engineering Simulation

During fall of 2006, production data from oil wells north and outside the CO_2 confinement area showed a steady increase in oil production. Production levels increased several times normal production for these 50+-year-old wells. These measured oil production data are suggestive that the seismic images successfully tracked the northward movement of the CO_2 long before engineering simulations or production data either detected or even considered this possibility. Continued monitoring of the CO_2 plume and enhancement to processing and interpretation workflows will not take place due to project termination by sponsor. Several publications previously submitted to reviewed but unrefereed journals will be refined and submitted to upper-tier refereed outlets under no-cost extensions of this project.

REFERENCES

KGS Project website: www.kgs.ku.edu/Geophysics/4Dseismic.

Byrnes, A.P., R.D. Miller, and A.E. Raef, 2005, Evolution of reservoir models incorporating different recovery mechanisms and 4-D seismic—Implications for CO_2 sequestration assurances [Abs.]: Poster presented at the annual conference of the American Association of Petroleum Geologists, June 19-22, Calgary, Alberta, Canada.

Miller, R.D., A.E. Raef, A.P. Byrnes, and W.E. Harrison, 2007, Technical progress report, year 3: 4-D high-resolution seismic reflection monitoring of miscible CO_2 injected into a carbonate reservoir: Kansas Geological Survey Open-file Report 2007-11.

Miller, R.D., A.E. Raef, A.P. Byrnes, and W.E. Harrison, 2005, Technical progress report, year 2, and plan for year 3: 4-D high-resolution seismic reflection monitoring of miscible CO_2 injected into a carbonate reservoir: Kansas Geological Survey Open-file Report 2005-32.

Miller, R.D., A.E. Raef, A.P. Byrnes, and W.E. Harrison, 2005, 4D seismic—Application for CO_2 sequestration assurances: AAPG Mid-Continent Section meeting, Oklahoma City, Oklahoma, September 10-13, abstract published online.

Miller, R.D., A.E. Raef, A.P. Byrnes, and W.E. Harrison, 2004, Progress Report Year 1: 4-D high-resolution seismic reflection monitoring of miscible CO_2 injected into a carbonate reservoir: Kansas Geological Survey, Open-file Report 2004-45.

Miller, R.D., A.E. Raef, A.P. Byrnes, and W.E. Harrison, 2004, Project Facts: 4-D high-resolution seismic reflection monitoring of miscible CO_2 injection into a carbonate reservoir; *in* DOE Fact Sheet CO_2 EOR Technology—Technologies for Tomorrow's E&P Paradigms: U.S. Dept. of Energy, Office of Fossil Energy, National Energy Technology Laboratory, Strategic Ctr. for Natural Gas and Oil, 2 p.

Miller, R.D., A.E. Raef, A.P. Byrnes, and W.E. Harrison, 2005, 4-D seismic—Application for CO_2 sequestration assurances [Abs.]: American Association of Petroleum Geologists Mid-Continent Section meeting, Oklahoma City, Oklahoma, September 10-13.

Miller, R.D., A.E. Raef, A.P. Byrnes, J.L. Lambrecht, and W.E. Harrison, 2004, 4-D high-resolution seismic reflection monitoring of miscible CO_2 injected into a carbonate reservoir in the Hall-Gurney field, Russell County, Kansas [Exp. Abs.]: Society of Exploration Geophysicists, p. 2259-2262.

Raef, A.E., R.D. Miller, A.P. Byrnes, E.K. Fransen, W.L. Watney, and W. E. Harrison, 2005, A new approach for weak time-lapse anomaly detection using seismic attributes: geology and production data integrated monitoring of miscible EOR-CO_2 flood in carbonates: Society of Exploration Geophysicists, Houston, November 6-11.

Raef, A.E., R.D. Miller, A.P. Byrnes, W.E. Harrison, 2006, Impact of improved seismic resolution and signal-to-noise ratio on monitoring pore-fluid composition changes: CO_2-injection, Hall-Gurney Field, Kansas, USA: Annual convention of the American Association of Petroleum Geologists, April 9-12, 2006, Houston.

Raef, A.E., R.D. Miller, A.P. Byrnes, and W.E. Harrison, 2006, Pore-fluid composition oriented 4D-seismic data processing and interpretation: implications for monitoring

EOR and/or sequestration CO_2: AAPG Rocky Mountain Section Annual Meeting, Billings, Montana, June 11-13.

Raef, A.E., R.D. Miller, A.P. Byrnes, and W.E. Harrison, 2004, 4-D seismic monitoring of the miscible CO2 flood of Hall-Gurney field, Kansas: *Leading Edge*, v. 23, no. 11, p. 1171-1176.

Raef, A.E., R.D. Miller, A.P. Byrnes, W.E. Harrison, and E.K. Franseen, 2005, Time-lapse seismic monitoring of enhanced oil recovery CO_2-flood in a thin carbonate reservoir, Hall-Gurney field, Kansas, U.S.A.: Poster presented at the annual meeting of the American Association of Petroleum Geologists, Calgary, Alberta, Canada, June 22; Kansas Geological Survey, Open-file Report 2005-24.

Raef, A.E., R.D. Miller, E.K. Franseen, A.P. Byrnes, W.L. Watney, and W.E. Harrison, 2005, 4-D seismic to image a thin carbonate reservoir during a miscible CO_2 flood—Hall-Gurney field, Kansas, USA: *Leading Edge*, v. 24, no. 5, p. 521-526.

Watney, W.L., E.K. Franseen, A.P. Byrnes, R.D. Miller, A.E. Raef, S.L. Reeder, and E.C. Rankey, 2006, Characterization of Seismically-Imaged Pennsylvanian Ooid Shoal Geometries and Comparison with Modern: Annual convention of the American Association of Petroleum Geologists, April 9-12, 2006, Houston; Annual Convention Abstracts Volume, p 113.